FINITE ELEMENT ANALYSIS AND EXPERIMENTAL VERIFICATION OF POLYMER MELT TEMPERATURE AND PRODUCT SHRINKAGE IN INJECTION MOLDING

GAN TECK WAN

DISSERTATION SUBMITTED IN FULFILLMENT

OF THE REQUIREMENTS

FOR THE DEGREE OF MASTER OF ENGINEERING

FACULTY OF ENGINEERING

UNIVERSITY OF MALAYA

KUALA LUMPUR

2012

UNIVERSITY MALAYA

ORIGINAL LITERARY WORK DECLARATION

Name of Candidate: **Gan Teck Wan** (I.C/Passport No:

Registration/Matric No: **KGA090027**

Name of Degree: **Master of Engineering Science**

Title of Project Paper/Research Report/Dissertation/Thesis ("this work"): **Finite Element Analysis and Experimental Verification of Polymer Melt Temperature and Product Shrinkage in Injection Molding**
Field of Study: **Manufacturing**

I do solemnly and sincerely declare that:

(1) I am the sole author/writer of this work;
(2) This work is original;
(3) Any use of any work in which copyright exists was done by way of fair dealing and for permitted purposes and any excerpt or extract form, or reference to or reproduction of any copyright work has been disclosed expressly and sufficiently and the title of the work and its authorship have been acknowledged in this work;
(4) I do not have any actual knowledge not do I ought reasonably to know that the making of this work constitutes an infringement of any copyright work;
(5) I hereby assign all and every rights in the copyright in this work to the University of Malaya ("UM"), who henceforth shall be owner of the copyright in this work and that any reproduction or use in any form or by any means whatsoever is prohibited without the written consent of UM having been first had and obtained;
(6) I am fully aware that if in the course of making this work I have infringed any copyright whether intentionally or otherwise, I may be subjected to legal action or any other actions as may be determined by UM.

Candidate's Signature Date:

Subscribed and solemnly declared before,

Witness's Signature Date:

Name:

Designation:

UNIVERSITI MALAYA

PERAKUAN KEASLIAN PENULISAN

Nama: **Gan Teck Wan** (No. K.P/Passport No: **850418-14-5401**)

No. Pendaftaran /Matrik: **KGA090027**

Name Ijazah: **Master of Engineering Science**

Tajuk Kertas Projek/Laporan Penyelidikan/Disertasi/Tesis ("Hasil Kerja ini"): **Finite Element Analysis and Experimental Verification of Polymer Melt Temperature and Product Shrinkage in Injection Molding**

Bidang Penyelidkan: **Manufacturing**

Saya dengan sesungguhnya dan sebenarnya mengaku bahawa:

(1) Saya adalah satu-satunya pengarang/penulis Hasil Kerja ini;
(2) Hasil kerja ini adalah asli;
(3) Apa-apa penggunaan mana-mana hasil kerja yang mengandungi hakcipta telah dilakukan secara urusan yang wajar dan bagi maksud yang dibenarkan dan apa-apa petikan, ekstrak, rujukan atau pengeluaran semula daripada atau kepada mana-mana hasil kerja yang mengandungi hakcipata telah dinyatakan dengan sejelasnya dan secukupnya dan satu pengiktirafan tajuk hasil kerja tersebut dan pengarang/penulisnya telah dilakukan di dalam hasil kerja ini;
(4) Saya tidak mempunyai apa-apa pengetahuan atau patut semunasabahnya tahu bahawa penghasilan hasil kerja ini melanggar suatu hakcipta hasil kerja yang lain;
(5) Saya dengan ini menyerahkan kesemua dan tiap-tiap hak yang terkandung di dalam hakcipta hasil kerja ini kepada Universiti Malaya ("UM") yang seterusnya mula dari sekarang adalah tuan punya kepada hakcipta di dalam hasil kerja ini dan apa-apa pengeluaran semula atau penggunaan dalam apa jua bentuk atau dengan apa juga cara sekalipun adalah dilarang tanpa terlebih dahulu mendapat kebenaran bertulis dari UM;
(6) Saya sedar sepenuhnya sekiranya dalam masa penghasilan hasil kerja ini saya telah melanggar suatu hakcipta yang lain sama ada niat atau sebaliknya, saya boleh dikenakan tindakan undang-undang atau apa-apa tindakan lain sebagaimana yang diputuskan oleh UM.

Candidate's Signature Date:

Subscribed and solemnly declared before,

Witness's Signature Date:

Name:

Designation:

ABSTRACT

It is not an easy task to control the final properties of the plastic product since there is a lot factors like mold design, processing parameters and behavior of the plastic material during injection molding have to be taken into consideration. Due to these factors, injection molded plastic part varies accordingly with the parameter setting and results in different dimensional variation from part to part. For better quality control, the effect of these processing parameters on shrinkage must be known before manufacturing. In this study, finite element analysis was used to determine this effect by using one-way interaction approach and two-way interaction approach. In one-way interaction approach, three finite element analysis tools namely computational fluid dynamic, transient thermal analysis and static structural analysis were used to model the mold filling, mold cooling and product shrinkage after ejection as separate process. In the two-way interaction approach, a highly intelligent multi-physics architecture composed of both computational fluid dynamic and finite element analysis tools were proposed to study the injection molding shrinkage problem as a single process. Two test mold cavities namely mold cavity-I and mold cavity-II were used in this study. Marlex HDPE 9500 was injection molded in mold cavity-I and TOYOLAC 250 ABS was injection molded in mold cavity-II. Both cavities product shape were respectively rectangular in geometry with dimension of 100 $mm \times 50\ mm \times 2\ mm$ and 67 $mm \times 40\ mm \times 4\ mm$. From analysis obtained from one-way interaction approach, it was found that the shrinkage of mold cavity-I increased from 4.7 - 4.8% to 4.9 – 5.0% when the melt temperature was adjusted from 220℃ to 240℃. The packing pressure effect on shrinkage was relatively small compared with melt temperature effect since it was not taken into account in static structural analysis. The two-way interaction approach result showed that the shrinkage was high at the center location of the plastic part. No shrinkage was

recorded when the mass flow rate was high. At low injection mass flow rate (0.05 *kg/s)*, the shrinkage improved with melt temperature. Shrinkage was 1 - 10% when melt temperature was 220 ℃ and shrinkage was 0 - 4.5% when melt temperature used was 240 ℃. One-way interaction approach simulation for mold cavity-II was compared with physical result obtained from experimental study. Both simulation and the physical results showed almost the same flow speed, temperature and thickness. Recorded experimental flow speed was 0.05 - 0.1 *s* faster than the simulation. The average recorded temperature obtained from the experimental result was about 9 ℃ higher than the simulation. Simulation over predicted the plastic product of mold cavity-II shrinkage by 1 - 4.8%. Taguchi method and analysis of variance (ANOVA) were used to optimize the processing parameter for minimum shrinkage of mold cavity-II product. According to the statistical result, melt temperature, mold cooling time and injection speed were the significant factors. Due to the small dimension of the injection gate, the material in this region cooled down and solidified very fast to the extent that the applied packing pressure and packing time had no significant effect on adding material into the cavity to reduce product shrinkage during packing phase. As a result, these two parameters were not significant according to Taguchi and ANOVA analysis.

ABSTRAK

Ia bukan satu tugas yang mudah untuk mengawal sifat sifat akhir produk plastik sebab terlalu banyak faktor seperti rekan bentuk acuan, parameter pemprocessan dan perubahan sifat bahan plastik semasa pengisian acuan. Disebabkan faktor-faktor in, produk plastik pengisian acuan akan berubah selari dengan pemprosesan yang berbeza dan menyebabkan perubahan dimensi yang berbeza walaupun pemprocesan yang sama diikuti. Untuk kawalan kualiti yang lebih baik, kesan parameter pemprocesan terhadap pengecutan perlu diketahui sebelum pembuatan. Dalam kajian ini, "Finite Element Analysis" telah digunakan untuk menentukan kesan ini dengan menggunakan interaksi dalam satu hala dan interaksi dalam dua hala. Dalam interaksi dalam satu hala, tiga jenis alat analysis "Finite Element Analysis" iaitu "Computational Fluid Dynamic", Transient Thermal Analysis" dan "Static Structural Analysis" telah digunakan untuk memodelkan pengisian acuan, penyejukan acuan dan pengecutan produk selepas ejeksi sebagai process yang berasingan. Dalam interaksi dalam dua hala, simulasi multi-fizik yang terdiri daripada kedua-dua "Computational Fluid Dyanamic" dan "Computational Structural Mechanic" telah dicadangkan untuk mengkaji masalah pengecutan dalam pengacuan suntikan sebagai process tunggal. Dua kaviti iaitu kaviti-I dan kaviti-II adalah masing masing dalam bentuk segi empat tepat dengan dimensi 100 $mm \times 50\ mm \times 2\ mm$ dan 67 $mm \times 40\ mm \times 4\ mm$. Marlex HDPE dipilih sebagai bahan pengisian acuan untuk kaviti-I dan TOYOLAC 250 ABS dipilih sebagai bahan pengisian acuan untuk kaviti-II. Daripada analisis yang diperolehi dari interaksi dalam satu hala, didapati bahawa pengecutan produk plastik menigkat dari 4.7 - 4.8% ke 4.9 – 5.0% apabila suhu leburan plastik diselaraskan dari 220 ℃ ke 240 ℃. Kesan tekanan pemampatan pada pengecutan adalah kecil berbanding dengan kesan suhu leburan kerana ia tidak diambil kira dalam "Finite Element Analysis". Sebaliknya, interaksi dalam dua hala

menunjukan bahawa pengecutan adalah tinggi di bahagian tengah produk plastik. Tiada pengecutan dicatatkan apabila kadar aliran jisim adalah tinggi. Pada kadar pengaliran jisim yang rendah (0.05 *kg/s*), pengecutan berkurangan dengan suhu leburan. Pengecutan adalah 5.5 - 14% apabila suhu leburan adalah 220 ℃ dan pengecutan adalah 0 - 4.5% apabila suhu leburan yang digunakan adalah 240 ℃. Simulasi yang didapati dengan menggunakan interaksi dalam satu hala bagi kaviti-II telah dibandingkan dengan hasil yang diperolehi daripada kajian eksperiment. Kedua-dua simulasi dan hasil kajian menunjukan laju kealiran, suhu dan ketebalan yang hampir sama. kelajuan aliran yang direkodkan dalam eksperiment adalah 0.05 - 0.1 *s* lebih cepat daripada simulasi. Sebaliknya, suhu purata yang diperolehi daripada eksperiemen adalah 9 ℃ lebih tinggi daripada simulasi. Simulasi terlebih meramalkan pengecutan pengecutan produk plastick bagi kaviti acuan-II dengan 1 - 4.8%. Kaedah Taguchi dan analisis variasi (ANOVA) telah digunakan untuk mengoptumumkan parameter pemprosesan untuk pengecutan minimum produk bagi kaviti acuan-II. Menurut keputusan statistik, suhu leburan, masa penyejukan dan kelajuan suntikan adalah faktor penting. Disebabkan oleh kawasan suntikan yang kecil, leburan plastik di kawasan ini menjadi agak sejuk dan memejal dengan cepat sehingga kuasa tekanan dan masa pemampatan yang digunakan tidak mempunyai kesan ketara ke atas penambahan leburan plastik ke dalam rongga acuan untuk mengurangkan pengecutan produk semasa fasa pemampatan. Kedua-dua parameter ini iaitu tekanan dan masa pemampatan tidak memberikan kesan yang ketara megikut kaedah Taguchi dan analisis ANOVA.

ACKNOWLEDGEMENT

This thesis is based on a research work carried out at the engineering lab, University of Malaya, Malaysia, from June 2009 until June 2011, under the supervision of Prof. Dr. Imtiaz Ahmed Choudhury and Dr Nukman bin Yusoff. I greatly appreciate the educational opportunity that they have provided me through these years. In addition, I would like express my sincere gratitude to them for their valuable suggestions, advices, criticisms and comments on this research.

Moreover, I would like to thank Institute of Postgraduate Studies, University of Malaya for providing me financial support (Fellowship of UM) and research grant (IPPP) in conducting this research. In addition, I would like to thank Mr. Azzudin on giving me a lot of advices and comments on designing the mold cavity for experimental work. Furthermore, I would like to thank all the technicians in engineering lab for assisting me in fabricating the mold cavity during the experimental study.

Finally, I would like to thank my family especially my parents for their encouragement and support.

TABLE OF CONTENTS

LIST OF FIGURES

LIST OF TABLES

LIST OF EQUATIONS

LIST OF SYMBOLS

Symbol	Definition	Unit
[B]	Strain displacement matrix, based on the element shape functions	
$[D]$	Elasticity or elastic stiffness matrix or stress strain matrix	
ε	Total strain vector	
ε^{th}	Thermal strain vector	
ε_x	Direct strain in the x direction	
ε_y	Direct strain in the y direction	
ε_z	Direct strain in the y direction	
ε_{xy}	Shear strain on the x-y plane	
ε_{yz}	Shear strain on the y-z plane	
ε_{xz}	Shear strain on the x-z plane	
e	Internal energy	J/kg
E	Young's modulus	Pa
$\{F_e^{nd}\}$	Nodal forces applied to the element	N
$\overrightarrow{g}$	Gravitational acceleration	m/s^2
G	Shear modulus	Pa
k	Thermal conductivity	$W/m\,°C$
$[N]$	Matrix of shape functions	
$[N_n]$	Matrix of shape functions for normal motions at the surface	
ρ	Density	kg/m^3
P	The applied pressure vector	Pa
q_r	Radiation heat flux vector	W/m^2
Q	Internal heat generation rate per unit volume	W/m^3
S	Shape function	
τ	Shear stress	Pa
t	Time	s
T	Current temperature at the point in question	$°C$
T_{ref}	Reference (strain free) temperature	$°C$
u	Cartesian velocity component in x- direction	m/s
$\{u\}$	Nodal displacement vector	m
ν	Poisson's ratio	
v	Cartesian velocity component in y- direction	m/s
ν_{xy}	Major Poisson's ratio	
ν_{yx}	Minor Poisson's ratio	
vol	Volume of element	m^3
$\vec{V}$	Velocity and its magnitude	m/s
V	Volume	m^3
w	Cartesian velocity component in z- direction	m/s
W	External work	J
$\{w_n\}$	Displacements within the element normal to the surface	

σ	Stress vector	N/m^2
σ_{ij}	Stress tensor	N/m^2
δ	Virtual operator	
α	Coefficient of thermal expansion	$^\circ C^{-1}$
η	Dynamic viscosity	kg/ms
Φ	Viscous dissipation	
$\dot{\gamma}$	Shear rate	*1/s*

LIST OF ABBREVIATIONS

Abbreviation	Definition
ABS	Acrylonitrile - Butadiene - Styrene
ANOVA	Analysis of Variance
area	Area of the distributed resistance
C	Carbon
CAD	Computer aided design
CFD	Computational Fluid Dynamic
CSM	Computational Structural Mechanic
Fe	Ferrite
HDPE	High density polyethylene
LDPE	Low density polyethylene
Mn	Maganese
PA 6	Polyamide
PP	Polypropylene
PS	Polystyrene
PVT	Pressure - Volume – Temperature
Si	Silicon
WLF	Williams-Landel-Ferry

CHAPTER 1: INTRODUCTION

Plastic injection molding is known as an important manufacturing process in plastic industry for wide range of products from consumer product to machinery, car and air plane.

In the manufacturing process, hot polymer melt is injected into mold in filling phase, high pressure is applied in packing phase to force more material into the cavity to compensate for volumetric shrinkage of the material as it cools. The hot plastic is allowed to cool in mold until it has enough strength to be ejected during mold cooling phase. After ejection, the cooling process continues until the molded part achieves equilibrium state with room temperature. This manufacturing technology is one of the most efficient processes where mass production through automation is feasible and products with complex geometry are easily attained. For a long time, controlling the injection molding product quality is the main issue of this manufacturing technique. Since non Newtonian material is used, it is very hard to control the final properties of the product especially when the mold cavity used is very complicated.

A lot of molding defects like short shot, warpage, sink mark, shrinkage and so on can happen when the plastic injection molding process is uncontrollable. Among all the molding defects, shrinkage is the most prominent molding defects. This molding defect is related to the dimensional accuracy of the final product. Driven primarily by the strong needs for the manufacturing of high precision complicated plastic parts at high production rates and low cost, products with slight dimensional variation must be rejected. To a production factory, high rejection rate will result in a loss to them. As a result, it is important to control the properties of the plastic product produced.

1.1 Importance and scope of study

In industry, injection molding is used for large quantity production. If dimensional accuracy is a problem for high precision plastic part during production, it can result in a deep loss to a factory since a lot of molded parts needed to be scrapped in this large quantity production process. Besides, the time and electricity for running the machine will be wasted. Therefore, controlling the end product shrinkage problem is very important to ensure the company loss is at minimum during production.

It is not an easy task to control the final properties of the plastic product since there is a lot factors like mold design, processing parameters and behavior of the plastic material have to be taken into consideration. As a result, this process is time consuming and not cost effective. In addition, repeated machining or new mold has to be made in order to rectify the molding problem. As a solution to this, plastic product must be carefully designed in the initial stage and not improved after the product is made. The molding problem must be known before the cavity is made.

In order to achieve the above goal, finite element analysis is used in this study to predict the molding problems in the design phase. Under different processing parameters, the dimensional accuracy of the end products is analyzed. The end product properties are a result of processing history. There is a strong interaction between the end product quality and the processing parameters. In this study, the effect of these processing parameters on the molding stage (mold filling, packing and cooling) and shrinkage are studied. Since finite element analysis is only a prediction made by using theoretical mathematical model, its reliability is determined by using real time experiment data.

1.2 Problem statement

Degree of shrinkage is directly reflected from the processing parameter applied during an injection molding process. Due to the complicated mold geometry, complicated molding process that involves four different sub processes from filling to cooling and also the number of processing parameter involved; controlling the shrinkage to get highly precise part is a challenging job.

Altering the mold geometry to fix this problem is a costly job but luckily the shrinkage can be minimized if the best processing parameter is applied. However, the optimization process is a difficult task too since the number of processing parameters involved are a lot like injection speed, packing pressure, mold clamping pressure, plastic melt processing temperature, mold temperature, packing time, mold cooling time, screw rotation speed and so on. To study the effect of all these parameters effect on shrinkage can be considered as impossible and indirectly post a difficulty for molder to produce good quality product.

When altering the processing parameter is not the option for shrinkage problem then the mold cavity must be modified. Conventionally, mold cavity is made without any knowledge of how the plastic flow into the cavity, how the heat exchange happens and how the dimension of the product changes during the cooling process. This has resulted a number of costly iteration of the mold modification to get the desired dimension of injection molded product. This conventional method must be changed. The problems of injection molding and the defects must be known before manufacturing to minimize the cost spend on mold fabrication.

Simulation is the tool that can help designer to foresee the problems before manufacturing. However, current commercial injection molding can lead one user to wrong decision on mass manufacturing process due to the unknown solving procedure of the software. However, the finite element analysis which is user defined software is seldom used to simulate this process due to the complexity of the molding process and also the solving procedure.

1.3 Objectives

The objectives of this study are

- To analyze plastic melt temperature, pressure, filling speed during injection molding and the effect of these parameters on part shrinkage by using computational fluid dynamic and finite element analysis techniques
- To verify polymer melt temperature, flow speed and product shrinkage predicted by computational fluid dynamic with experimental results
- To optimize the processing parameters for minimum product shrinkage

1.4 Thesis outline

Chapter 1 has presented a brief introduction to the injection molding manufacturing process and the problems associated with this manufacturing technique. This chapter has also presented a brief discussion on plastic product shrinkage formation under different circumstances. Chapter 2 presents the relevant background information on finite element analysis, studies done by the previous researcher and optimization process of plastic injection molding. Chapter 3 presents the numerical approach used to model the injection molding process. The formulation on shrinkage formation in the simulation model used is broadly discussed in this chapter. In addition, the experimental set up, apparatus,

instrument, mold design, part design and design of experimental are discussed in this chapter too. The effect of processing parameter on molding situation (mold filling, packing and cooling) and product quality (shrinkage) are discussed in Chapter 4. Chapter 5 presents the conclusions of the thesis work, and recommendations for future work.

CHAPTER 2: LITERATURE REVIEW

Controlling the properties of plastic injection molding product is important to produce consistent high quality plastic product and to save cost and reduce time wasted in the manufacturing process. In literatures, a lot of attempts were made by previous researchers on this topic using different approaches like finite element analysis, statistical method and experimental method to study the effect of the molding processing parameters on shrinkage. The previous researchers' works are presented as follows.

2.1 Shrinkage analysis by simulation

Present day competitive conditions force us to produce high quality product faster and cheaper. Computer aided analysis and engineering software must be used in order to meet this necessity (Ozcelik & Erzurumlu, 2006). These kinds of software are not only easy to use but allow us to foresee the problem before manufacturing. It is a good learning tool for both novice and experienced user since a lot of illustrative results which are not available by using experimental means are available for user. As a result, a lot of commercial computer aided engineering (CAE) software available for plastic injection molding like MoldFlow, Moldex or CadMould are extensively used to investigate the molding situation to optimize the injection molding condition.

Due to the increasing demand for a more accurate property data for the large number of polymers, Sridhar & Narh (2000) studied effect of temperature dependent thermal conductivity and specific heat data on cavity pressure, average flow velocity, bulk temperature, frozen layer fraction and volumetric shrinkage by using CadMould. They found that the temperature dependent variables appeared to affect the cooling time in term of its effect on the prediction of bulk temperature and prediction for part shrinkage.

Li (2001) found a new design synthesis approach to solve the initial cooling channel design for a complex shape plastic product by using CadMould. In his study, a complex shape plastic part was decomposed into simpler shape features to obtain the best cooling system design for the individual feature. Then they were combined to form the final cooling system of the entire plastic product.

Spina (2004) used MoldFlow to study the fabrication of a plastic arm of the body interior of a medium sized car in order to evaluate effect of different hot runner systems, gating and product configurations on surface appearance. A deep investigation of thermal stress and strain distribution was performed to predict defect presence in the final product and he found that simulation allowed the deflections of warped surface to be estimated and in depth analyses can be performed in order to aid process engineers on how to position gates and modify mold design.

Imihezri et al. (2005) used MoldFlow to see the effects of increasing gate number on fill time, pressure distribution, weld line and temperature for “X” and “V” ribbing. They concluded that injection molding simulation provides an insight to unforeseen problems commonly related to injection molding process such as weld line and warpage.

Ozcelik & Erzurumlu (2006) used MoldFlow to find the best gate design, filling profile and minimum shrinkage and warpage for PC Button Base using Taguchi method. Packing pressure, mold temperature and melt temperature were found as significant factors for warpage and shrinkage in their study.

Oktem et al. (2007) used MoldFlow and Taguchi optimization technique to reduce warpage problem resulted from the shrinkage variation which depended on process parameters during production of thin shell plastic components for orthose part. Taguchi

optimization was found to be sufficient to solve the warpage and shrinkage problems for thin shell plastic components of orthose part in their study.

Shen et al. (2008) used MoldFlow to study effect of gate design on mold filling situation of an electronic dictionary battery cover. Through numerical simulation, they found that two injection locations at both side of the thin shell product is better than one injection location molding.

Wan Abdul Rahman et al. (2008) used MoldFlow to study difference between solid and hollow designs of window frame made of rice husk filled high density polyethylene on filling, packing and cooling situation during injection molding and the most feasible window frame design was selected for stress analysis. In their research work, they found that the window frame with hollow design was preferable owing to the advantage of filling, packing and cooling properties. However, pressure and clamping tonnage required was unfavorable for hollow design.

Hwang et al. (2008) studied the feasibility of microcellular injection molding over injection molding for textile roller made of polybutyleneterephthalate (PBT) with 30 wt% glass and wollastonite fiber using CadMould and experimental analysis. Through numerical analysis, they found that the unbalance melt flow resulted thickness variation. Due to the introduction of inert gas for injection molding, shrinkage of textile roller made using microcellular injection molding was comparatively lower than that of part made by using injection molding process.

Zhil'tsova (2009) used MoldFlow to study the effects of processing parameter (injection speed, packing pressure, packing time and hot nozzle temperature) on the characteristics (dimensional stability, weight variation and visual appearance) of injection

molded high density polyethylene (HDPE) acetabular cups for total hip replacement implants. From the numerical analysis, packing pressure was found as the most significant factor on part dimension and weight. In addition, injection speed rise was found to have negative influence on the part weight and dimensions.

Ozcelik & Sonat (2009) used MoldFlow and Taguchi method to study warpage of thin shell phone cover produced with polycarbonate/acrylonitrile butadiene styrene (PC/ABS) thermoplastic. Structural analysis software, CATIA V5R12 was used to determine the forces that cause the plastic part to fail. The most significant factor was found to be the packing pressure and the strongest material for the cell phone cover is made of PC/ABS reinforced with 15% of carbon fiber.

From the literature above, commercial injection molding simulation software (MoldFlow and CadMould) can be considered as very powerful software which allows user to replicate real processing condition, provides insight into the manufacturing process, helps user to prevent and avoids any poor design or molding problems before manufacturing and assists user to obtain feasible design for mass production. However, there is some limitation on the meshing procedure, convergence criteria, solving formula and theory associated with the software if compared with finite element analysis. Finite element analysis is user defined software which allows user to do manual setting on the simulation model set up. Highly accurate result can be generated by using this user defined software depending on the user knowledge on the meshing method, convergence criteria, formula and theory as well as the resolution of the simulation.

2.2 Finite element analysis of injection molded product shrinkage

Finite element analysis is user defined software. Depending on user defined setting: the numerical procedure applied, the mesh generated, convergence criteria, residual plot and the model used; highly accurate prediction can be generated by this analysis tool. As a result, finite element analysis is used to obtain solutions to large class of engineering problems involving stress analysis, heat transfer and fluid flow (Moaveni, 1999). In this simulation process, the medium of interest is divided into a number of small sub regions and nodes (discretization). Then, the complete solution is generated by connecting or assembling the information obtained from these small sub regions and nodes individually.

Kansal et al. (2001) used thermal analysis to thoroughly study the temperature distribution and thermal residual stresses which were developed due to non uniform cooling of the molten plastic inside the mold cavity in the injection molded polystyrene gear. Their main intention of the investigation was to understand the thermal residual stresses built up as a result of the temperature distribution of the plastic material inside the mold cavity. They found that the analysis tool was able to reduce the scrap rate at the mold design phase.

Liu, (2009) used a special experimental set up which includes an injection mold equipped with tubular needles for guiding embedded thermocouples to measure the temperature inside the cavity. A transient heat transfer finite element model was used in their study to simulate the temperature variation in injection molded products too. From their study, they found that the numerical prediction coincided satisfactorily with the measured temperature data.

Wen-Bin (2004) used a simple thermal viscoelastic model to calculate the residual stress developed in the post filling stage based on the calculation of the injection molding

process. The entire model was divided into two regions, liquid and solid. Residual stress calculation was applied in the solid region. From his study, he found that he developed model was useful for determining the residual stress for different molding conditions and complicated cavity geometry.

Dimla et al. (2005) used finite element analysis and thermal heat transfer analysis to determine an optimum and efficient design for conformal cooling/heating channels in the configuration of an injection molding tools. In their study, they determined the best location for gate and cooling channels. Analysis of virtual models showed that those with conformal cooling channels predicted a significant reduced cycle time as well as marked improvement in the general quality of the surface finish when compared with conventionally cooled mold.

Tang et al. (2006) performed thermal analysis on simple rectangular geometry part to assess the effect of cooling channel on thermal residual stress in the mold using two dimensional finite element analysis. From the two dimensional contour plot of temperature distribution, the results showed that the shrinkage was likely to occur in the region near the cooling channels as compared to other regions. To provide thermal regulation in the injection molding process,

Hassan et al. (2010) studied the effect of the cooling system design on the solidification and heat transfer of polymer by injection molding. A full three dimensional time dependent injection molding numerical analysis was carried out in their experiment for a mold with cuboids shape cavity. After the validation of the numerical model was presented, they found that when cooling channels approached to the product surface, the cooling efficiency increased. They also found that the rectangular geometry cooling channel has the highest efficiency in the cooling.

Bikas et al. (2002) used finite element analysis to design the guidance of melt either by tuning the gates' geometry or by introducing appropriate vacuum at specific areas of the mold. They found that the numerical procedure applied leads to flow balancing and improved part quality by minimizing flow generated defects such as non uniform shrinkage, sink marks and so on.

Galantucci & Spina (2003) evaluated gating system configurations to optimize the filling conditions of thermoplastic injection molded part through data integration between finite element analysis and design of experiment approach. They found that a deeper investigation of stress and strain distribution can be performed to predict defect presence in the final product through the data integration approach applied. They found that this methodology is sensitive to existing differences between property of the real part and of its model.

Hassan et al. (2010) did the same thing as Tang et al. (2006) did but the later considered the effect of cooling system on the shrinkage rate of polystyrene by using 2D finite element analysis. Through numerical analysis, they showed that the position of the cooling channels has great effect on the final product temperature and shrinkage rate distribution throughout the product.

Choi & Im (1999) analyzed the shrinkage and warpage of injection molded parts made of amorphous polymer numerically in consideration of the residual stresses produced during the packing and cooling stages of injection molding. In their model, the temperature field was assumed to be independent of the in plane x and y directions and no bending of the parts in the mold was assumed. Besides, the residual stress generated during injection stage was not taken into consideration. It was found that the model proposed over predicted

the tensile residual stresses at the surface of injection molded parts but the predicted shrinkage was found to be reasonable to describe the effects of processing conditions well.

Although finite element analysis is a powerful analysis tool but due to the complexity of the solving procedure, it is seldom used to analyze the shrinkage problem of plastic injection molding. Much of the efforts are spent on analyzing the effect molding parameters on temperature distribution, mold filling situation and stress distribution field. In the industry, these research outcomes are not practical on improving the product quality. The research outcome must be focused more on shrinkage or warpage since these molding problems can indirectly result in loss to a company. Although, few attempts were made on this topic but certain assumptions must be made or certain parameters must not be taken into account for shrinkage study. The finite element analysis models made by previous researchers on shrinkage were still not perfect. As a result, this study is conducted to create a better finite element model for plastic product shrinkage simulation.

Well known finite element analysis software ANSYS 12.1 is used in this study. For modeling the shrinkage of injection molded components, both computational fluid dynamic (CFD) and computational solid mechanic (CSM) are used. CFD is a computer based tool for simulating the behavior of system s involving fluid flow, heat transfer and other related physical processes (ANSYS, 2006). A typical CFD interface of ANSYS 12.1 is presented Figure 2.1. As shown in this figure, it works by solving the equation of fluid flow over a region of interest (fluid region/mold cavity) with specified conditions on the boundary of that region (gate and air vent of the mold cavity). The set of equations which describe the processes of momentum, heat and mass transfer are known as the Navier-Stokes equations. There are a number of different solution methods which are used in CFD codes. The most common, and the one on which ANSYS CFX uses is known as the finite volume technique.

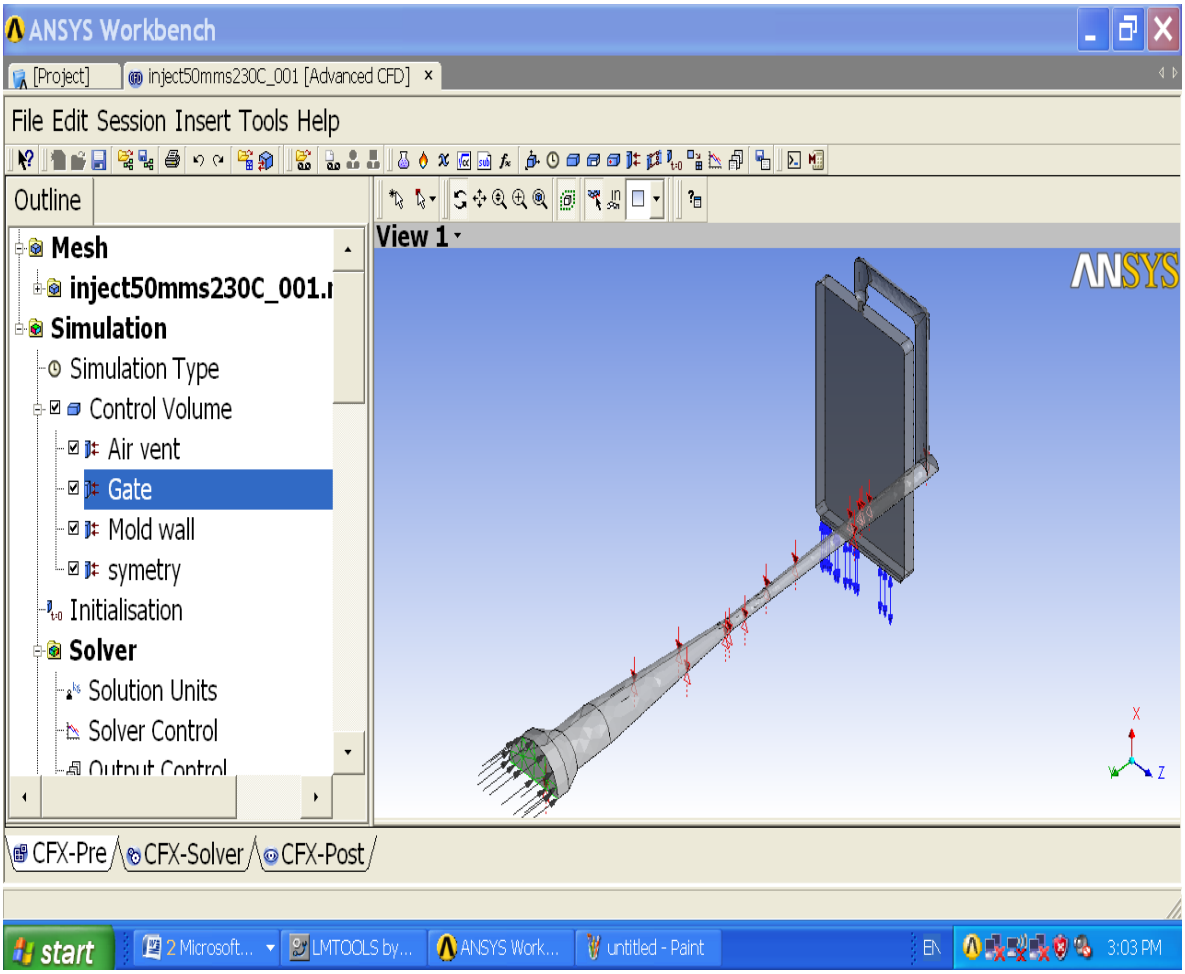

Figure 2.1: Computational fluid dynamic interface of ANSYS 12.1 (ANSYS, 2006)

In this technique, the region of interest (mold cavity) is divided into small sub-regions, called control volumes. The equations are discretized and solved iteratively for each control volume. As a result, an approximation of the value of each variable at specific points throughout the domain can be obtained. In this way, one derives a full picture of the behavior of the flow.

On the other hand, CSM is the branch of mechanics, physics, and mathematics that concerns the behavior of solid matter under external actions (external forces, temperature changes, applied displacements and so on). Under CSM, the analysis types available are structural (static and transient) analysis, heat transfer (steady state and transient) analysis,

dynamic (modal, harmonic, random vibration, flexible and rigid dynamics) analysis and magnetostatic analysis. A typical user interface of CSM for ANSYS 12.1 is presented in Figure 2.2. In the analysis of plastic injection molding shrinkage, both structural and heat transfer analysis are selected.

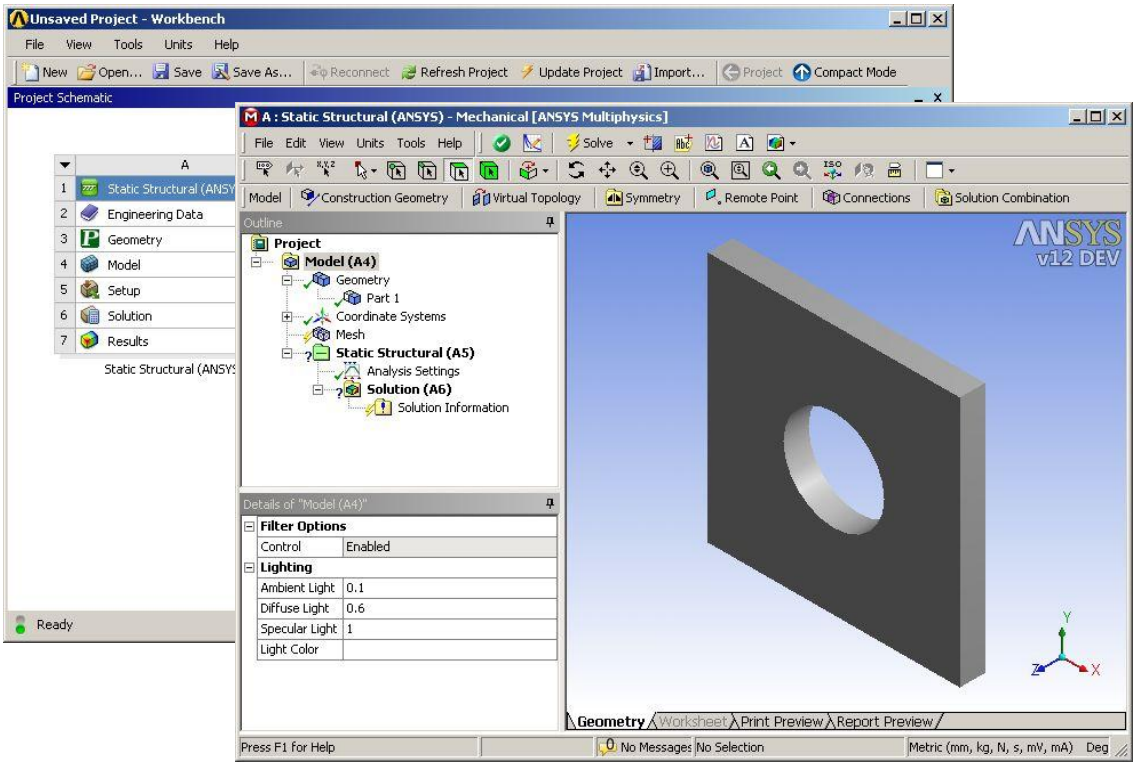

(b)

Figure 2.2: CSM user interface of ANSYS 12.1 (ANSYS, 2006)

The heat transfer analysis (thermal analysis) determines temperatures and other thermal quantities that vary over time (Moaveni, 1999). The variation of temperature distribution over time is of interest in many applications such as with cooling of electronic packages or a quenching analysis for heat treatment. Also of interest are the temperature distribution results in thermal stresses that can cause failure and dimensional change. In such cases the temperatures from a transient thermal analysis are used as inputs to a structural analysis for thermal stress and dimensional evaluations.

Structural analysis determines the displacement, stress, strains and forces in structures or components caused by loads that do not induce significant inertia and damping effects (Moaveni, 1999). Steady loading and response conditions are assumed. The loads and structure's response are assumed to vary slowly with respect to time. The types of loading that can be applied in a static analysis include:

- Externally applied forces and pressures
- Steady state inertial forces (such as gravity or rotational velocity)
- Imposed (nonzero) displacements
- Temperatures (for thermal strain)

The stress, strain and dimensional change are the main interest of static structural analysis.

1.6 Experimental analysis on shrinkage of injection molded part

It is very important to understand the influence of processing parameter on final quality of the end product. In practical, the visual inspection is not possible on plastic injection molding. As a result, it is very hard to understand what is actually happening during injection molding process. For a long time, the quality of the injection molding product is monitored through a trial and error basis. Through this method, the cost and time spent are very high since mold cavity might need to be remade in some cases if plastic injection molding is not successful. Although the difficulty on this research topic is very high but the result obtained is real as compared with simulation prediction.

To obtain precisely controlled surface contour, Lu & Khim (2001) investigated experimentally some effects of the molding conditions on the surface contour of injection molded polycarbonate lens. The injection molded lens contour was measured using laser interferometer and the birefringence of the molded lenses was measured using a polarimeter

to characterize the residual stresses in the lens. They found that mold shrinkage and stress play a vital role in determining the lens surface contours.

Chen & Gao (2003) studied the effect of packing profile (constant, ramp and step change) on plastic part shrinkage, evenness and thickness in searching the proper setting of injection molding parameters. From their research, they found that the increasing packing profiles of both the ramp and step change types tend to reduce shrinkage greater than the constant packing profiles with the same mean pressure. Besides, near gate location thickness was found to increase with packing pressure.

Postawa & Koszkul (2005) investigated the weight and shrinkage of a plastic product using different processing parameters (mold temperature, injection temperature, cooling time, hold pressure and injection speed) via Taguchi method. Taking the advantage of design of experiment theory, they found that the change in mass and processing shrinkage of the injection molded pieces made of polyoxymethylene or polystyrene depends much on the holding pressure and injection temperature.

Wang & Young (2005) studied the residual stress in a plastic part via layer removal technique. The stress distribution under different processing conditions was determined. Kim & Youn (2007) used the same technique to evaluate the residual stresses in injection molded part. The residual stress was simulated using commercial injection molding software, MoldFlow. Both experimental and predicted results showed the same residual stress behavior and they concluded that the layer removal method was applicable for residual stress measurements involving polymeric materials and especially for complex geometry parts.

Tsai et al. (2009) studied the effects of process parameters on light transmission, surface waviness and surface finish of optical lenses using Taguchi method. Form their research, they found that the most significant process affecting surface waviness was the melt temperature, followed by mold temperature, injection pressure and packing pressure. They found that the process parameter had little effect on light transmission and surface finish.

Zhil'tsova et al. (2009) studied the effects of processing conditions like filling rate, packing pressure, packing time and hot nozzle temperature of the mold on the dimensional stability of injection molded HDPE acetabular cups for the total hip replacement implants. Information regarding cycle time duration was obtained using MoldFlow analysis. From their research, they found that the packing pressure was the most significant factor affecting the part dimensions and weight. Injection speed rise had a negative effect on weight and dimensions. The influence of hot nozzle temperature and packing time were considered irrelevant for the range of process parameters under analysis.

Mirigul (2010) used Taguchi and ANOVA methods to study shrinkage of rectangular shaped polypropylene and polystyrene specimens. They found that the packing pressure and melt temperature were the most significant parameters.

Although the visual inspection is not possible but some researchers have been struggling to achieve this target in their study by using special instrument or tool like capacitive transducer, glass insert mold, thermocouple or pressure transducer for robustness monitoring of the quality of the final part. Yokoi et al. (2002) used an insert mold made of glass to measure the flow front position of the injection molding by using high speed camera. In practical, such insert was not advised to be applied in plastic injection molding since the strength of the material was not enough to withstand the injection pressure of the

molten plastic. However, they successfully captured the flow front behavior at flow front velocities up to 350mm/s and abnormal flow behavior like flow mark and formation of silver streaks.

Min (2003) derived a series of regression equations to optimize the injection molding processing parameters. In his study, the online parameters like pressure and temperature were measured using pressure transducer and thermocouple. By using regression analysis derived from response surface analysis for online process parameter, he found the optimum processing condition for plastic injection molding in their study.

Chen et al. (2004) developed a soft sensor measurement of the melt flow length. In their research, the soft sensor prediction was compared with online measured melt flow length using capacitive transducer. The experimental result shows that such a developed soft sensor can predict well flow length for filing of molds.

Michaeli & Starke (2005) used ultrasonic instrument to measure cavity pressure, melt flow profile and shrinkage of plastic injection molding. This approach produced promising result on monitoring the molding process but the cost spent on installation of high technology instrument like this was very high.

Wong et al. (2008) again used capacitive transducer to measure the filling time of injection molding. The sensor used had excellent ability of detecting start/end of mold filling and tracing the melt flow position in the cavity. The output can be further correlated to online part weight prediction and measurement of part solidification rate. According to Chen et al. (2004), it was neither economical nor practical for all mold to be fitted with such sensor since the installation was only possible on simple geometry cavity and the installation cost was very high.

Kurt et al. (2009) investigated the effects of cavity pressure and mold temperature on the quality of the final products by using pressure sensor and thermocouple. According to them, cavity pressure and mold temperature were the dominant factors determining the quality of the final product in injection molding.

In order to obtain more accurate prediction of the service performance and service life of polymer, Wang et al. (2009) modified the molding machine for online testing of PVT (pressure, volume and temperature) of polymer under different processing conditions. The modified machine allowed direct PVT data of polymer to be retrieved from an injection molding process. In their study, five polymers (ABS, PS, LDPE, PA 6 and PP) were measured and compared with those obtained by the confining fluid technique. They found that the PVT curve were consistent, which proves that the new online measurement was feasible. Instead of using sensor to monitor pressure, temperature and flow profile,

Dumitrescu et al. (2005) used near infrared spectroscopy to analyze the material used in injection molding, to identify color change due to applied temperature and pressure and also to monitor the moisture in materials.

The experimental result is reliable as compared with simulation result. However, to monitor the parameters (cavity pressure, flow front, cavity temperature and so on) involved during the molding process, expensive instrument must be used. For better quality product, the investment on these instruments is unavoidable. To save money and time, usually simulation is chosen for injection molding analysis but the reliability of the result must be verified with certain experimental values before it is used as an analysis tool.

2.4 Summary

From the above mentioned literature, it was found that the commercial injection molding software is a very powerful and is usually used to replicate the real processing condition of injection molding process. However, the unknown meshing procedure, convergence criteria, solving procedure and theory can lead a user to get wrong prediction and decision.

As a finite element analysis which is user defined software is recommended to be used for the simulation of the process instead of the commercial software in order to get better simulation result. Due to the complexity of the finite element analysis, it is seldom used to study thoroughly the entire complicated molding process. In addition, models available for this process are quite limited. This has post a problem to previous researcher to do injection molding simulation by using this software even they are good.

In general, simulation is a wonderful tool which allows one to predict the problems before manufacturing. Moreover, it helps designer to save time and cost in the design phase. Conversely, the reliability of the software must be known to avoid wrong decision on the manufacturing process that can lead to huge loss to a company. Consequently, a lot previous researchers prefer using experimental way to study the effect of processing parameter on the quality of injection molded product. However, the cost on conducting the experiment on injection molding is very high.

CHAPTER 3: METHODOLOGY

The purpose of the investigation in this study was to determine the influence of chosen important input parameters (injection speed, melt temperature, packing pressure, mold cooling time and packing time) on the output (shrinkage) by finite element analysis (ANSYS 12.1). The reliability of the numerical model proposed for this study was verified with experimental parameter and result. Two numerical models were proposed in this study and they were named as i) one-way interaction approach and ii) two-way interaction approach. Two mold cavities geometry were used in this study too and they were named as mold cavity-I and cavity-II. For mold cavity-I, only finite element analysis was used to analyze the plastic product shrinkage by using different injection packing pressure, injection mass flow rate and melt temperature. The packing pressure and melt temperature were varied at five different levels in one-way interaction approach simulation. On the other hand, the melt temperature and injection mass flow rate used in two-way interaction simulation were varied at 3 different levels. The validity of finite element analysis prediction was made by comparing with experimental result of a previous researcher (Chen and Gao, 2003). For mold cavity-II, an initial guess of the processing parameter used in the experimental study was simulated using one of the proposed numerical models, depending on which numerical model was better. Then the predicted flow speed, melt temperature during injection molding and part thickness were verified experimentally. In the experimental study, a special mold insert was made to clamp and guide the thermocouple into the mold cavity-II to measure plastic melt temperature during injection molding. The recorded melt temperature was used to estimate the plastic melt speed during injection molding as well. The ejected plastic part thickness was measured using a Mitutoyo micrometer. After the predicted processing parameter reliability was ensured, the

processing parameter obtained from the simulation was varied at three different levels according to an L_{27} orthogonal array (OA) of Taguchi design of experiment to further investigate the impact of the processing parameters on the physical plastic product shrinkage.

3.1 Part geometry and mold design

CAD engineering software, ProEngineer 4.0 was used to design the plastic parts and mold cavity.

The mold cavity-I was not created for experimental study and the control volume involved in the analysis for this mold cavity is presented in Figures 3.1 and 3.2. As shown in these figures, a rectangular plastic part with dimension of 150 $mm \times 100\ mm \times 2\ mm$ was designed as the mold cavity and a fan gate was used to guide the plastic melt into the cavity. Figure 3.1 shows the thickness and temperature measurement locations for one-way interaction approach. Figure 3.2 shows the thickness and temperature measurement locations for two-way interaction approach simulation.

The control volume involved in injection molding for mold cavity-II is presented in Figure 3.3. The product was a thin rectangular plastic part with dimension of 67 $mm \times 40\ mm \times 4\ mm$ as illustrated in Figure A-1 of APPENDIX A. To replicate the real injection molding situation, the control volume of plastic melt in the barrel was taken into account. During plastic injection, the screw pushed the plastic melts in the barrel to move plastic out of the nozzle into mold cavity. The injection speed on the injection molding machine was a control on how fast the screw pushing the plastic melts in the barrel. Hence, the injection force applied was important to be taken into account. As a result, the control volume for barrel was incorporated in this analysis.

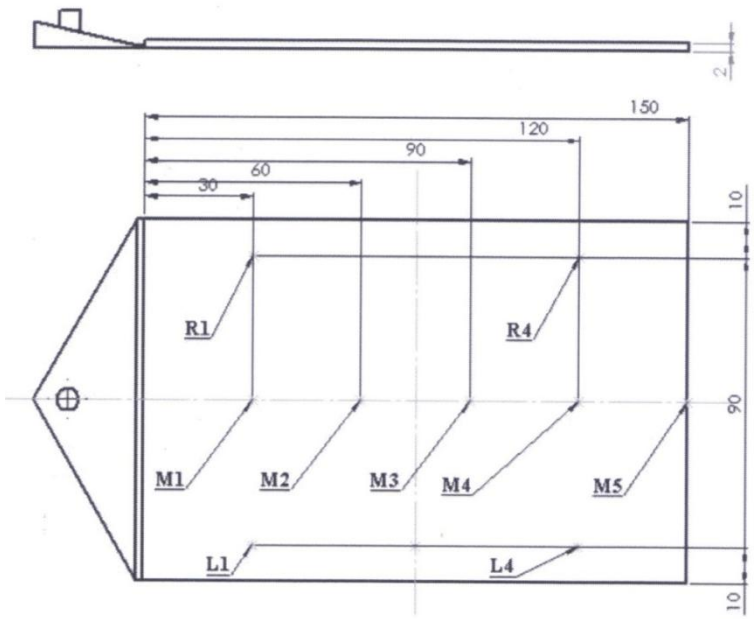

Figure 3.1: Part design and measurement locations for one-way interaction approach

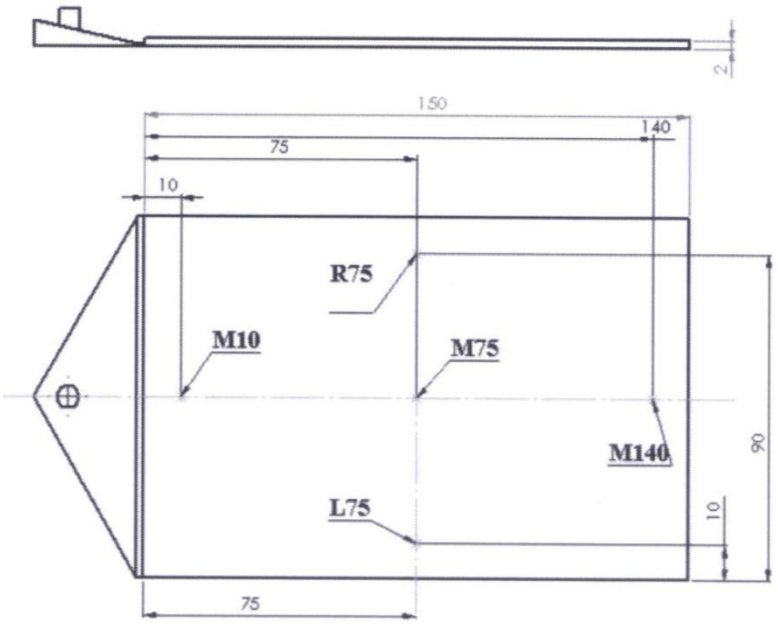

Figure 3.2: Part design and measurement locations for injection molding modeling using two-way interaction approach

For mold cavity-II, all of the molding experiments were conducted using a two cavities test mold. The mold components that assembled into this cavity shape included plate *A* and plate *B* are illustrated in Figures A-2 and A-4 of APPENDIX A.

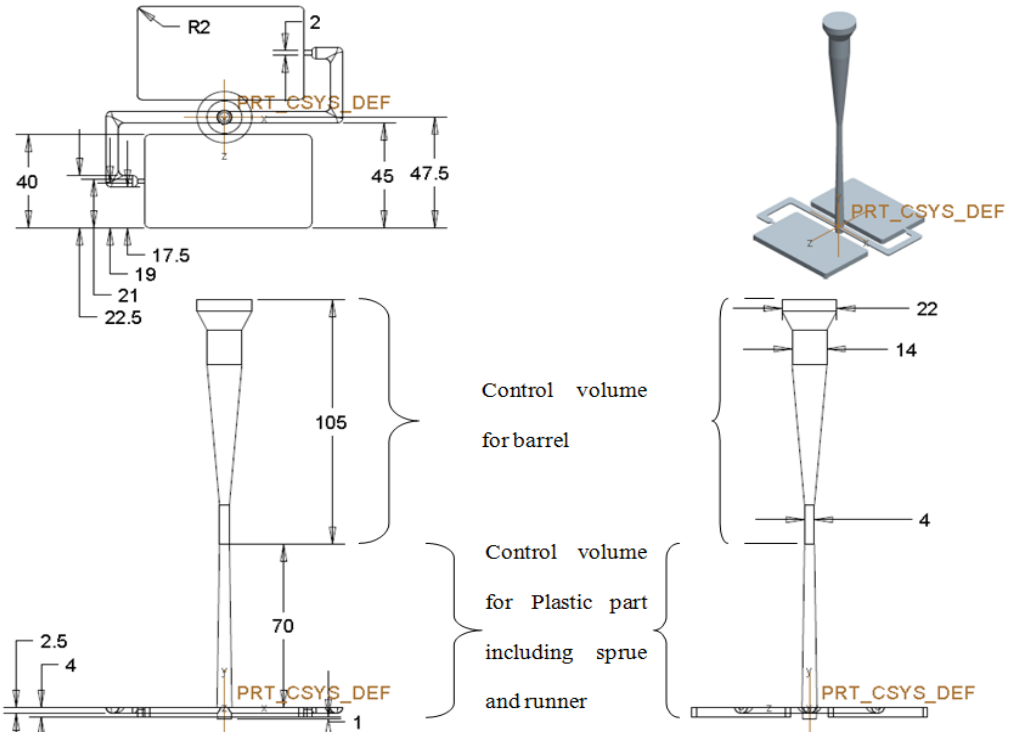

Figure 3.3: The control volume involved in simulation for mold cavity-II

Runner, air vent and ejector pin holes were made on plate *A* as illustrated in Figure A-2 of APPENDIX A. Cold half round runner system of radius 3 *mm*, a sprue diameter of diameter 10 *mm* and two half round pin gate with radius of 1.5 *mm* were machined on this plate surface. Plate *A* used for plastic injection molding was installed on moving side of injection molding machine. An insert was made on plate *A* as illustrated in Figure A-2 of APPENDIX A. The main function of the insert made was to clamp and hold the thermocouple on desire position for thermal analysis. The structure of the mold insert is presented in Figure A-3 of APPENDIX A and it was made of two parts (insert 1 and insert 2). A tiny hole was machined on this mold insert for the thermocouple probe used during

thermal analysis. To clamp and hold the thermocouple on fixed position, two screw holes were machined on insert 1 and 2. Once the desired position of the thermocouple probe was located, the insert 1 and 2 were clamped together by using screw to hold the thermocouple on fixed position for injection molding. Plate *B* was installed on stationary side of injection molding machine. On plate *B*, a hole on the center of the plate as shown in Figure A-4 of APPENDIX A was made to guide the plastic melt from sprue into the mold cavity. Injection started here when the plastic melt started to flow from inside of the barrel through the sprue and into the cavity.

3.2 Materials and their properties

Two types of plastic materials were used for plastic injection molding. They were high density polyethylene (HDPE) and Acrylonitrile-Butadiene-Styrene (ABS). Marlex HDPE 9500 was injection molded in mold cavity-I and Toyolac 250 ABS was injection molded in mold cavity-II. The information of these two materials properties was obtained from MoldFlow plastic insight 6.1 material databases (MoldFlow, 2011).

3.2.1 Non Newtonian behavior

Both plastic materials were modeled as non Newtonian fluid in ANSYS 12.1. To describe the non Newtonian flow behavior, a Cross WLF model was used. The governing mathematical equation for this model is as follows (MoldFlow, 2011):

$$\eta = \frac{\eta_0}{1+\left(\frac{\eta_0 \dot{\gamma}}{\tau^*}\right)^{1-n}} \tag{3.1}$$

where n is the power law index, τ^* is the stress level of the asymptotic transition region between the power-law and Newtonian fluids, $\dot{\gamma}$ is shear rate, η is dynamic viscosity and it

is a function of shear rate, temperature and pressure, η_0 is the zero shear rate viscosity represented by the WLF functional form as follows:

$$\eta_0 = D_1 . exp\left[\frac{-A1(T-T^*)}{A2+ D_3P +(T-T^*)}\right] \quad (3.2)$$

$$T^*(P) = D_2 + D_3P \quad (3.3)$$

The model constants and information related to this model is presented in Table 3.1.

Table 3.1: Cross WLF model constants (MoldFlow, 2011)

Symbol	Unit	Marlex HDPE 9500	Toyolac 250 ABS
n (Power law index)		0.1	0.3364
τ^* (Stress level of the asymptotic transition region between the power law and Newtonian fluids)	Pa	1.693×10^5	5.0777×10^4
D_1 (Model coefficient)	$Pa\ s$	1.518×10^{19}	1.44×10^{14}
D_2 (Model coefficient)	℃	153.15	100.00
D_3 (Model coefficient)	℃/Pa	0	0
A_1 (Model coefficient)		43.37	33.891
A_2 (A function of pressure)	℃	51.6	51.6

3.2.2 Melt compressibility

To include the effect of melt compressibility, the PVT (pressure, specific volume and temperature) equation was used. The PVT relation considered the specific volume of a material as a function of temperature, pressure, and cooling rate. To illustrate this melt compressibility behavior, the PVT diagrams for both Marlex HDPE 9500 and TOYOLAC 250 ABS are plotted as shown in Figures 3.4 and 3.5.

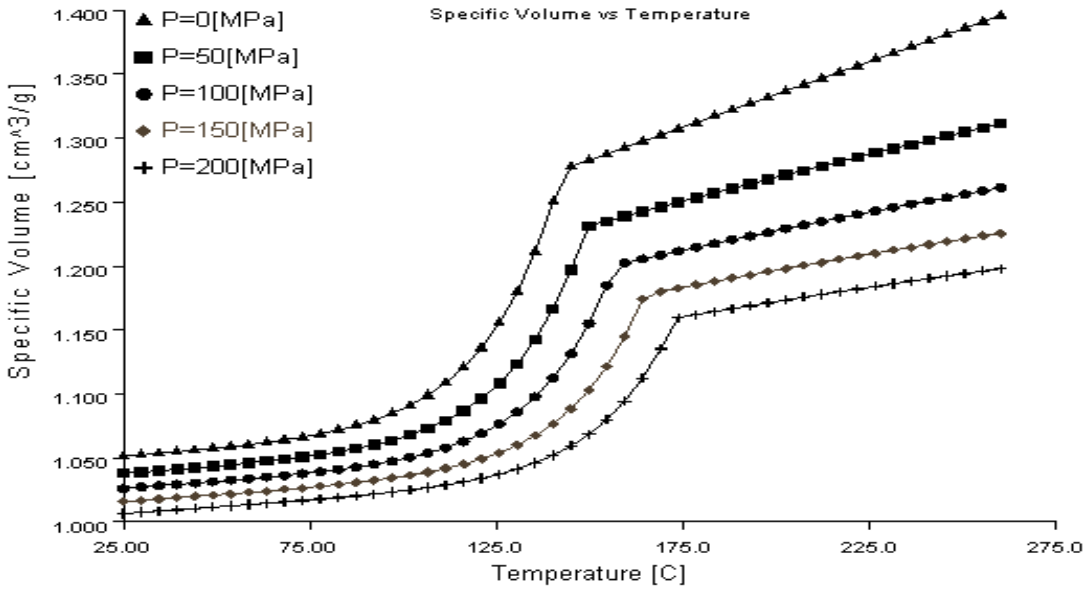

Figure 3.4: PVT behavior of Marlex HDPE 9500 (MoldFlow, 2011)

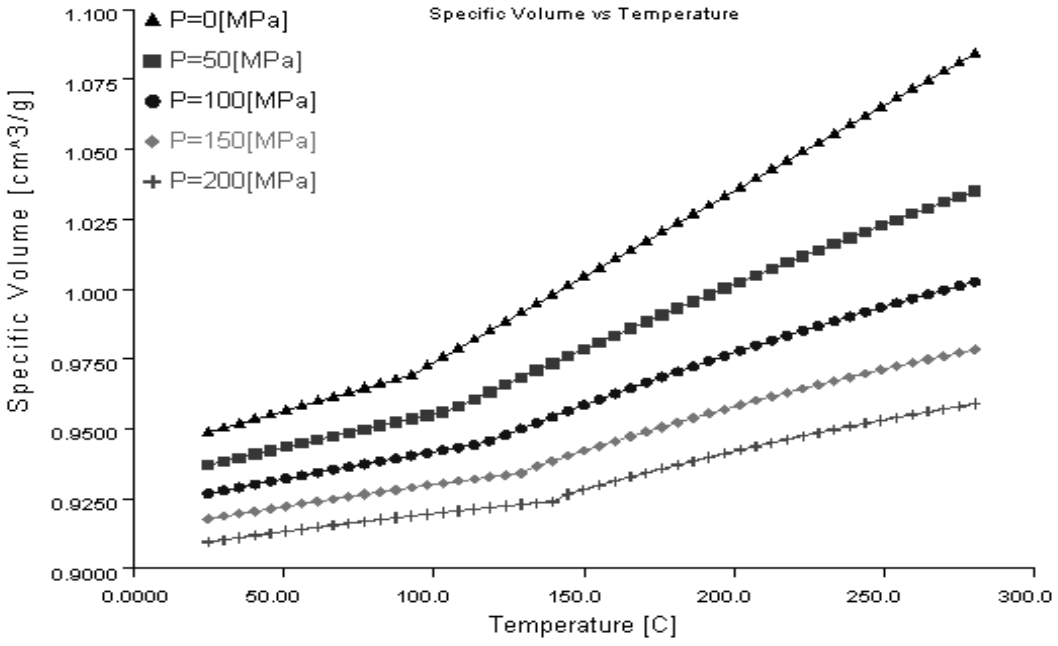

Figure 3.5: PVT behavior of TOYOLAC ABS 250 (MoldFlow, 2011)

The governing equation for PVT Tait equation is as follows (MoldFlow, 2011):

$$v(T,P) = v_0(T).\left[1 - 0.0894ln(1 + \frac{P}{B(T)})\right] + v_t(T,P) \quad (3.4)$$

where T is temperature, P is pressure, $v(T,P)$ is the specific volume at temperature T and pressure P. $v_0(T)$ is the specific volume at zero gauge pressure. $B\ (T)$ is used to take into account the pressure sensitivity of the material. The specific volume at zero gauge pressure, $v_0(T)$ and pressure sensitivity, $B\ (T)$ of this model are defined as follows:

At upper temperature region($T > Ttrans$):

$$T > T_{trans} \begin{cases} v_0 = b_{1m} + b_{2m}.(T - b_5) \\ B(T) = b_{3m}.\exp[-b_{4m}.(T - b_5)] \end{cases} \quad (3.5)$$

At lower temperature region($T < Ttrans$):

$$T < T_{trans} \begin{cases} v_0 = b_{1s} + b_{2s}.(T - b_5) \\ B(T) = b_{3s}.\exp[-b_{4s}.(T - b_5)] \end{cases} \quad (3.6)$$

The dependence of glass transition temperature, T_{trans} on pressure can be described by as follows:

$$T_{trans}\,(P) = b_5 + b_6.P \quad (3.7)$$

In this PVT equation, b_{1m} , b_{2m} , b_{3m} , b_{4m} , b_{1s} , b_{2s} , b_{3s} , b_{4s} , b_5 and b_6 are data-fitted coefficients. The data fitted coefficients associated with this equation are presented in Table 3.2. The information of these two materials, both Marlex HDPE 9599 and TOYOLAC 250 ABS were retrieved from the MoldFLow material database.

Table 3.2: Data fitted constant for PVT Tait equation as obtained from MoldFlow database (MoldFlow, 2011)

Symbol	Unit	Marlex HDPE 9500	Toyolac 250 ABS
$b_{1,m}$	m^3/kg	0.001274	0.000969
$b_{2,m}$	$m^3/kg\,K$	1.026×10^{-6}	6.139×10^{-7}
$b_{3,m}$	Pa	9.263×10^{7}	2.03208×10^{8}
$b_{4,m}$	K^{-1}	0.004941	0.005269
$b_{1,s}$	m^3/kg	0.001075	0.000969
$b_{2,s}$	$m^3/kg\,K$	2.077×10^{-7}	3.021×10^{-7}
$b_{3,s}$	Pa	3.324×10^{8}	3.54252×10^{8}
$b_{4,s}$	K^{-1}	2.46×10^{-6}	0.004331
b_5	K	414.5	366.03
b_6	K/Pa	1.543×10^{-7}	2.55×10^{-7}

The thermal data and mechanical properties of Marlex HDPE 9500 and TOYOLAC 250 ABS are presented in Table 3.3.

Table 3.3: Thermal and mechanical data of the plastic materials used in injection molding (MoldFlow, 2011)

Material data	Symbol	Unit	Marlex HDPE 9500	Toyolac 250 ABS
Thermal data				
Specific heat	C_P	$J/kg\,°C$	3307.4	2400
Glass transition temperature	T_g	$°C$	153.15	100.00
Thermal expansion coefficient	α	$°C^{-1}$	2.3×10^{-4}	7×10^{-5}
Thermal conductivity	k	$W/m\,°C$	0.3098	0.18
Reference temperature	T_{ref}	$°C$	240	240
Mechanical properties				
Young's modulus	E	GPa	1.2755	2.24
Poisson ratio	ν		0.423	0.392
Tensile yield strength		MPa	30	49
Tensile ultimate strength		Mpa	37	53

The information on the thermal data and mechanical properties were retrieved from the MoldFlow material database too. Thermal data like specific heat, glass transition

temperature, thermal expansion coefficient, thermal conductivity and reference temperature were used in transient thermal analysis to estimate heat transfer and its effect on phase transition and degree of dimensional change with temperature. On the other hand, mechanical properties like Young's modulus, Poisson ratio, tensile yield strength and tensile ultimate strength were used to calculate the dimensional variation of the plastic according to the degree of dimensional change obtained from transient thermal analysis.

3.3 Injection molding simulation by using finite element analysis

For mold cavity-I, two finite element models were proposed to study the effect of processing parameters on mold filling, pressure and temperature distribution in the mold cavity during injection molding and part shrinkage. These models were named as one-way interaction approach and two-way interaction approach. They were described in the following sections. For mold cavity-II, one of the proposed numerical models was chosen to study the shrinkage problem depending on which numerical model was better.

3.3.1 One-way interaction approach

The entire one-way interaction model is presented in Figure 3.6. Initially, a 3D part file was imported into ANSYS workbench, discretized and generated into mesh. The mesh generated was imported into ANSYS analysis tools to study the plastic injection molding process. As shown in this figure, three main CAE analysis tools were used to simulate this process. The analysis tools involved were CFD, transient thermal analysis and static structural analysis. The entire injection molding process was divided into three parts (mold filling, mold cooling and shrinkage analysis). CFD was used for mold filling problem, mold cooling process of the plastic was analyzed by using transient thermal analysis and finally static structural analysis was used to compute the thermal stress and shrinkage of the plastic

part. ANSYS multiphysic on the other hand, as a post processing tool was used to calculate the mesh deformation of the plastic part for shrinkage analysis.

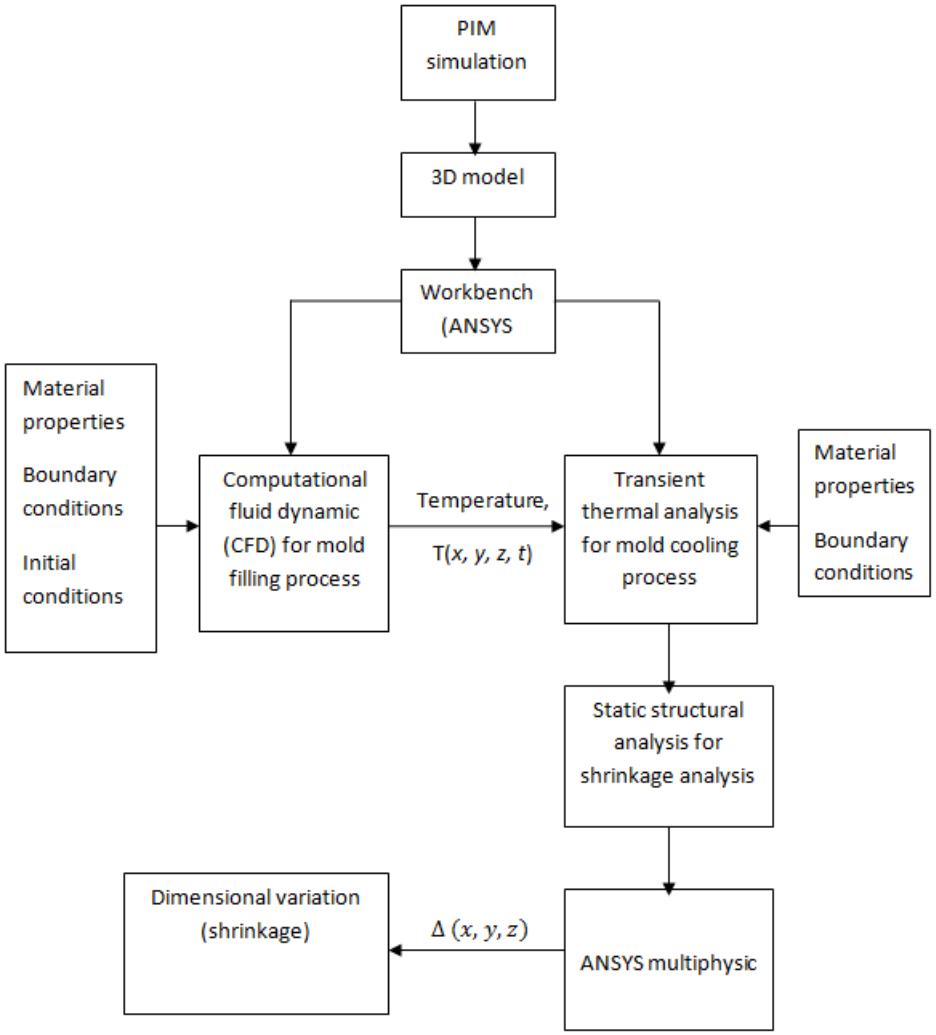

Figure 3.6: One-way interaction approach to analyze shrinkage of plastic part

3.3.1.1 Mold filling and post mold filling

In the first part, the mold filling and post mold filling process of injection molding was modeled as a computational fluid dynamic problem. Mold cavity-I and mold cavity-II meshes used in this study are presented in Figures 3.7 and 3.8. Both meshes were generated using CFD meshing method.

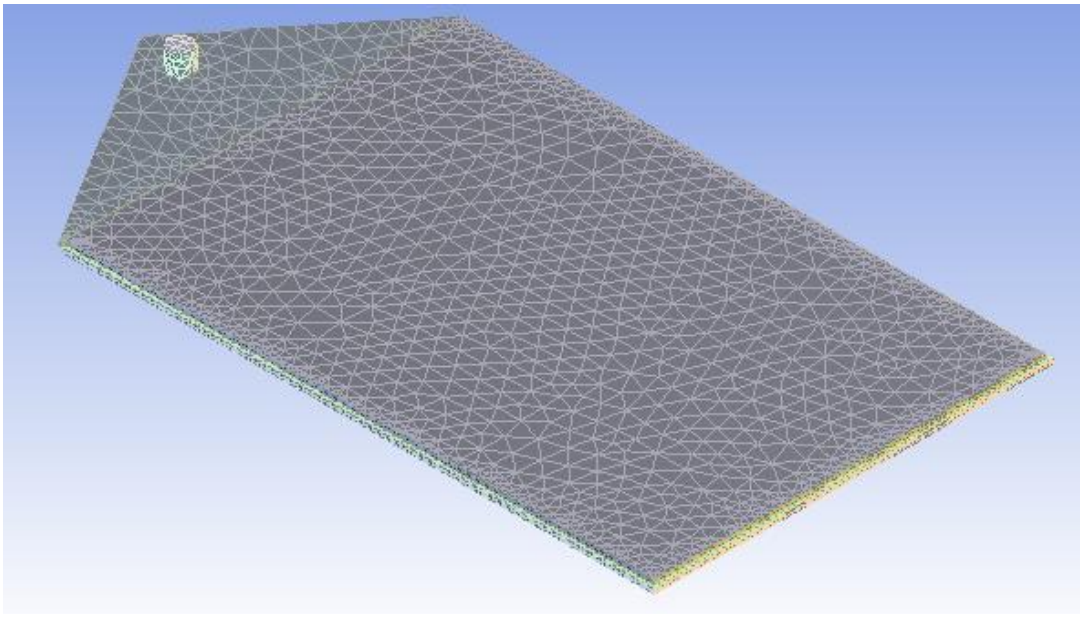

Figure 3.7: The CFD mesh generated for mold cavity-I

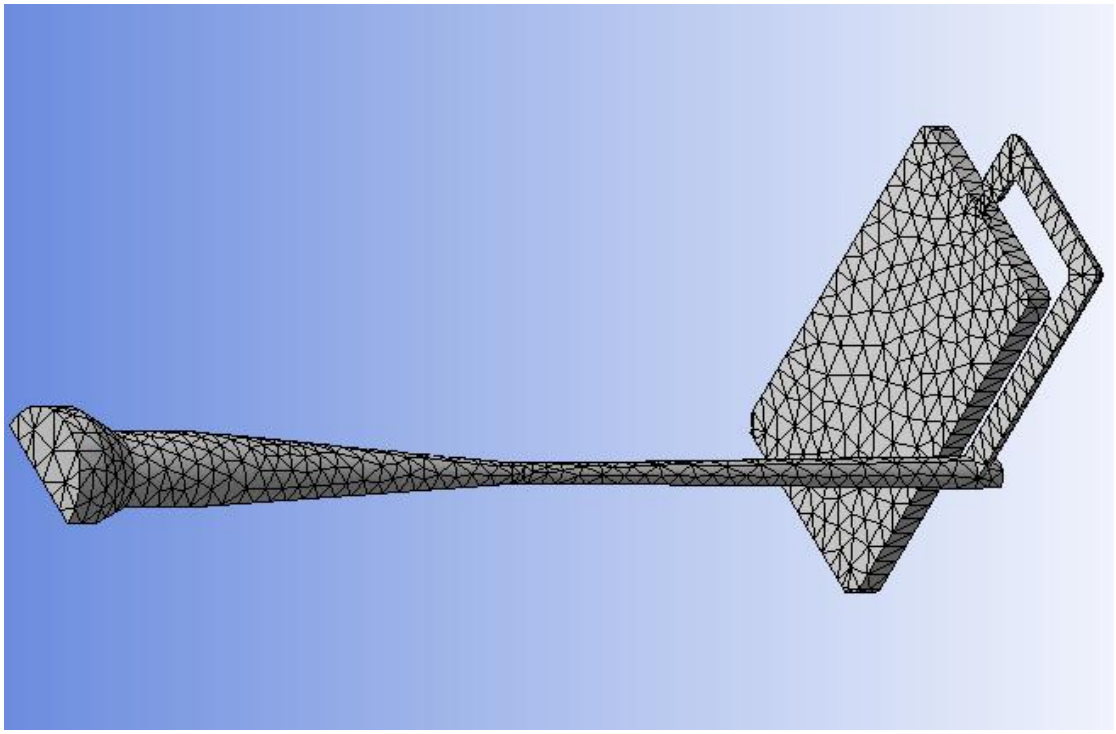

Figure 3.8: The CFD mesh generated for half portion of mold cavity-II

The governing fluid flow equations for the mold filling process were continuity equation, conservation of linear momentum equation (Cengal & Cimbala, 2006) and

thermal energy equation (Kenneth et al., 2001). The governing equations were solved together with rheological characteristic of the material selected. The conservation of mass or continuity equation is presented in Equation 3.8. Equation 3.9 shows the continuity equation in Cartesian coordinates (Cengal & Cimbala, 2006).

$$\frac{\partial \rho}{\partial t} + \vec{\nabla}.\left(\rho \vec{V}\right) = 0 \tag{3.8}$$

where,

$$\vec{\nabla}.\left(\rho \vec{V}\right) = \frac{\partial (\rho u)}{\partial x} + \frac{\partial (\rho v)}{\partial y} + \frac{\partial (\rho w)}{\partial z} \tag{3.9}$$

Equation 3.8 was valid for incompressible and compressible flows. The conservation of linear momentum equation or also known as Cauchy's equation was presented as follows:

$$\frac{d}{dt}\left(\rho \vec{V}\right) + \vec{\nabla}.\left(\rho \vec{V} \vec{V}\right) = \rho \vec{g} + \vec{\nabla}.\sigma_{ij} \tag{3.10}$$

where σ_{ij} is the stress tensor, $\vec{g}$ is the gravitational acceleration and ρ is the density. Equation 3.10 hold for any control volume regardless of its size and shape and it is valid for compressible as well as incompressible flow.

The thermal energy equation was used to take into account the viscous dissipation of the polymer melt. The thermal energy equation was (Kenneth et al., 2001):

$$\rho \frac{De}{Dt} + P\nabla.\vec{V} + \nabla.q_r - \dot{Q} = \frac{\partial}{\partial x}\left(k\frac{\partial T}{\partial x}\right) + \frac{\partial}{\partial y}\left(k\frac{\partial T}{\partial y}\right) + \frac{\partial}{\partial z}\left(k\frac{\partial T}{\partial z}\right) + \eta \Phi(x, y, z) \tag{3.11}$$

where e is internal energy per unit mass, k is thermal conductivity, q_r is radiation heat flux vector, $\dot{Q}$ is internal heat generation rate per unit volume and Φ is the viscous dissipation and η is dynamic viscosity. A multiphase approach was adopted for the mold filling process

to take into account of the air and polymer melts as the two phases involved in the process. After the multiphase approach was activated, the polymer melt pushed the air out of the cavity during injection molding simulation. For locating the flow front at every time step, volume of fluid method was used.

3.3.1.2 Transient Thermal Analysis

In the second part, the cooling process of the plastic melt was considered in two stages, the cooling in mold cavity and the cooling at room temperature after the part was ejected. Mold cavity-I and mold cavity-II meshes used in this analysis are presented in Figures 3.9 and 3.10.

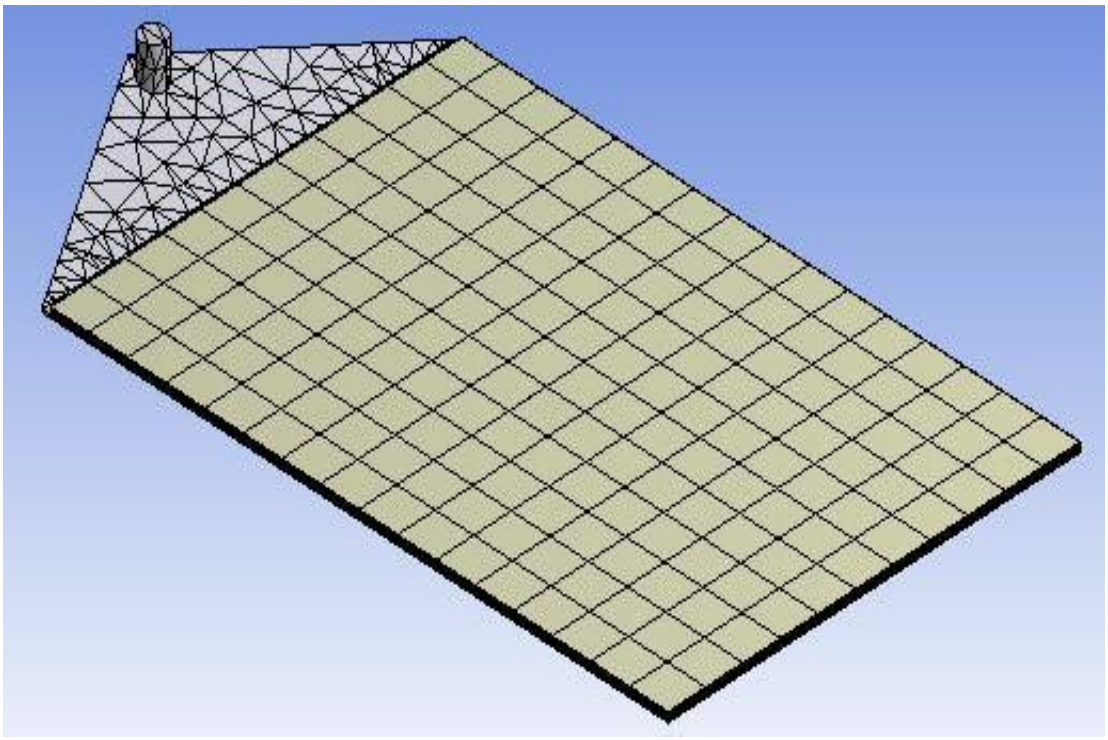

Figure 3.9: The mechanical mesh generated for transient thermal analysis and structural analysis for mold cavity-I

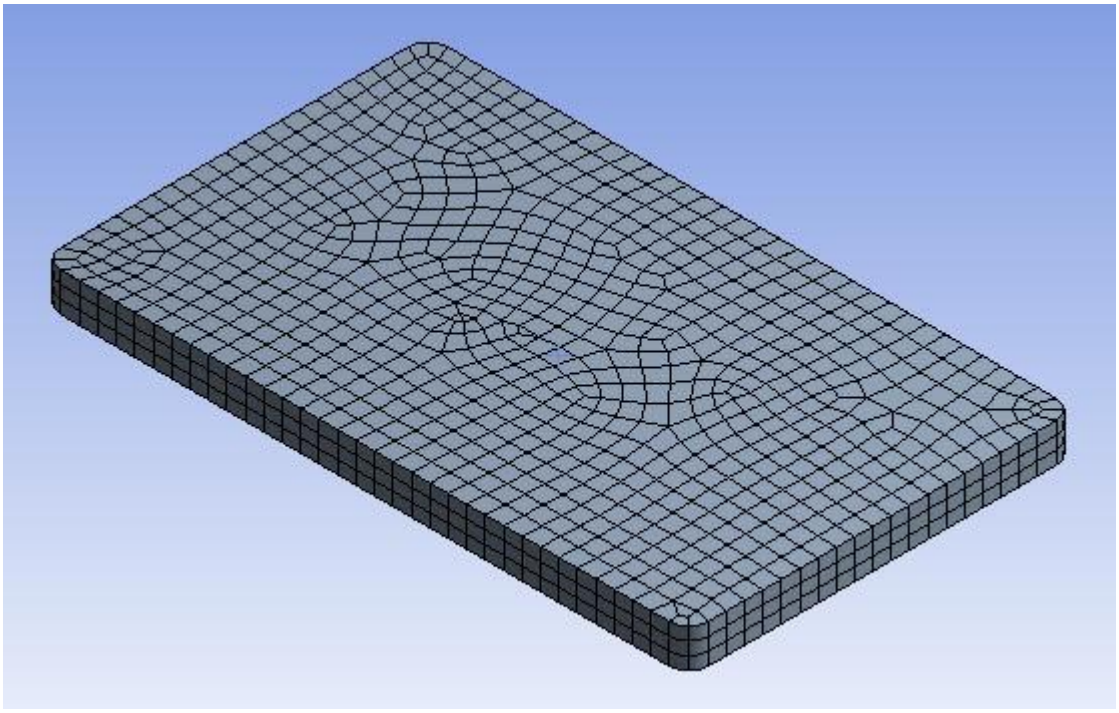

Figure 3.10: The mechanical mesh used for transient thermal analysis and structural analysis for mold cavity-II

Both of these meshes were generated using mechanical meshing method. Moreover, the governing heat transfer equation (Huang & Usmani, 1994) for transient thermal analysis was given as follows:

$$\rho c\left(\frac{\partial T}{\partial t}+\ u\frac{\partial T}{\partial x}+\ v\frac{\partial T}{\partial y}+\ w\frac{\partial T}{\partial z}\right)=\ \nabla.k\nabla T+Q \qquad (3.12)$$

where c is specific heat in this equation.

3.3.1.3 Static Structural Analysis

In the third part, the dimensional change of the plastic part due to thermally induced stress and temperature change was analyzed by using static structural analysis. The meshes used in this analysis are presented in Figures 3.9 and 3.10. The polymer shrunk

during cooling and the shrinkage was measured as nodal displacement for each element in the model.

3.3.1.4 Constitutive equation of mesh displacement as a function of temperature

The two types of elements used for meshing are presented in Figures 3.11 (a) and (b). Only the general formulation of tetrahedral element on nodal displacement and temperature measurement was explained in this section. Further shrinkage measurement for both of these elements can be referred to ANSYS help content (ANSYS, 2006). The nodal displacement of tetrahedral element is presented in Equation 3.13 as follows.

$$u = C_{11} + C_{12}X + C_{13}Y + C_{14}Z$$

$$v = C_{21} + C_{22}X + C_{23}Y + C_{24}Z$$

$$w = C_{31} + C_{32}X + C_{33}Y + C_{34}Z \quad (3.13)$$

Considering the nodal displacement, the following conditions must be satisfied:

$$u = u_i \; at \; X = X_i, \; Y = Y_i, \; Z = Z_i$$

$$u = u_j \; at \; X = X_j, \; Y = Y_j, \; Z = Z_j$$

$$u = u_k \; at \; X = X_k, \; Y = Y_k, \; Z = Z_k$$

$$u = u_l \; at \; X = X_l, \; Y = Y_l, \; Z = Z_l \quad (3.14)$$

The lowercase letters; *i*, *j*, *k*, and *l* are any arbitrary nodal value associated with the *x* direction displacement. Same with other directional displacement, they must satisfy this requirement as well.

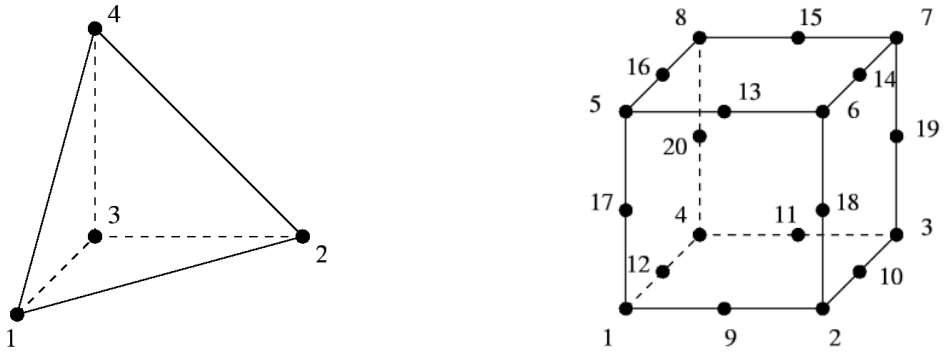

(a) (b)

Figure 3.11: (a) Four node tetrahedral element for the gate and (b) 20 nodes brick element for the part

Substitution of respective nodal values from Equation 3.14 into Equation 3.13 results in 12 equations and 12 unknowns. Solving for the unknown C coefficients and substituting the results back into Equation 3.13 and regrouping the parameters, we obtain:

$$u = S_1 u_i + S_2 u_j + S_3 u_k + S_4 u_l$$
$$v = S_1 v_i + S_2 v_j + S_3 v_k + S_4 v_l$$
$$w = S_1 w_i + S_2 w_j + S_3 w_k + S_4 w_l \quad (3.15)$$

The shape functions of four node tetrahedral element associated with the nodal displacement were:

$$S_1 = \frac{1}{6V}(a_i + b_i X + c_i Y + d_i Z)$$
$$S_2 = \frac{1}{6V}(a_j + b_j X + c_j Y + d_j Z)$$
$$S_3 = \frac{1}{6V}(a_k + b_k X + c_k Y + d_k Z)$$
$$S_4 = \frac{1}{6V}(a_l + b_l X + c_l Y + d_l Z) \quad (3.16)$$

where V, the volume of the tetrahedral element was computed from

$$6V = det\begin{vmatrix} 1 & X_i & Y_i & Z_i \\ 1 & X_j & Y_j & Z_j \\ 1 & X_k & Y_k & Z_k \\ 1 & X_l & Y_l & Z_l \end{vmatrix} \tag{3.17}$$

The a_i, b_i, c_i, d_i,…., and d_l terms were determined as follows:

$$a_i = det\begin{vmatrix} X_j & Y_j & Z_j \\ X_k & Y_k & Z_k \\ X_l & Y_l & Z_l \end{vmatrix} \tag{3.18}$$

The other terms can be determined by using similar determinants by rotating through the *i, j, k,* and *l* subscripts using the right hand rule. It was important to note that for thermal problems; only a single degree of freedom was associated with each node of the four node tetrahedral element. Hence, the variation of temperature over a four node tetrahedral element was expressed by:

$$T = T_i S_1 + T_j S_2 + T_k S_3 + T_l S_4 \tag{3.19}$$

The nodal displacement, temperature and volume for each element were obtained by solving the equations associated with each element together with the material model assigned to each element. The material model used was described in Section 3.2.

To predict plastic part shrinkage by using formulation as discussed previously, the relationship between stress and strain must be derived first. The stress and strain relationship (ANSYS, 2006) was given by as follows:

$$\{\varepsilon\} = \{\varepsilon^{th}\} + [D]^{-1}\{\sigma\} \tag{3.20}$$

where ε^{th} was thermal strain and it was defined as follows:

$$\varepsilon^{th} = \alpha^{se}(T - T_{ref}) \tag{3.21}$$

where α^{se} was defined as the temperature-dependent secant coefficient of thermal expansion and it was computed as follows:

$$\alpha^{se} = \frac{\varepsilon^{ith}}{T - T_{ref}} \tag{3.22}$$

Equation 3.22 assumes that when $T = T_{ref}$, $\varepsilon^{th} = 0$. If this was not the case, the ε^{th} was shifted automatically by a constant value so that it was true. α^{se} at T_{ref} was calculated based on the slopes from the adjacent user-defined data points. Hence, if the slopes of ε^{ith} above and below T_{ref} were not identical, a step change in α^{se} at T_{ref} will be computed. ε^{th} was related to α by:

$$\varepsilon^{ith} = \int_{T_{ref}}^{T} \alpha dT \tag{3.23}$$

where α is thermal expansion coefficient and its value is listed in Table 3.3.

Combining Equation 3.22 with Equation 3.21:

$$\alpha^{se} = \frac{\int_{T_{ref}}^{T} \alpha dT}{T - T_{ref}} \tag{3.24}$$

The flexibility or compliance matrix $[D]^{-1}$ was defined as:

$$\begin{bmatrix} 1/E_x & -\nu_{xy}/E_x & -\nu_{xz}/E_x & 0 & 0 & 0 \\ -\nu_{yx}/E_y & 1/E_y & -\nu_{yz}/E_y & 0 & 0 & 0 \\ -\nu_{zx}/E_z & -\nu_{zy}/E_z & 1/E_z & 0 & 0 & 0 \\ 0 & 0 & 0 & 1/G_{xy} & 0 & 0 \\ 0 & 0 & 0 & 0 & 1/G_{yz} & 0 \\ 0 & 0 & 0 & 0 & 0 & 1/G_{xz} \end{bmatrix} \tag{3.25}$$

By expanding Equations 3.20 - 3.22, the principal and shear strain can be written as follows:

$$\varepsilon_x = \alpha_x^{se}\Delta T + \frac{\sigma_x}{E_x} - \frac{v_{xy}\sigma_y}{E_x} - \frac{v_{xz}\sigma_z}{E_x} \quad (3.26)$$

$$\varepsilon_y = \alpha_y^{se}\Delta T + \frac{\sigma_y}{E_y} - \frac{v_{xy}\sigma_x}{E_x} - \frac{v_{yz}\sigma_z}{E_y} \quad (3.27)$$

$$\varepsilon_z = \alpha_z^{se}\Delta T + \frac{\sigma_z}{E_z} - \frac{v_{xz}\sigma_x}{E_x} - \frac{v_{yz}\sigma_y}{E_y} \quad (3.28)$$

and,

$$\varepsilon_{xy} = \frac{\sigma_{xy}}{G_{xy}}; \varepsilon_{yz} = \frac{\sigma_{yz}}{G_{yz}}; \varepsilon_{xz} = \frac{\sigma_{xz}}{G_{xz}} \quad (3.29)$$

where α_x^{se}, α_y^{se} and α_z^{se} were the secant coefficient of thermal expansion in the *x*, *y* and *z* directions. ε_x, ε_y and ε_z were the principal strains in the x, y and z directions. ε_{xy}, ε_{yz} and ε_{xz} were respectively *xy*, *yz* and *xz* planes shear stress.

The principle of virtual work (ANSYS, 2006) had stated that a virtual (very small) change of the internal strain energy must be offset by an identical change in external work due to the applied loads or

$$\delta U = \delta W \quad (3.30)$$

where U was the strain energy (internal work) and W was the external work

Two types of virtual energy were to be taken into account. The first type was virtual strain energy, δU_1 and was given as

$$\delta U_1 = \{\delta u\}^T \int_{vol}[B]^T[D][B]d(vol)\{u\} - \{\delta u\}^T \int_{vol}[B]^T[D]\{\varepsilon^{th}\}d(vol) \quad (3.31)$$

where in this equation, the strain was related to the nodal displacements by:

$$\{\varepsilon\} = [B]\{u\} \tag{3.32}$$

Another form of virtual strain energy was when a surface moves against a distributed resistance, as in a foundation stiffness. This was written as:

$$\delta U_2 = \{\delta u\}^T \int_{area_f} [N_n]^T [N_n] d(area_f) \{u\} \tag{3.33}$$

The displacements within the element were related to the nodal displacements by:

$$\{w_n\} = [N_n]\{u\} \tag{3.34}$$

Next, the external work will be considered. Three types of external work were considered. The first type was the inertial effects and this effect was represented by:

$$\delta W_1 = -\{\delta u\}^T \rho \int_{vol} [N]^T [N] d(vol) \frac{\delta^2}{\delta t^2} \{u\} \tag{3.35}$$

The second external work was pressure force and its formulation was written as follows. Pressure was applied on the outside surface of an element.

$$\delta W_2 = \{\delta u\}^T \int_{area_p} [N_n]\{P\} d(area_P) \tag{3.36}$$

The last external work in static structural analysis was nodal force. Nodal forces applied to the element can be accounted for by:

$$\delta W_3 = \{\delta u\}^T \{F_e^{nd}\} \tag{3.37}$$

By combining Equations 3.30, 3.31, 3.33, 3.35, 3.36 and 3.37, the equilibrium equation of the material model assigned to an element was represented as follows:

$$\left([K_e] + \left[K_e^f\right]\right)\{u\} - \{F_e^{th}\} = [M_e]\{\ddot{u}\} + \left\{F_e^{pr}\right\} + \{F_e^{nd}\} \tag{3.38}$$

where,

$$[K_e] = \int_{vol}[B]^T[D][B]d(vol)$$

$$\left[K_e^f\right] = K\int_{area_f}[N_n]^T[N_n]\,d(area_f)$$

$$\{F_e^{th}\} = \int_{vol}[B]^T[D]\{\varepsilon^{th}\}d(vol)$$

$$[M_e] = P\int_{vol}[N]^T[N]d(vol)$$

$$\{\ddot{u}\} = \frac{\delta^2}{\delta t^2}\{u\} \text{ and}$$

$$\left\{F_e^{pr}\right\} = \int_{area_p}[N_n]^T\{P\}d(area_P)$$

$[K_e]$ was the element stiffness matrix, $\left[K_e^f\right]$ was the element foundation stiffness matrix, $\{F_e^{th}\}$ was the element thermal load vector, $[M_e]$ was the element mass matrix, $\{\ddot{u}\}$ was the acceleration vector such as gravity effects and $\left\{F_e^{pr}\right\}$ was the element pressure vector. Depending on type of element, the deformation of the part was measured by solving the above equation (27) together with the type of the element selected.

3.3.1.5 Computational Domain & Boundary Conditions

The detail input and output for all the analysis tools used in one-way interaction approach model is presented in Figure 3.12. The entire injection molding cycle was divided into three parts to study the effect of processing conditions on part shrinkage as discussed previously. In mold filling and post mold filling, computational fluid dynamic method was used to study the filling time required for injection molding, pressure distribution and temperature distribution of the polymer melt. Temperature field at the end of post mold filling was imported into transient thermal analysis as initial condition to analyze the cooling process taking place for the plastic material. Heat flux and temperature change

were the output from transient thermal analysis. To determine the effect of temperature change on part shrinkage, the temperature change obtained from transient thermal analysis was imported into static structural analysis. The deformation or the dimensional change of the plastic part during cooling was calculated according to the material properties defined within the analysis.

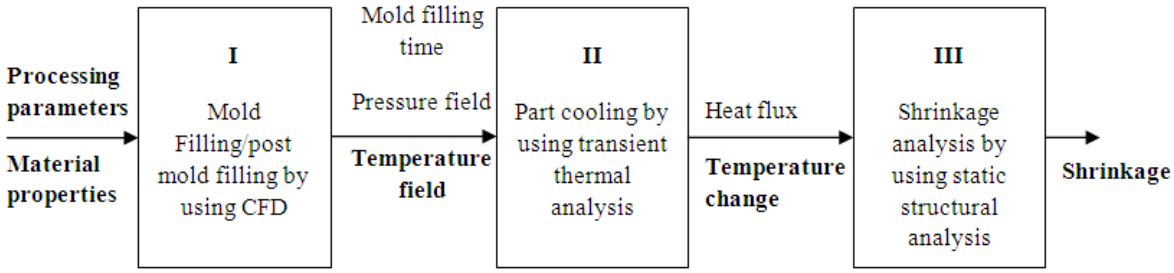

Figure 3.12: Simulation process flow chart

A homogeneous multiphase approach with the air as one phase and polymer melt as another phase was used to model the initial condition of the mold filling problem. Initially, it was assumed that the cavity was full with air and polymer melt phase was completely absent in the mold. The boundary conditions used for mold filling analysis were defined as follows:

On mold wall : $u = v = w = 0;\ T = T_{mold}$

At inlet : $T = T_{in}$

At outlet : $P_{outlet} = P_{atm};\ T = T_{room}$

where u, v and w were the x, y and z directional velocity vectors. The boundary condition on mold cavity wall surface was defined as no slip. The velocity vectors on the wall surface were zero and the mold temperature, T_{mold} was 50 ℃. At gate where the plastic melt was injected into the cavity, the melt temperature of the plastic melt and injection speed were

defined within the computational fluid domain. The post filling stage started once after mold filling. The packing pressure applied during post filling phase was defined at the gate region. Air vent was provided for the air in the cavity to escape in this model and it was defined as opening boundary condition where the air was allowed to enter and escape through this region. The opening pressure was $1\ atm$ and the room temperature, T_{mold} surrounding the air vent was 25 ℃.

After packing phase, the plastic melt was allowed to cool in mold cavity until it had enough strength to be ejected. The cooling process was still taking place after ejection and continues until the plastic part achieved equilibrium state at the room temperature. Transient thermal analysis was used to model this heat transfer problem. The initial condition and boundary conditions for this problem was defined as follows:

Initial condition : $T(x, y, z, 0) = T_0(x, y, z)$

The temperature field obtained from the mold filling analysis was used as initial condition, T_0. The heat exchange between plastic melt and mold material when the plastic melt was still in the mold and the heat exchange between plastic melt and surrounding air when the part was ejected were treated as boundary conditions. The convection boundary conditions were presented as follows:

Cooling in mold : $$-\boldsymbol{k}\frac{\boldsymbol{\partial T}}{\boldsymbol{\partial n}} = \boldsymbol{h}(T_{mold} - T_{melt}) \quad (3.39)$$

Cooling at room temperature : $$-\boldsymbol{k}\frac{\boldsymbol{\partial T}}{\boldsymbol{\partial n}} = \boldsymbol{h}(T_{room} - T_{melt}) \quad (3.40)$$

The temperature difference between the mold, T_{mold} and plastic melt, T_{melt} and the temperature difference between plastic melt, T_{melt} and room temperature, T_{room} were modeled as a function of temperature. $\boldsymbol{n}$ was the line normal to the plane of the surface

element and *h* was the heat transfer coefficient. The plastic in the mold cavity was allowed to cool until it had enough strength to be ejected. When the plastic was still in the mold cavity, the difference between mold temperature and plastic melt temperature was taken as the boundary condition. For cooling at room temperature, new boundary condition was applied. The temperature difference between the plastic temperature after ejection and room temperature was treated as the new boundary condition. The temperature change of the plastic melt due to the difference between the plastic melt temperature and mold temperature and room temperature during the whole injection cycle was simulated. The effect of pressure on temperature was not taken into account in this analysis.

For static structural analysis, the temperature change obtained from transient thermal analysis was used as input to calculate the part shrinkage. The reference temperature used in the shrinkage analysis was same with melt temperature. Reference temperature was defined as the temperature where zero strain occurs. No structural loads and supports were imposed on the plastic part in this analysis. The part was allowed to shrink freely during the cooling process. The plastic was assumed to be solid in static structural analysis and an elastic model was used to describe the mechanism of deformation of the plastic part. Pressure effect on shrinkage was not taken into account in shrinkage analysis but its effect on temperature distribution was considered in the shrinkage analysis.

3.3.2 Two-way interaction approach

The two-way interaction approach model used to analyze the part thickness variation due to plastic injection molding process is presented in Figure 3.13. This model was highly intelligent multi-physics (mechanical and fluid dynamic) architecture composed of two different regions and an interface for connecting these two regions. The fluid domain of the injected polymer as illustrated in Figure 3.14 was one of the regions and

finite volume method was adopted to solve the fluid dynamic problem. The second region comprised of two steel and two polymer layers representing the structural domain as shown in Figure 3.15 and finite element method was used to solve this mechanical problem.

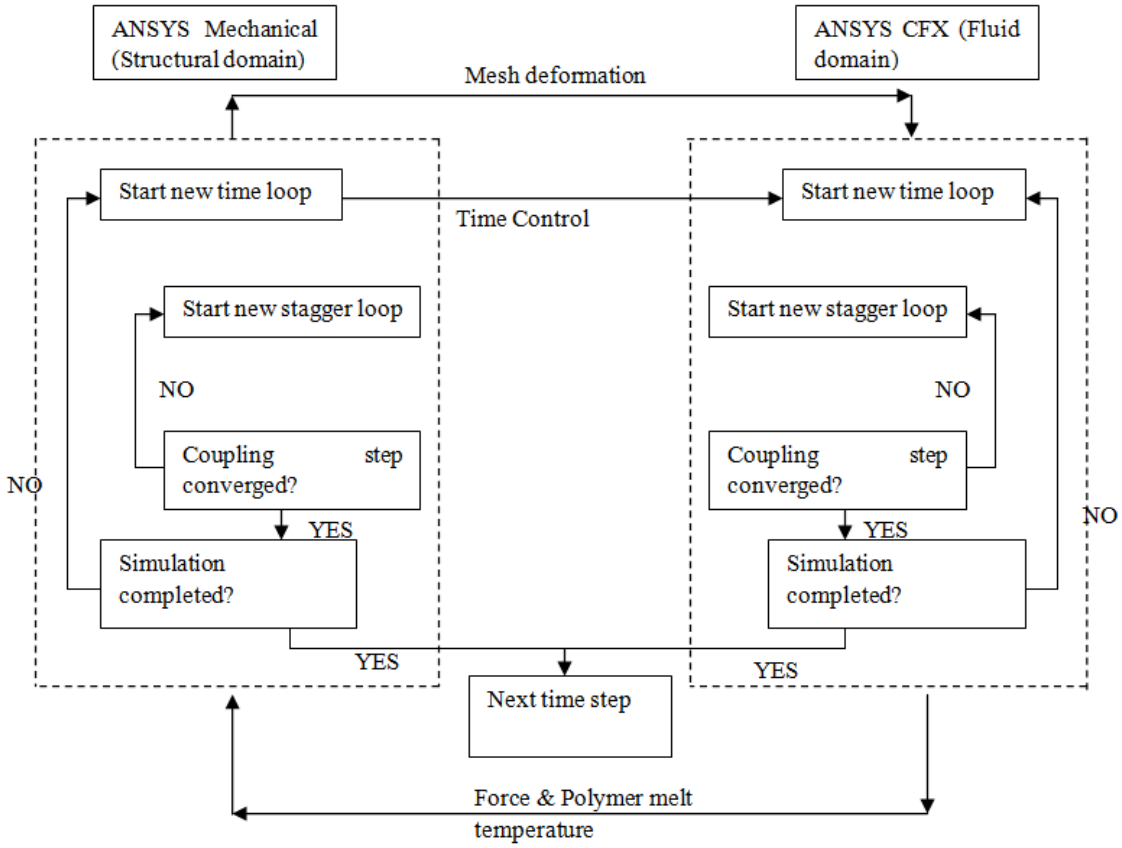

Figure 3.13: Injection molding simulation using two-way interaction approach

The steel layers were fixed throughout the simulation process and it acted as mold surface to prevent the injected polymer to deform outward. The polymer layers were fixed at their circumference throughout the simulation process but the region other than the fixed circumference was allowed to react according to injection molding parameters. The fluid solid interaction was established by means of an interface placed in between the fluid domain and structural domain. Data exchange via this interface: the force, pressure and temperature acting on the element as obtained from the fluid domain was transmitted to

structural domain and the dimensional variation in term of mesh deformation was transmitted back to fluid domain. Communication between these two machines was programmed via loops (time loop and stagger loop) defined by user within each time step until convergence of the load transfer between fields then simulation continued to the next time step until end to the injection molding cycle.

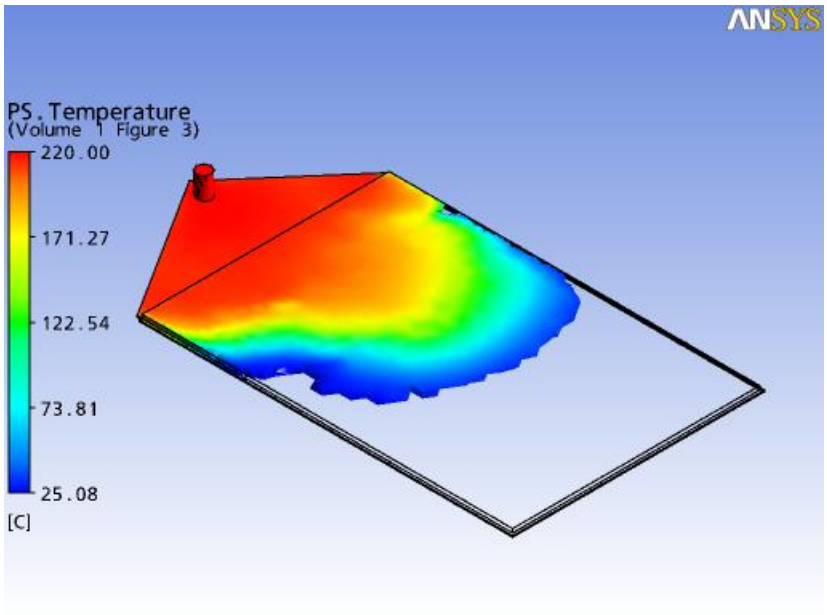

Figure 3.14: Control volume for fluid domain (air vent size is 0.5mm)

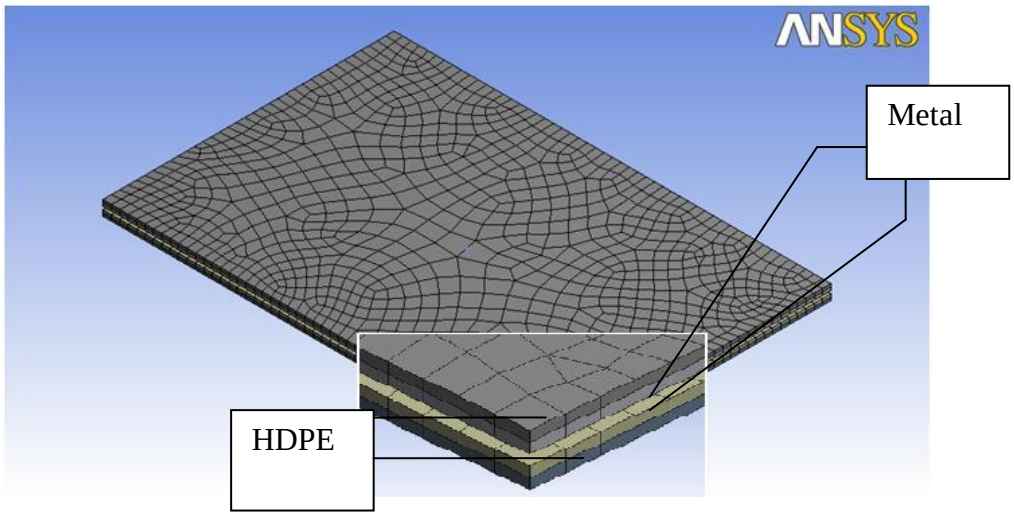

Figure 3.15: Structural domain

This simulation technique allowed robust communication between different physics simulation machines. This made it possible to accurately simulate the polymer behavior during injection molding and reproduce the deformation of the plastic part coupling with the material rheology, the PVT behavior and process rate sensitivity. Furthermore, the proposed model almost took into consideration every important effect (pressure, temperature and shear effect) on thickness variation as never done before by previous researcher and it was believed that this model can reliably predict the dimensional variation of the plastic part very well.

3.3.2.1 Fluid domain simulation

The plastic behavior in the fluid domain as depicted in Figure 3.14 during injection molding was solved using fluid dynamic theory (finite volume method). The CFD mesh as shown in Figure 3.7 was used in this study. The governing fluid flow equations for the injection molding process were continuity equation (Cengal and Cimbala, 2006), conservation of linear momentum equation (Cengal and Cimbala, 2006) and thermal energy equation (Kenneth et al., 2001) as described in Section 3.3.1.1.

Same boundary conditions as described in Section 3.3.1.5 were applied in this model. A homogeneous multiphase approach with air as one phase and polymer melt as another phase was used to model the initial condition of the mold filling problem. It was assumed that the cavity was full of air and polymer melt phase was completely absent in the mold cavity initially. Mold cavity wall was assumed as in no slip condition and the temperature on this surface was constant, 25 ℃. Melt temperature (T_{melt}), injection speed and packing pressure were defined at the inlet. Air vent was defined as a small opening for the mold cavity used in this study where air was allowed to enter and escape to the

surrounding room environment through this air vent region. The air vent temperature and pressure were defined as room temperature (T_{room}), 25 ℃ and room pressure, 1 *atm*.

3.3.2.2 Structural domain

As depicted in Figure 3.15, the structural domain in this analysis was made of two layers of metal surface and two layers of polymer surface. This figure also shows the mechanical mesh used for structural analysis. The metal surface acted as mold surface which constrains the polymer from deforming outward during injection molding. The polymer surface acted as the interface connecting fluid domain with structural domain. The dimensional variation due to processing parameter in structural domain was solved using finite element method. To achieve this objective, a linear elastic model was employed to calculate the element reaction (mesh displacement) according to temperature, pressure and shear stress. In this process, the mechanical solver computed the stress generated due to the processing parameter applied and the mesh displacement was calculated according to the stress level in each simulation time step. The governing equation involved in this analysis was described in Section 3.3.1.4.

A reference temperature was used in this analysis and it was same with the melt temperature used in injection molding. The plastic layers were assumed to be attached to the metal surfaces during injection and packing phase. No separation between the both layers was defined during these two injection phases. After packing phase, the interaction between these layers was defined as frictional where separation was allowed and the plastic layers was allowed to deformed according to shrinkage due to temperature, pressure and shear stress effect.

3.3.2.3 Load transfer through interface

Load transfer between structural domain and fluid domain was based on two layers of interface (polymer surfaces) inserted in between these two different physic domains. In this process, one field transmitted mesh based quantities to another field as illustrated in Figure 3.13. Under the two-way interaction simulation approach, the transferring of information occurred from a surface to a surface and across dissimilar meshes (finite volume mesh and finite element mesh). Globally conservative interpolation method was used to transfer the data over this interface. In this procedure, each node on the sender side maps onto an element on the receiver side. The node on the sender was split to meet the node distribution of the receiver side. Through this method, the total force, mesh displacement and temperature profile was balanced on this interface and adequately captured.

3.3.2.4 The Computational Domain and Boundary Conditions

In this two-way interaction approach, a homogeneous multiphase approach with the air as one phase and polymer melt as another phase was used as initial condition for the injection molding process. The boundary condition applied throughout the injection molding cycle is tabulated in Table 3.4. In structural domain, the metal surface acted as mold surface, its motion was fixed throughout the molding cycle. The polymer surface was assumed not exist yet in filling phase. The polymer surface was fixed from moving in packing phase since the polymer melt was assumed to be attached to mold surface. After packing, the polymer surface motion was defined as free in mold cooling and ejection phases and the polymer surface was used to capture the thickness variation due to the processing parameter applied throughout the molding cycle. The surrounding environment temperature during injection molding was defined within this structural domain and it was

25 ℃. To compute the mesh deformation of the polymer surface resulted from heat transfer, a reference temperature was defined within this domain.

Table 3.4: Boundary condition for injection molding simulation

Injection molding	**Structural domain**		**Fluid domain**		
Sub process	**Metal surface**	**Polymer surface**	**Air vent**	**Gate (Inlet)**	**Mold wall**
Filling	Fixed	-	Pressure = 1 *atm*	Mass flow rate = 0.1, 0.3 and 0.5 *kg/s* Melt temperature = 220, 230 and 240 ℃	No slip
Packing	Fixed	Fixed	Pressure = 1 *atm*	Packing pressure = 100*MPa* Melt temperature = 220, 230 and 240 ℃	No slip
Mold cooling	Fixed	Free	Pressure = 1 *atm*	Pressure = 1 *atm*	No slip
Ejection	Fixed	Free	Pressure = 1 *atm*	Pressure = 1 *atm*	No slip

In fluid domain, the air vent pressure was 1 *atm* (room pressure) throughout the molding cycle. The air vent size was 0.5 *mm* and it was located at the bottom circumference of the control volume (mold cavity) as shown in Figure 3.14. Air vent only allowed air to escape from the mold cavity. However, gate which was the injection location only allowed polymer melt to flow into the mold cavity. Mass flow rate, packing pressure and injection melt temperature for simulation were applied at this location. In mold cooling and ejection phase, the polymer melt was allowed to shrink within these two phases. No slip condition was applied on the mold surface throughout the entire molding cycle. The polymer melt velocity was zero at mold wall surface during injection molding.

3.4 Experimental set-up

Figure 3.16 shows all the experimental components used for shrinkage analysis. The components used were: a) Data acquisition system (TC-08), b) mold insert, c)

thermocouple, d) and g) plate *A* and plate *B*, e) mold cavity, f) computer and h) mold core. The mold cavity was made up of plate *A* and plate *B*. Plate *A* was installed on the moving side of injection molding machine. Plate *B* was installed on mold core. The mold core was assembled on the stationary side of injection molding machine. Real time temperature monitoring was conducted during injection molding in this study and a type *K* thermocouple was used to measure the plastic melt temperature as illustrated in this figure. A data acquisition system (DAQ) provided by Pico technology was used to record the temperature obtained from thermocouple. A personal computer was used to store the data obtained for analysis. The detailed structure of the mold component was presented in APPENDIX B.

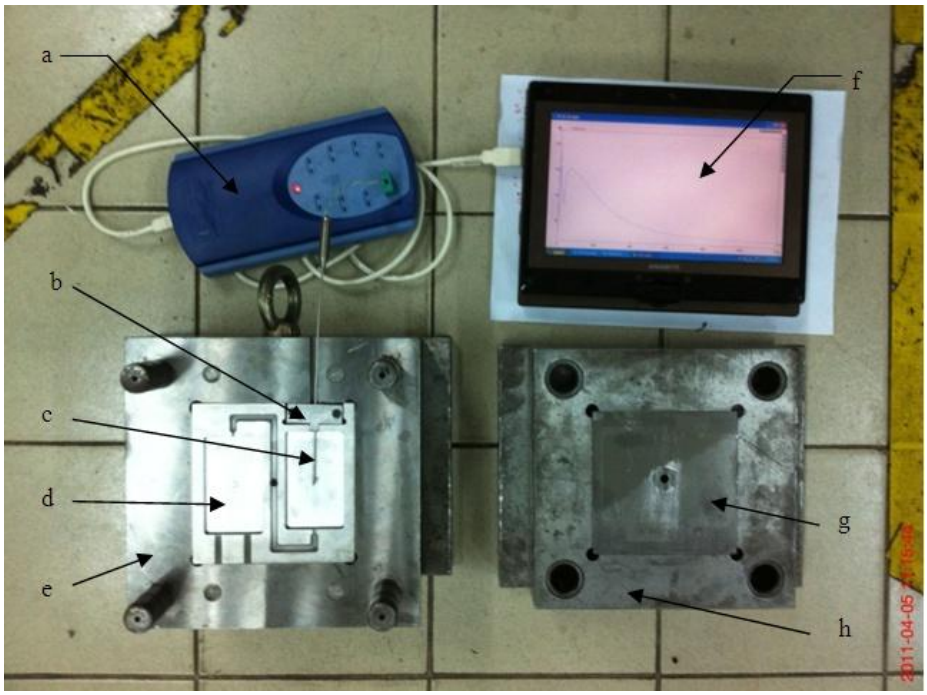

Figure 3.16: Mold cavity and core with data acquisition system

3.4.1 Machines and tools

To realize the mold cavity-II for experimental analysis, a series of milling operations were conducted to produce the mold components (plate *A*, plate *B* and mold

insert) for the thin plastic part on a CINCINATI MILACRON SABRE 750 three axis vertical milling machine as shown in Figure 3.17 by using the programming code generated from NX Unigraphics 2.0 CAM software.

Figure 3.17: Cincinnati Milacron – SABRE three axis vertical milling machine

Milling operations were performed in a block with dimensions of 110 *mm* × 110 *mm* × 20 *mm* for fabrication of plate *A* and *B* and in a block with dimension of 50 *mm* × 20 *mm* × 10 *mm* for fabrication of mold insert. The work piece material was machinable carbon steel (Assab Steel 760) that had chemical properties of 0.5% C, 98.5% Fe, 0.7% Mn and 0.3% Si. The mold components were hardened to increase the durability of the material. The material hardness was 210*BHN* (MatWeb, 1990). All of the experimental analysis for plastic injection molding were conducted on an injection molding machine BOY 22M as illustrated in Figure 3.18. The injection unit screw diameter was 22 *mm*, maximum injection force is 65 *kN* and maximum stroke volume was 64 cm^3.

Figure 3.18: Injection molding machine, BOY 22M

3.4.2 Instrumentation and implementation

Figure 3.19 shows the schematic temperature measurement process used in this study. As illustrated in this figure, the DAQ system was connected to a computer via a USB cable and the thermocouple was connected to the DAQ system through a thermocouple input connector. Computer supplied electricity for the DAQ device via the USB cable and the DAQ system supplied electricity to the thermocouple via thermocouple input connector. The DAQ system, TC-08 was provided by Pico Technology Ltd and it supported type *B*, *E*, *J*, *K*, *R*, *S* and *T* thermocouples. This device was a temperature and voltage logger designed to support 8 temperature measurements at the same time via miniature temperature connector. It can measure voltages in the range of $\pm 70\ mV$ and the uncalibrated accuracy was $\pm 0.2\%$ and $\pm 0.5\ ℃$. The resolution of the smallest sampling rate for TC-08 was 1 millisecond but in this study the sampling rate was adjusted to 50 milliseconds. A general purpose type *K* thermocouple was used for temperature measurement. Figure 3.20 shows

the type *K* thermocouple used in this study. It was obtained from Pico Technology Ltd and the product code name was Pt 100. The length and diameter of the thermocouple were respectively 150 *mm* and 2 *mm* respectively. The operating temperature range of the thermocouple was -270 ℃ to +1370 ℃ and the sensitivity was 41 $\mu V/°C$.

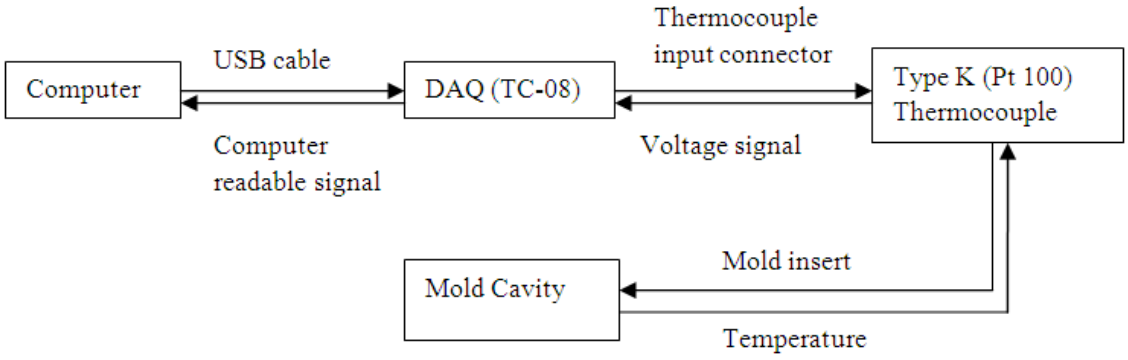

Figure 3.19: Plastic melt temperature measurement using the supplied DAQ system

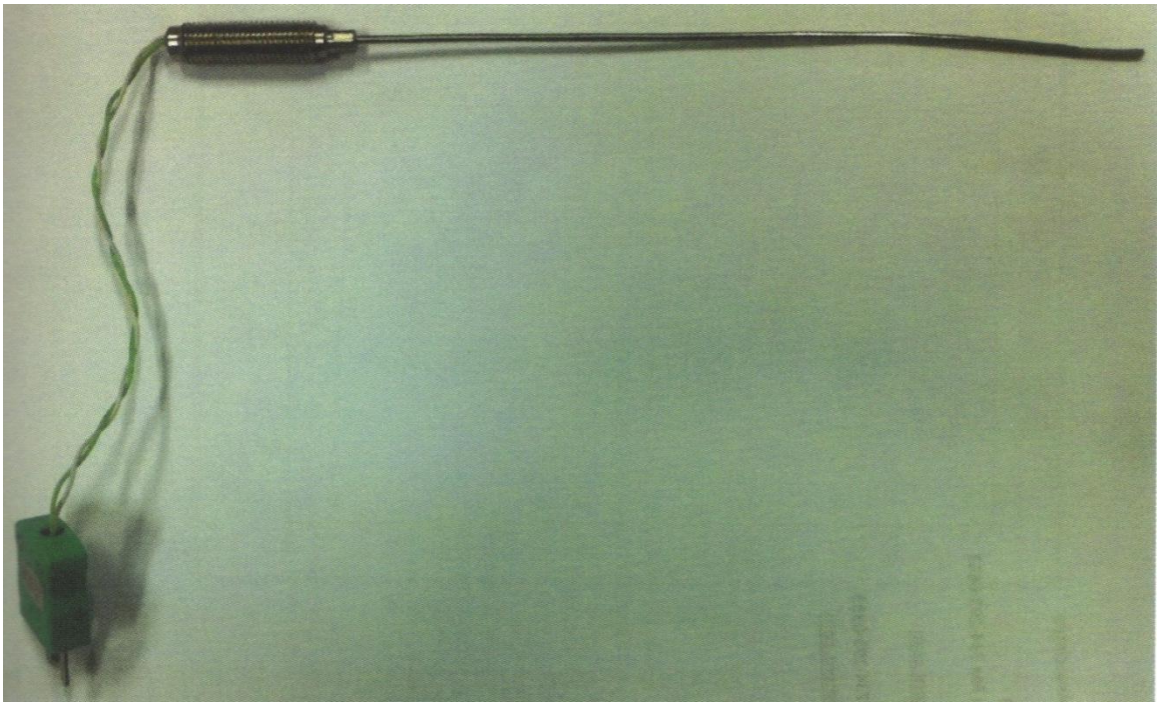

Figure 3.20: Pico technology type K thermocouple (Product code name was Pt 100)

The thermocouple was installed on the mold cavity for temperature measurement using a special mold insert as shown in Figure A-3 of APPENDIX A. During injection molding, the detected temperature change was converted into voltage signal by the thermocouple used in this study. The voltage signal was transmitted back to TC-08 through the thermocouple input connector. The voltage signal was processed into computer readable signal within this DAQ device. By using the connected computer, recorded computer readable signal (as illustrated in Figure 3.21) can be used to observe the temperature distribution of the plastic melt during injection molding.

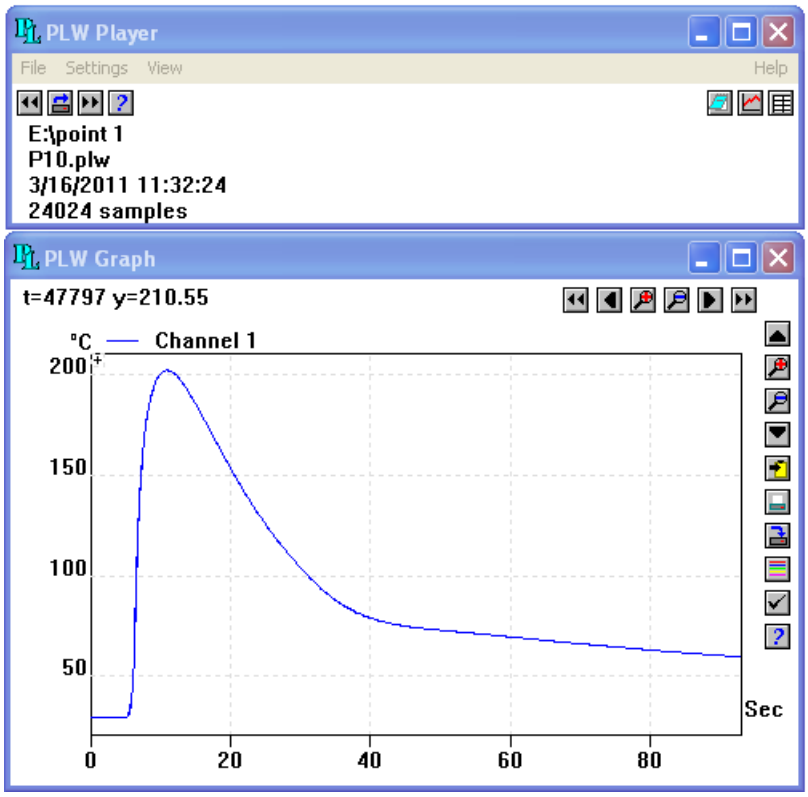

Figure 3.21: A typical example of temperature data as obtained from a thermocouple during plastic injection molding

Changing the length of the thermocouple probe by using this tool insert, cavity temperature at different locations was recorded during experiment. The thermoplastic used

was molded onto this thermocouple and the molded part was ejected together with thermocouple and tool insert at the same time at the end of the molding cycle. Two cavities test mold was used, the plastic part molded on thermocouple was scrapped and another plastic part obtained from the plastic molding was used for shrinkage analysis in this study. The temperature measurement was made at three positions along the flow length of the plastic part as shown in Figure A-1 of APPENDIX A starting from the gate location. These locations were respectively 5 *mm*, 33.5 *mm* and 62 *mm* measured from the gate location. All these locations were situated along the center line of the width and thickness direction of the plastic part.

3.5 Design of experiment

Different processing parameters were selected to study the effect of molding conditions on plastic product shrinkage.

For mold cavity-I, the packing pressure and melt temperature used in injection molding process were varied at 5 different levels in one-way interaction approach to investigate the effect of these two variables on shrinkage. The melt temperatures used were 220, 225, 230, 235 and 240 ℃ and the packing pressures used were 7, 8, 9, 10 and 11*M Pa*. During the plastic injection molding, the mold temperature was set at 25 ℃ throughout the entire cycle until the part was ejected. The packing time, injection mass flow rate and holding time used for the simulation were 6 *s*, 40 *kg/s* and 60 *s* respectively. In two-way interaction approach simulation, the melt temperature and injection mass flow rate used were varied at 3 different levels. The injection mass flow rates used were 40, 50 and 60 *kg/s* and the melt temperatures used were 220, 230 and 240 ℃. The mold temperature was set at 25 ℃ as well. The packing pressure, packing time and holding time were respectively 10*M Pa*, 6 *s* and 60 *s*.

For mold cavity-II, the required processing parameter for the experimental study was predicted using one of the proposed numerical models. According to the dimension of the mold cavity-II, the initial processing parameter required for this simulation roughly were injection speed of 40 *kg/s*, melt temperature of 250 ℃, packing pressure of 10*M Pa*, cooling time of 15 *s* and packing time of 10 *s*. After the reliability of this processing parameter was ensured after verification with the experimental result, the variables used in this processing parameter were varied at three levels according to a three level design of Taguchi's orthogonal array (OA) to study the effect of processing parameter on shrinkage. The OA, L_{27} (3^{13}) as illustrated in Table C-1 of APPENDIX C was used in this study. The variations of the processing parameters are tabulated Table 3.5. Other process parameter settings were held constant throughout the experiments.

Table 3.5: Process parameter used in three level eight factorial molding experiments

Factors	level 1	level 2	level 3
A: Injection speed, *mm/s*	40	50	60
B: Melt temperature, *℃*	210	230	250
C: Packing pressure, *M Pa*	1	5	10
D: Mold cooling time, *s*	10	15	20
E: Packing time, *s*	5	10	15
Others processing parameters			
Screw rotation speed, *mm/s*	100		
Back pressure , *M Pa*	10		
Feed stroke	50/52 (for suck back)		
Cushion setting, *mm*	12 (V/P switch over at 8 *mm*)		
Melt cushion position, *mm*	3		

The layout for the orthogonal array used is presented in Table C-1 of APPENDIX C. As illustrated in this table, the interaction effect between process parameters was also investigated in this study. The interaction effect between variable **A** and **B** was assigned to column 3. The interaction effect between variable **A** and **C** was assigned to column 6. The

last interaction effect between variable **B** and **C** was assigned to column 8 of the L_{27} (3^{13}) orthogonal array. Analysis of variance (ANOVA) was performed to study the contribution of each factor and also contribution of each interaction effect on plastic part shrinkage. *F-test* was used in this analysis to analyze this effect and a confident level of 90% was used to examine whether these factors or interactions were significant or not (Roy, 2010).

3.5.1 Experimental verification of finite element result

The plastic melt temperatures obtained from simulation experimental study were compared. Both experimental and experiment were conducted using the same parameter setting for this purpose. The parameters used were injection speed of 40 *mm/s*, melt temperature of 250 ℃, packing pressure of 10*M Pa*, mold cooling time of 15 *s* and packing time of 10 *s*. The plastic temperature was recorded at different positions (*Y1*, *Y2* and *Y3*) along the melt flow length direction as illustrated in Figure A-1. The thickness at these three positions for both simulation and experiment were compared to verify the reliability of the proposed numerical model for shrinkage analysis.

3.6 Product characterization

For shrinkage measurement of mold cavity-I, five locations along the flow direction: M1, M2, M3, M4 and M5 as illustrated in Figure 3.1 were selected as the point of interest for shrinkage study in one-way interaction approach. On the other hand, shrinkage measurement locations in two-way interaction approach are illustrated in Figure 3.2. These locations were respectively M10, M75 and M140 which were situated along the flow direction and L75, M75 and R75 that were situated in the transverse flow direction. The nodal displacements at each of these points were recorded and the thickness was calculated as the difference between the node value at the top and bottom surface. Shrinkage was

computed as the difference between the mod cavity thickness dimensions with plastic part thickness.

For mold cavity-II, the investigation included the determination of the molding conditions (injection speed, melt temperature, packing pressure, mold cooling time and packing time) on part shrinkage. The length (*X1*, *X2* and *X3*), width (*Z1*, *Z2* and *Z3*) and thickness (*Y1*, *Y2* and *Y3*) of the plastic part were measured at three respective locations as illustrated in Figure A-1 of APPENDIX A. The average readings of the plastic part length, width and thickness were used to calculate the part volume. The plastic part volume was calculated by Equation 3.39 as follows:

$$Part\ volume = \bar{X} \times \bar{Y} \times \bar{Z} \tag{3.41}$$

where, $\bar{X}$ is the average value of *X1*, *X2* and *X3*, $\bar{Y}$ is the average value of *Y1*, *Y2* and *Y3* and $\bar{Z}$ is the average value of *Z1*, *Z2* and *Z3*. Shrinkage is defined as dimensional variation between the desired part dimension (mold cavity dimension) and actual plastic part dimension. Hence, the plastic part volume obtained for each experimental runs were used to calculate volumetric shrinkage as given in Equation 3.40 below:

$$Shrinkage\ (\%) = \frac{Desired\ \ plastic\ \ part\ \ volume - actual\ \ plastic\ \ part\ \ volume}{Desired\ \ plastic\ \ part\ \ volume} \times 100 \tag{3.42}$$

Precision plastic part generally strived for lowest contour error. Therefore for shrinkage, the smaller the better (STB) was chosen as the quality characteristics in this analysis. According to the Taguchi experimental method, the S/N (signal to noise) for STB, (n_{STB}), was defined in Equation 3.41 as follows:

$$n_{STB} = -10log\left[\frac{1}{n}\sum_{i=1}^{n} y_i^2\right] \quad (3.43)$$

Best processing parameter was selected from this S/N analysis. Since the smaller the better was chosen as the quality characteristic hence the best processing parameter for minimum shrinkage was chosen from the S/N plot by selecting the lowest S/N ratio reading for each parameter. The combined selection was the best parameter for minimum shrinkage.

In addition, ANOVA analysis was performed to study the effect of each factor and effect of each interaction on part shrinkage by using F test. A confident level of 90% was used in this analysis and a factor or interaction was considered significant when the calculated confident ratio was less than 0.1 (Roy, 2010).

After running the ANOVA test, the significant factors were used to calculate the S/N ratio. This reading was used for confirmation test to check whether the S/N ratio of minimum shrinkage was same with this reading.

3.7 Summary

In this study, finite element analysis was used to determine the effect of processing parameter on shrinkage by using one-way interaction approach and two-way interaction approach in computational fluid dynamic and finite element software (ANSYS 12.1). In one-way interaction approach, three finite element analysis tools namely computational fluid dynamic, transient thermal analysis and static structural analysis were used to model the mold filling, mold cooling and product shrinkage after ejection as separate process. In the two-way interaction approach, a highly intelligent multi-physics architecture composed of both computational fluid dynamic and finite element analysis tools was proposed to study the injection molding shrinkage problem as a single process. Two test mold cavities

namely mold cavity-I and mold cavity-II were used in this study. Both cavities product shape were respectively rectangular in geometry with dimension of 100 *mm* × 50 *mm* × 2 *mm* and 67 *mm* × 40 *mm* × 4 *mm*. An optimization process was conducted on the mold cavity-II plastic product for minimum shrinkage by using Taguchi and ANOVA analysis according to an L_{27} (3^{13}) orthogonal array.

CHAPTER 4: RESULTS AND DISCUSSION

4.1 Finite element analysis of mold cavity-I plastic product by one-way interaction approach

The effect of melt temperature and packing pressure on plastic product shrinkage of mold cavity-I was studied. The mold filling for this cavity was analyzed first. Several locations in the mold cavity were chosen to study how the pressure and temperature of the plastic melt changed during injection molding. The selected locations (M1, M2, M3, M4, M5, L1, L4, R1 and R4) are illustrated in Figure 3.1. After that, the effect of processing parameter on product shrinkage variation was studied. The difference between the product thickness on selected locations (M1, M2, M3, M4 and M5) and cavity thickness (2 *mm*) was selected as the quality characteristic for shrinkage.

4.1.1 Mold filling analysis

A computational fluid dynamic (CFD) method was used to study the filling process using Marlex HDPE 9500 for mold cavity-I and Figure 4.1 shows a typical simulation result obtained using this method. This figure demonstrates the 3D analysis contour plot of mold filling and pressure distribution at different time intervals during the mold filling process for molding procedure using melt temperature of 230 ℃ and mass flow rate of 0.04 *kg/s*. Initially, the flow front pressure recorded was 0.940*M Pa* at 0.2 *s*. No back pressure occurred at this time interval and the plastic melt flow was very smooth. As the plastic melt travelled to the center region after 1 *s*, the hot plastic melt cooled down and became hard to move due to increased viscosity of the melt.

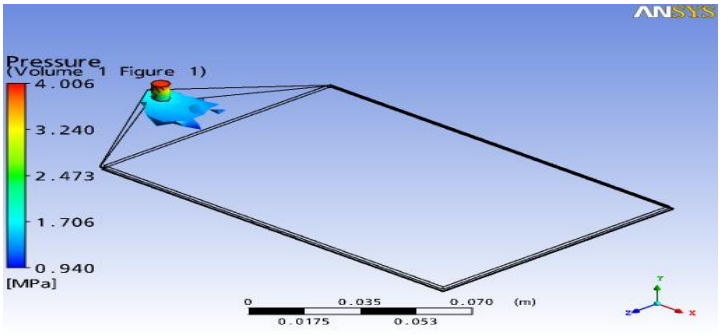

a) 0.2 *s*

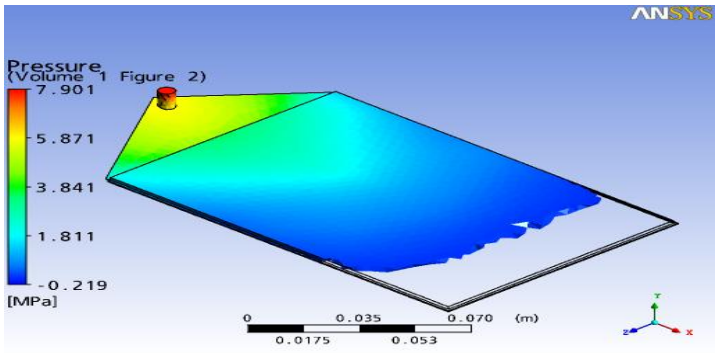

b) 1.0 *s*

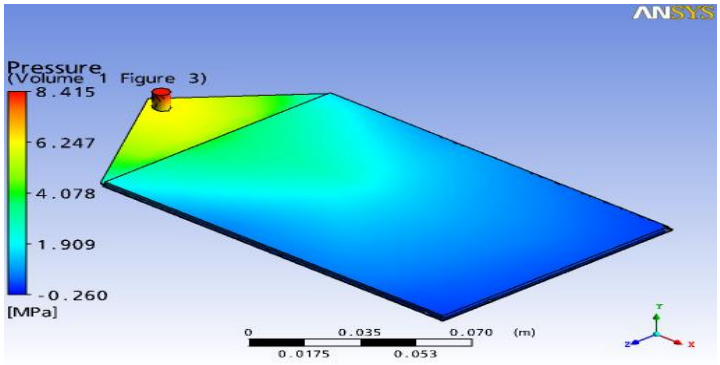

c) 2.6 *s*

Figure 4.1: Pressure distribution in injection phase; (a) after 0.2 *s*, (b) after 1 *s* and (c) after 2.6 *s*

The recorded pressure for flow front was below positive value, -0.219*M Pa*. The plastic melt experienced difficulty to move at this region. Further down to the cavity, the back pressure was even higher, -0.260*M Pa*. Higher back pressure indicated that the mobility of the plastic was poorer. Although after 1 *s*, the cavity was 75% filled but due to

pressure drop and air trap, the plastic melt became hard to move at the end of the cavity. As a result, the complete mold filling took 2.6 *s* to finish.

To further analyze the plastic melt behavior under different processing parameters, the cavity pressure and temperature at different locations were measured. The temperature and pressure time response graphs at these locations are presented in Figures 4.2 – 4.9.

Figures 4.2 and 4.3 show the cavity temperature at M1 and M4 respectively. M1 was the nearest point from gate. As depicted in Figure 3.1, it was located at mid section of the plastic part and 30 *mm* from the gate as measured along the flow direction.

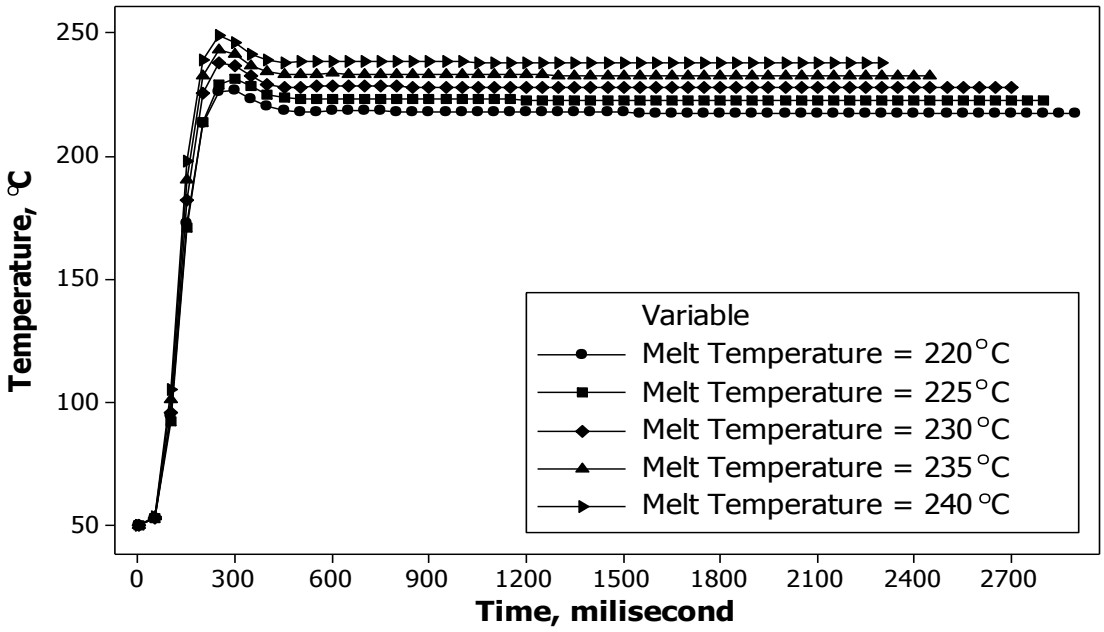

Figure 4.2: M1 temperature in the mold

The plastic melt took about 0.3 *s* to reach this position. The highest temperature recorded at this position using molding temperature of 240 ℃ was 248.94 ℃ at 0.25 *s*. For molding activity using melt temperature of 220 ℃, the highest melt temperature recorded was 226.90 ℃ at 0.3 *s*. The plastic melt for molding procedure using melt temperature of

240 ℃ reached M1 earlier than molding using melt temperature of 220 ℃. It was obvious that the highest temperature recorded was higher than the melt temperature used. The viscous dissipation under high shear rate had increased the melt temperature but the increment was no more than 10 ℃.

M4 was located at 120 *mm* from the gate as measured along the flow direction. Maximum temperature was recorded at about 1 *s* at this position. The highest temperature recorded for molding using melt temperature of 240 ℃ was 236.33 ℃ at 1.1 *s* and the highest temperature recorded for molding using melt temperature of 220 ℃ was 213.40 ℃ at 1.35 *s*. The highest temperature recorded for both processing parameters was lower than the actual melt temperature used. Due to the applied mold temperature and the distance from the gate, the difference between mold temperature and melt temperature had resulted in significant heat loss from the plastic melt.

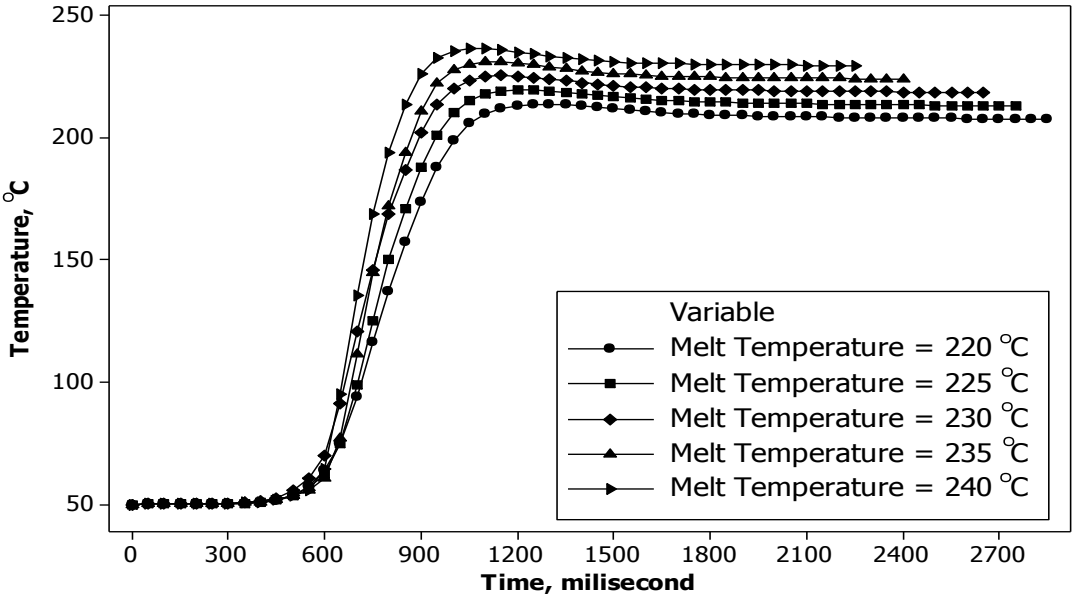

Figure 4.3: M4 temperature in the mold

The viscous dissipation effect was more significant at region near the gate but at region near to the end of the cavity, the effect of heat loss was more significant. Again, the plastic melt flow for molding process using melt temperature of 240 ℃ was faster than that of 220 ℃. The viscosity decreased with temperature and as a result the plastic melt at higher temperature had better mobility. The complete mold filling was 2.9 *s* for molding using melt temperature of 220 ℃ and the complete mold filling by using melt temperature of 240 ℃ was 2.3 *s*.

The temperature in the transverse direction at the beginning of flow is presented in Figure 4.4. Three points L1, M1 and R1 were used to investigate the temperature distribution across the transverse direction of the plastic flow. These three locations were respectively situated at left edge, mid section and right edge of the plastic part. All of them were located at 30 *mm* away gate as measured along the flow direction.

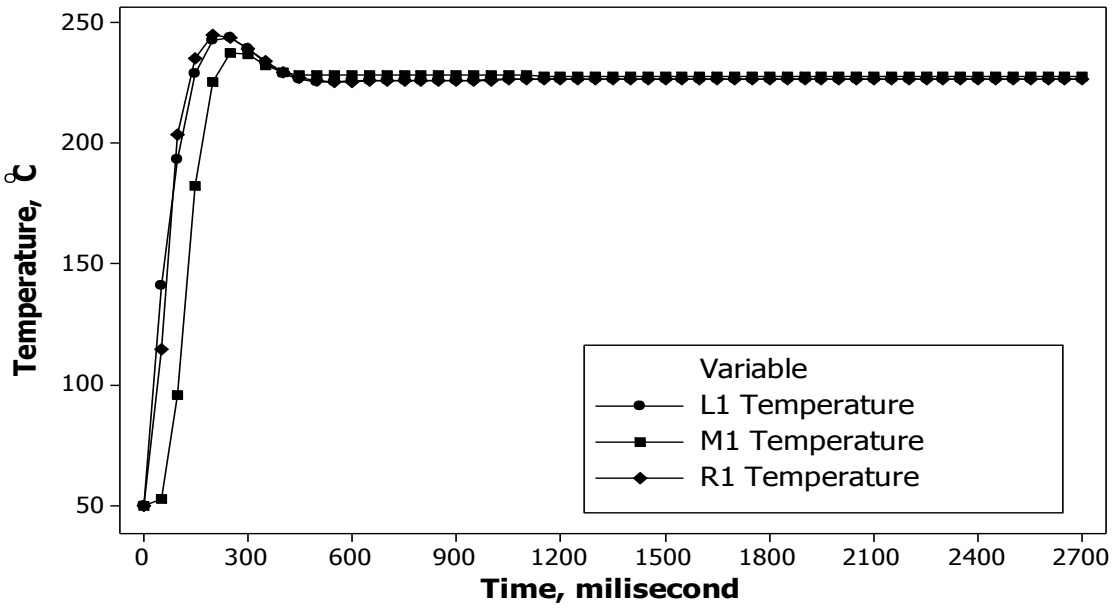

Figure 4.4: Temperature distribution across transverse direction as obtained using melt temperature of 230 ℃ and mass flow rate of 0.04 *kg/s*

The result was generated by using melt temperature of 230 ℃ and mass flow rate of 0.04 *kg/s*. The highest temperature recorded at M1 was 236.8 ℃ at 0.25 *s*. The highest temperature reading at L1 and R1 were 242.6 ℃ and 244.7 ℃ at 0.2 *s*. The plastic melt flow at M1 was slower than plastic melt flow at L1 and R1. The main function of fan gate was to ensure balancing of flow. Balance flow was crucial to ensure the plastic melt to cool down and shrink at uniform rate. Although the plastic melt in the mid section of the cavity was slightly slower but the flow was almost balanced. In addition, the temperature recorded for all the points were almost same, 226 - 228 ℃ after certain time interval, after about 0.5 *s*,

Figure 4.5 shows the temperature distribution across the transverse direction at the far end of the cavity. All the locations at far end of the cavity including L4, M4 and R4 were respectively situated at left edge, mid section and right edge of the plastic part. All of them were located at 120 *mm* away gate as measured along the flow direction.

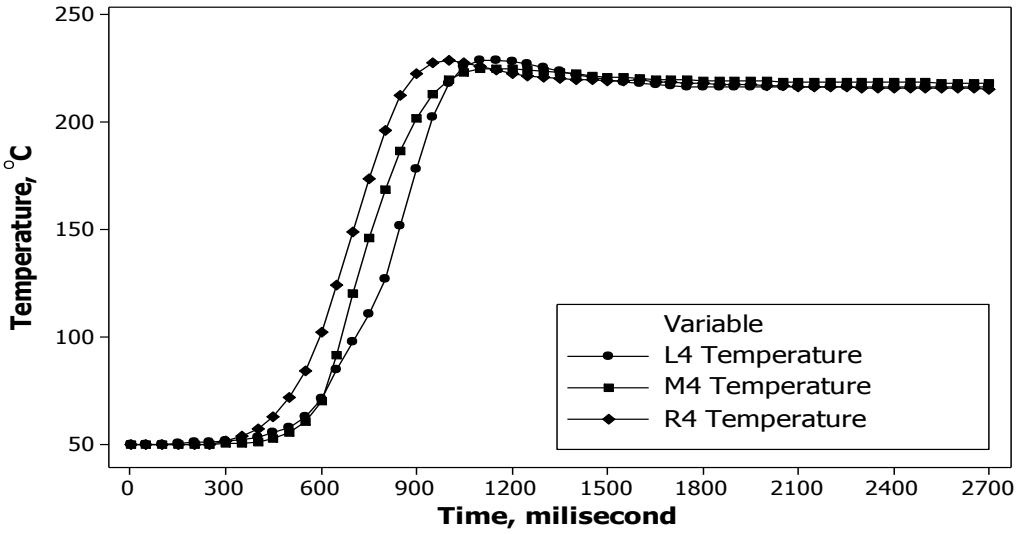

Figure 4.5: Temperature distribution across transverse direction as obtained using melt temperature of 230 ℃ and mass flow rate of 0.04 *kg/s*

The highest temperature recorded for M4, L4 and R4 were 224.7 ℃, 228.9 ℃ and 227.5 ℃ respectively after time period of 1.15 *s*, 1.15 *s* and 1.00 *s*. The plastic melt flow measured at L4 and R4 were slightly faster, 0.15 *s* faster than plastic melt flow measured at M4. The flow speed across the transverse direction was almost identical and the temperature distribution was almost the same too, within 224 – 229 ℃ after 1 *s*. The melt temperature dropped to 215 – 219 ℃ at the end of filling. The temperature and flow distribution were almost same for both beginning of flow and end of the flow. The fan gate applied had resulted in uniform plastic melt speed and temperature distribution.

Figures 4.6 and 4.7 show the pressure time response graph for M1 and M4.

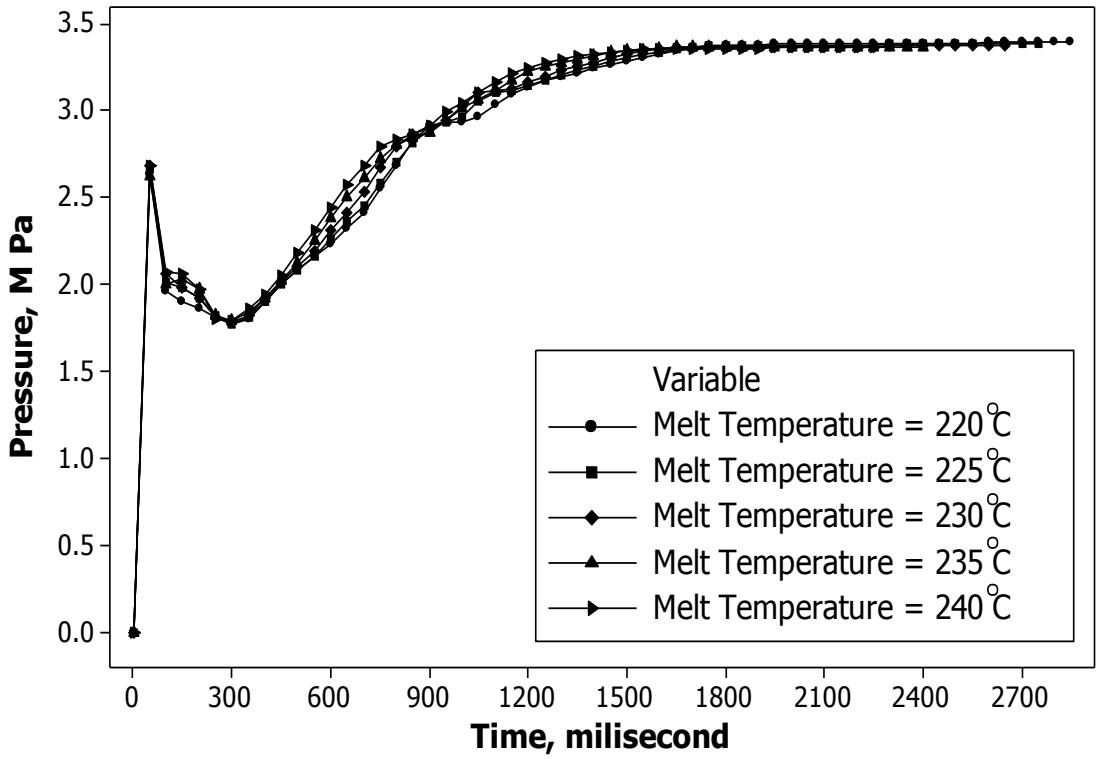

Figure 4.6: Pressure at M1 of the mold cavity-I during injection molding

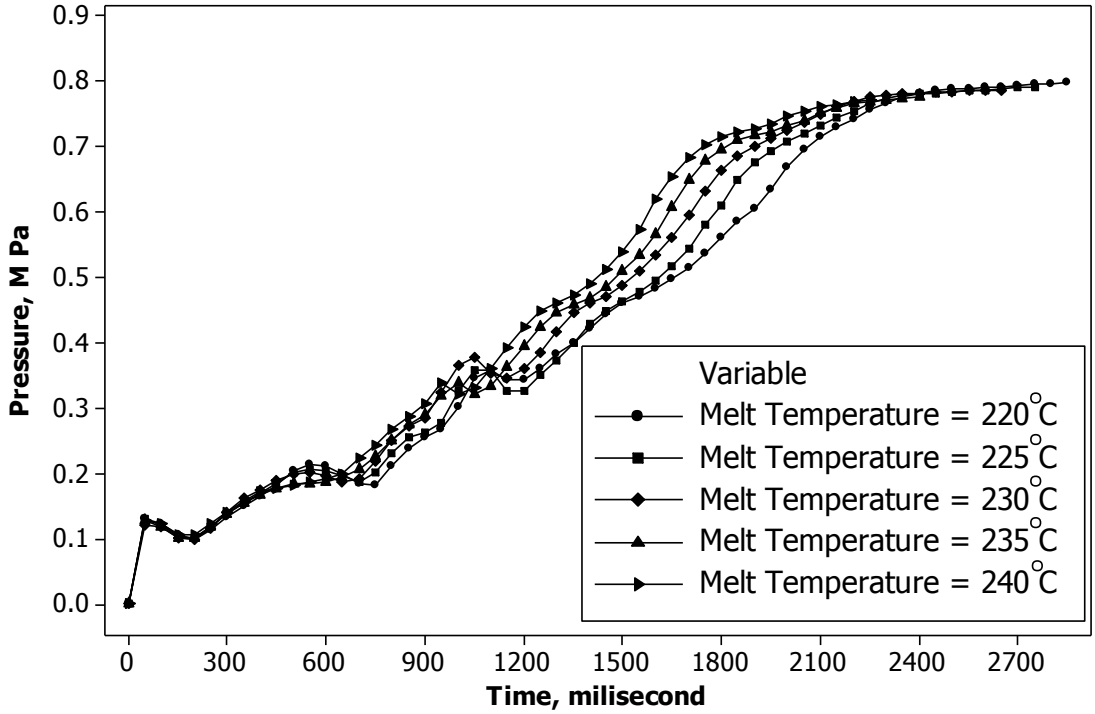

Figure 4.7: Pressure at M4 of the mold cavity-I during injection molding

M1 and M4 were located at mid section of the plastic part and respectively 30 and 120 *mm* from the gate as measured along the flow direction. Figure 4.6 shows the pressure distribution near gate area at M1 by using different melt temperatures. A drastic increase in pressure was observed initially at the beginning of the mold filling. This drastic increase in pressure was the indication for beginning of mold filling. However, M4 or the far end cavity pressure did not have this phenomenon because it was located at region far from the gate.

Molding using injection melt temperature of 220 ℃ has the highest pressure reading at position near to the beginning of the cavity. The highest pressure value was 3.39*M Pa* which was 0.03*M Pa* more than the pressure recorded for molding using melt temperature of 240 ℃. The pressure loss was 51.5% for molding using melt temperature of 220 ℃ and 52.0% for molding using melt temperature of 240 ℃. The overall pressure loss at this

position was about half of the injection pressure. At M4, near end of the cavity, the highest injection pressure recorded was 0.80*M Pa* for molding using melt temperature of 220 ℃ and 0.77*M Pa* for molding using melt temperature of 240 ℃. The pressure loss was 88.6% for molding using melt temperature of 220 ℃ and 89.0% for molding using melt temperature of 240 ℃.

In mold filling, pressure was the driving force for the plastic melt to move. The pressure used was converted into kinetic energy. As a result, the pressure loss increased with the melt flow length. The pressure recorded for melt temperature of 240 ℃ was slightly lower than of molding using melt temperature of 220 ℃. Lower pressure was required to drive hotter melt to move since the hot plastic melt has better mobility.

The pressure distributions across the transverse direction of flow are presented in Figures 4.8 and 4.9.

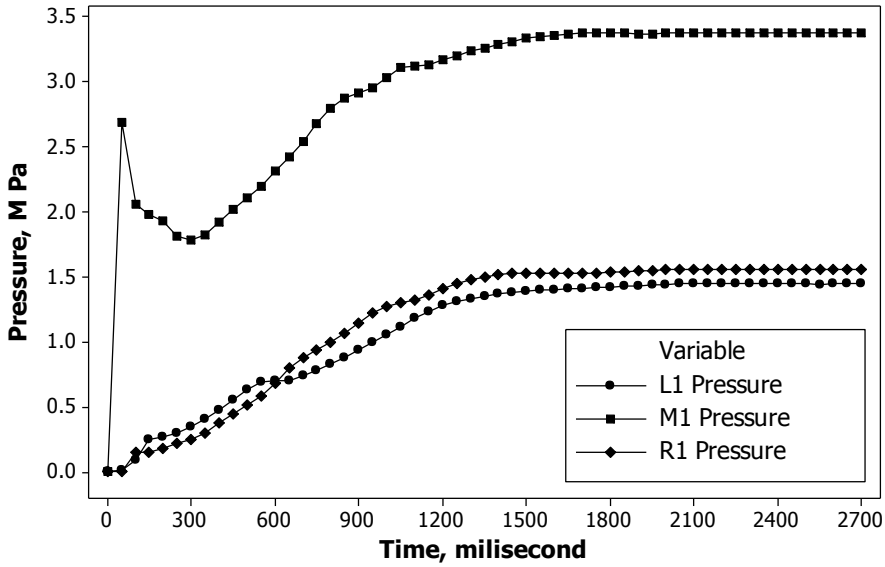

Figure 4.8: Pressure distribution across the transverse direction as obtained using melt temperature of 230 ℃ and mass flow rate of 0.04 *kg/s*

L1, M1 and R1 in **Error! Reference source not found.** were respectively situated t left edge, mid section and right edge of the plastic part. All of them were located at 30 *mm* away gate as measured along the flow direction. The recorded pressure reading was very high at M1 compared with L1 and R1. As discussed previously, pressure was converted into kinetic energy and the pressure loss with the moving distance of the plastic melt. M1 which was situated at the mid section of the plastic part and the flow length was relatively shorter than L1 and R1 which were located at region near the edge of the plastic part. As a result, the pressure reading for L1 and R1 were relatively lower than that of M1. The pressure became stagnant after about 1 *s* for all the points selected and all the points took about the same time period for the pressure to become stable. The highest pressure reading for M1 was 3.38*M Pa* at the end of filling.

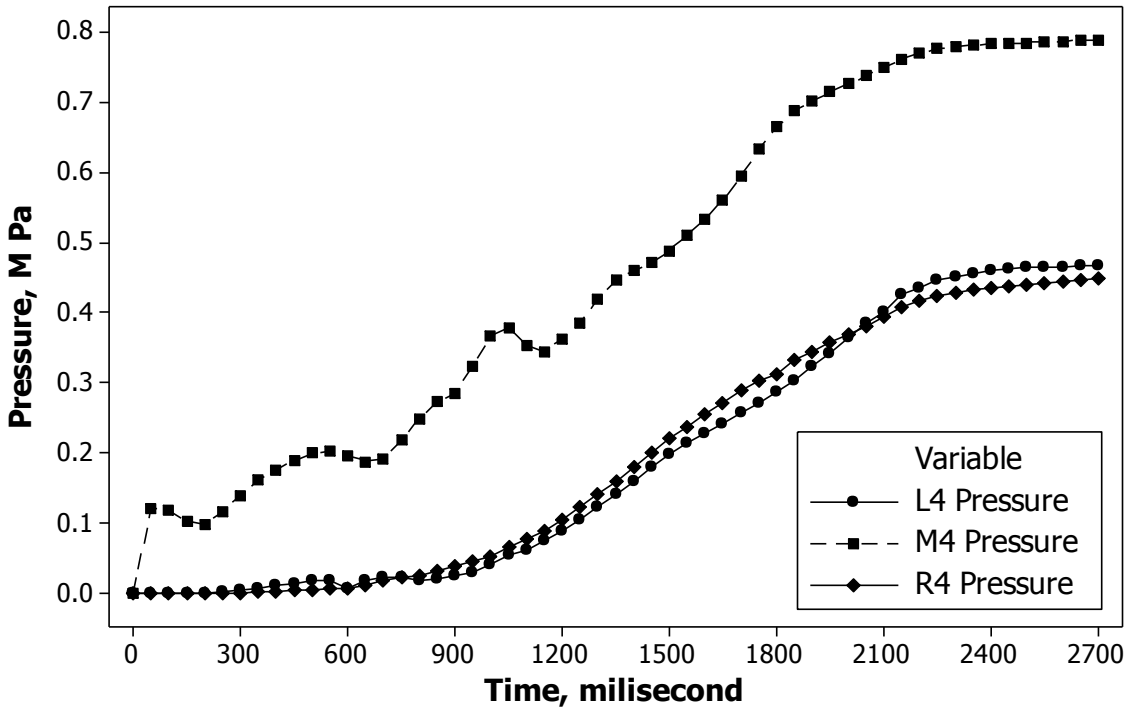

Figure 4.9: Pressure distribution across the transverse direction as obtained using melt temperature of 230 ℃ and mass flow rate of 0.04 *kg/s*

Figure 4.9 shows the same pressure distribution pattern as shown in Figure 4.8. L4, M4 and R4 were respectively situated at left edge, mid section and right edge of the plastic part. All of them were located at 120 *mm* away gate as measured along the flow direction. The pressure recorded for M4 was higher than that of L4 and R4. M4 flow length was relatively shorter than R4 and L4. As a result the pressure reading for M4 was higher. The pressure development for all the points involved took more than 2 *s* to become stable. The pressure reading for M4 was 0.79*M Pa* at the end of filling. For L4 and R4, the pressure readings at the end of filling were 0.47*M Pa* and 0.45*M Pa* respectively. Conversely, M4 pressure showed non uniform pressure increment at about 1 *s*. Due to the low temperature melt and the frozen layer formed at this region, the pressure from the injected gate was very hard to be conveyed to the plastic at this region. As a result, slight pressure fall was observed but eventually the pressure applied can overcome these two factors and move the plastic toward to the end of cavity. The pressure increased back after the slight pressure fall. Comparing readings from Figures 3.8 and 3.9, the pressure loss for the plastic melt to move from M1 to M4 was 76.7%, recorded at 2.7 *s*. On the hand, the pressure loss for the plastic melt to move from L1 to L4 and R1 to R4 were respectively 67.7% and 71.2%. The pressure loss at mid section was more than the edge.

4.1.2 Experimental verification

The simulation result for mold cavity-I was compared with previous researcher's (Chen and Gao, 2003) experimental result. Both simulation and experiment were conducted using same processing parameters and part design. The melt temperature applied was 230 ℃, injection speed was 20 *mm/s*, the packing pressure used was 50*M Pa*, packing time was 6 *s* and the mold temperature was controlled at 50 ℃ throughout the injection cycle. A Chen Hsong reciprocating screw injection molding machine (model JM88MKIII) was used

in the experiment and the material used was Marlex HDPE HMN 6060. For simulation, finite element software, ANSYS 12.1 was used for the analysis and the material selected was Marlex HDPE 9500. Both results are presented in Figure 4.10. The *x* axis in this figure indicates the plastic part thickness along the flow direction as measured form the injection gate. The thickness was measured along the center location of the plastic part width. The thickness of the plastic part was initially high at 15 *mm* from the injection gate, which was the nearest point to where plastic melt was injected. It was 1.990 *mm* for the simulation result. The thickness decreased when measured along the flow direction. The minimum thickness value for the simulation result was 1.962 *mm* at 95 *mm* from gate. Further from the gate, the thickness of the plastic part increased slightly to 1.965 *mm* at 135 *mm* form gate. For experimental result, the highest thickness reading was taken at 95 *mm* from gate, 1.983 *mm* and the lowest reading was obtained at 15 *mm* from gate, 1.973 *mm*. The thickness was high at the middle section of the plastic part.

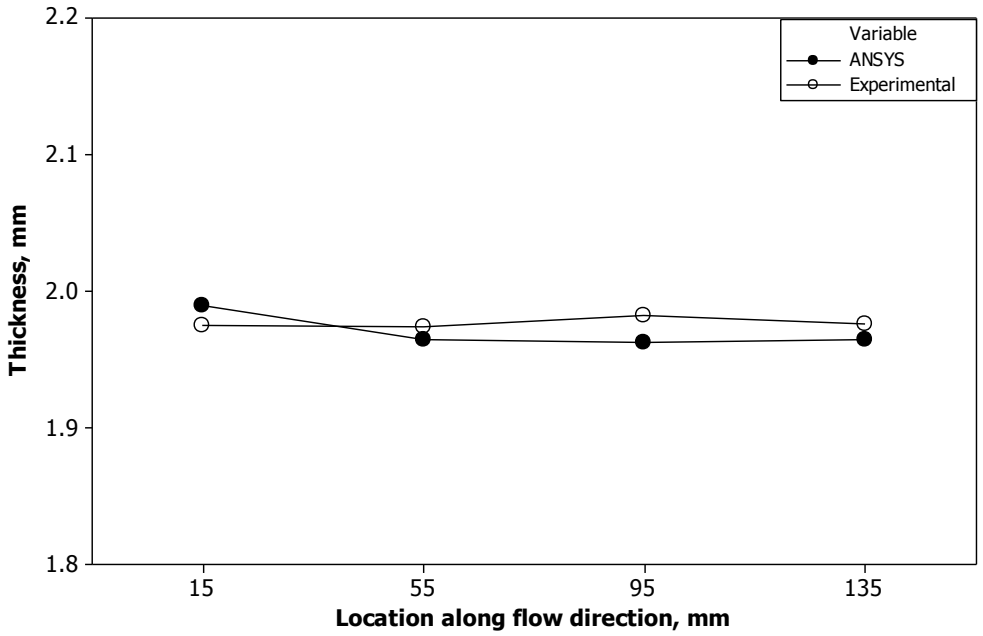

Figure 4.10: Experimental verification of simulation result

Figure 4.11 shows the shrinkage of both simulation and experimental results. At 15 *mm* from the gate, the shrinkage was 1.3% for experimental result and 0.5% for simulation result. At 95 *mm* from gate, the shrinkage was 0.85% for experimental result and 1.9% for simulation result. At 55 *mm* and 135 *mm* from gate, the shrinkages were respectively 1.7% and 1.8% for simulation result and 1.3% and 1.2% for experimental result. Although the thickness distribution for both experimental and simulation results were different but the shrinkage for both results were almost the same. The shrinkage values in either case were below 2% which was acceptable shrinkage limit for HDPE.

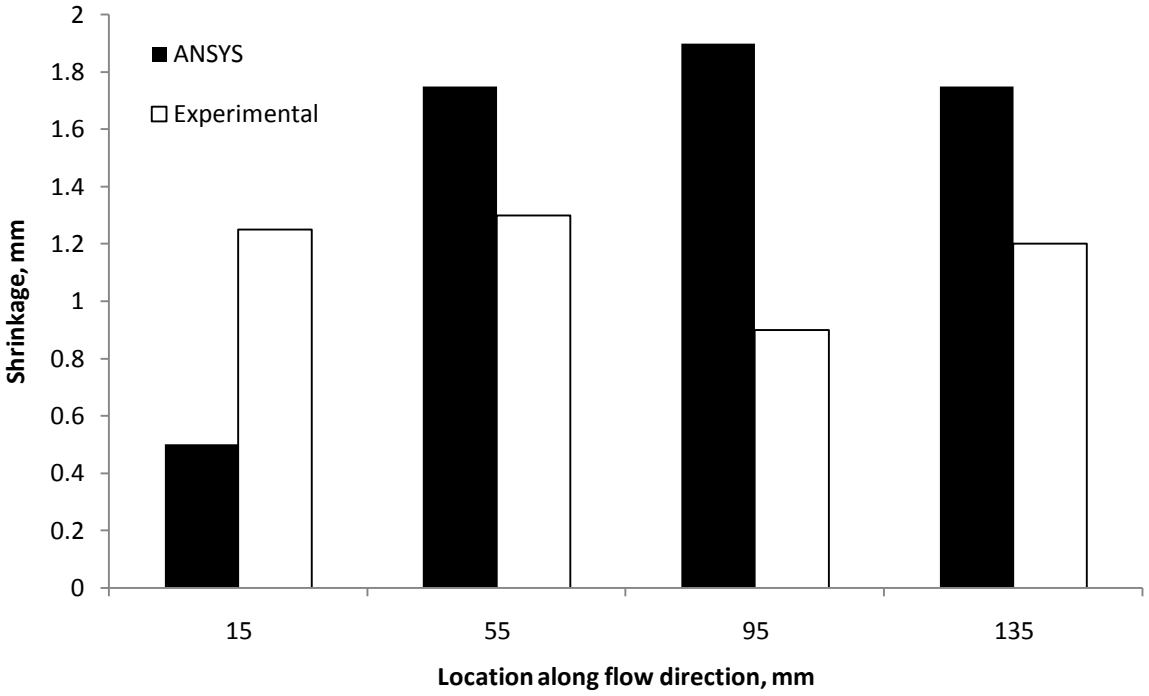

Figure 4.11: Shrinkage of both simulation and experimental results

4.1.3 Mold cavity-I product shrinkage

The plastic melt in the cavity shrunk during cooling. Depending on the temperature distribution, the shrinkage varied according to the temperature distribution and the cooling rate of the plastic melt during the cooling process. The plastic melt was allowed to cool in

the mold for 60 *s* and then ejected. Figure 4.12 shows the temperature change of the plastic melt in the cavity during the mold cooling process. When the polymer melt had solidified and had cooled to room temperature, the shrinkage was measured.

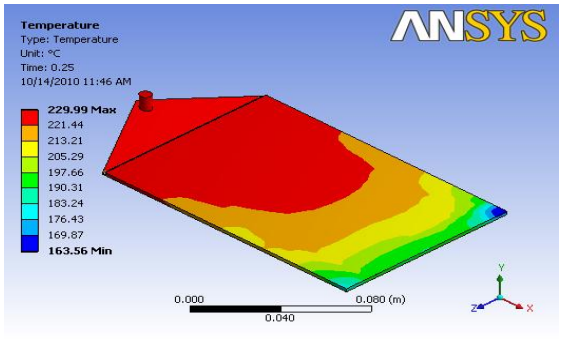

(a) 0.0 *s*

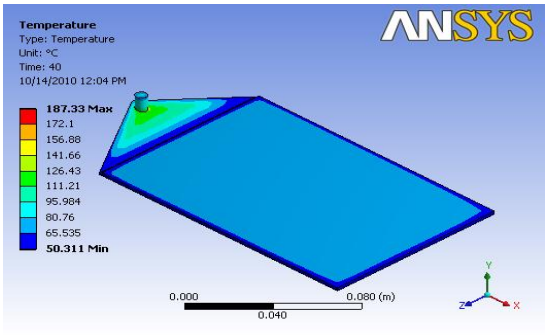

(b) 40.0 *s*

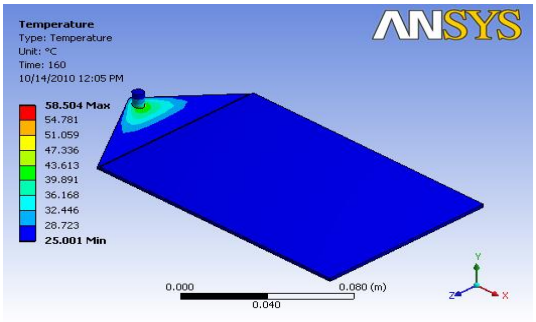

(c) 60.0 *s*

Figure 4.12: Transient thermal analysis during the cooling phase; (a) end of packing temperature, (b) after 40 *s* cooling in mold, (c) after 60 *s* cooling in mold

Figure 4.13 shows product shrinkage of mold cavity-I obtained from finite element analysis. The undeformed wireframe was used to illustrate the shrinkage of the plastic part. Different packing pressures of 7, 8, 9, 10 and 11*M Pa* and different melt temperatures of 220, 225, 230, 235 and 240 ℃ were used. To characterize the shrinkage, the thicknesses at five different points on the part surface were measured. The selected points are illustrated in Figure 3.1.

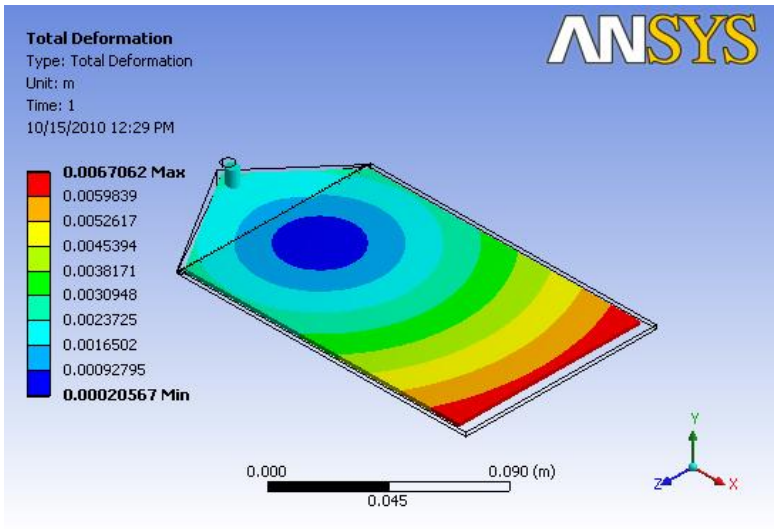

Figure 4.13: Shrinkage of the plastic part after injection molding

4.1.4 Effect of packing pressure and melt temperature on part thickness

The part thickness was measured as the average reading of the five points selected on the plastic part as illustrated in Figure 3.1. The effect of packing pressure and melt temperature on shrinkage is presented in Figure 4.14. The compressibility was not taken into account in static structural analysis but the effect of packing pressure on temperature distribution was considered in static structural analysis. As a result, the effect of packing pressure on shrinkage was not much different as compared with melt temperature effect.

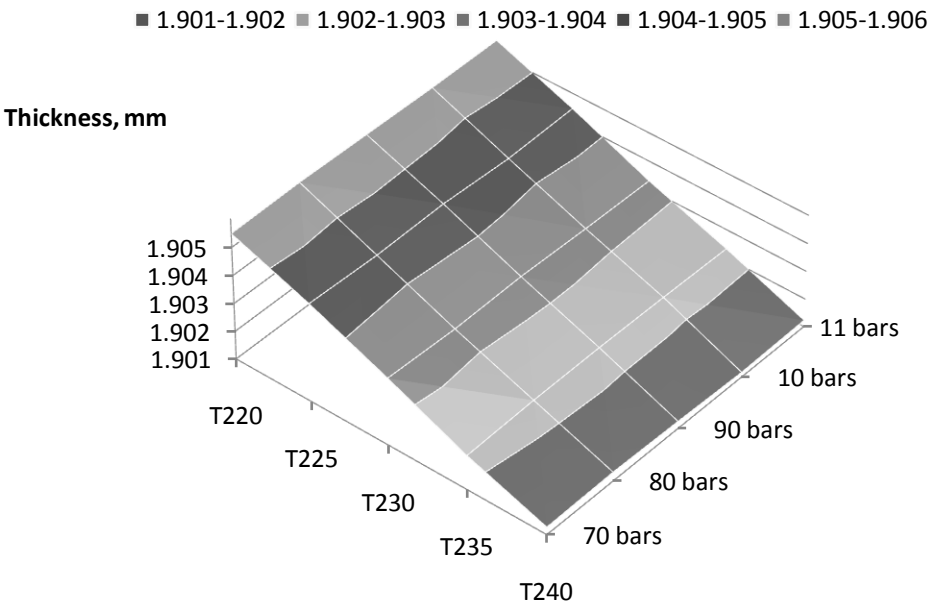

Figure 4.14: Effect of packing pressure and melt temperature on shrinkage

The natural behavior of polymer was a very important issue for shrinkage analysis. Most plastic materials shrunk during cooling and the shrinkage rate depended on the material selected and also the applied temperature and pressure. Figure 4.14 shows that the average thickness value was 1.905 - 1.906 *mm* for molding process using melt temperature of 220 ℃ and 1.901 - 1.902 *mm* for molding using melt temperature of 240 ℃. The original part thickness was 2 *mm* and the thickness difference were 0.094 - 0.095 *mm* and 0.098 - 0.099 *mm* for molding using melt temperature of 220 ℃ and 240 ℃ respectively. The shrinkage increased about 0.2% when the melt temperature used increased by 20 ℃.

To better illustrate the effect of packing pressure and melt temperature on the part thickness, Figures 4.15 – 4.19 are plotted. These figures show the effect of packing pressure on part thickness under different melt temperatures. The x axis of the figures shows the location of the points of interest along the melt flow length and the y axis shows the thickness reading.

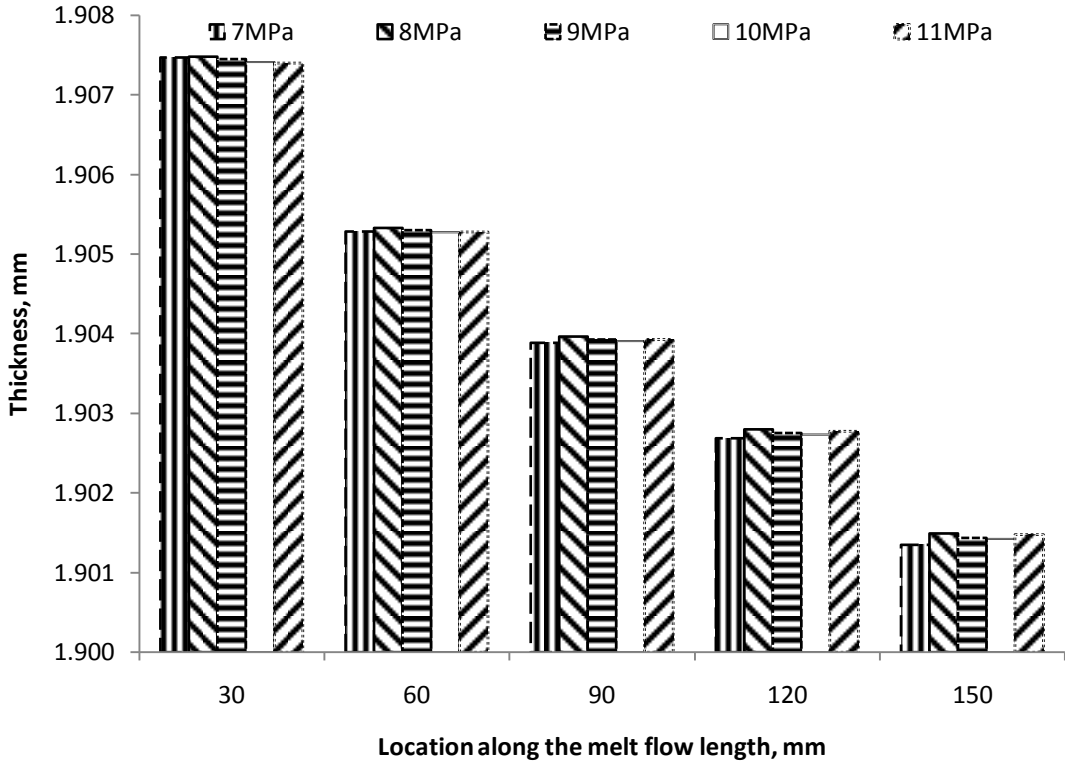

Figure 4.15: Effect of packing pressure on part thickness at melt temperature of 220 ℃

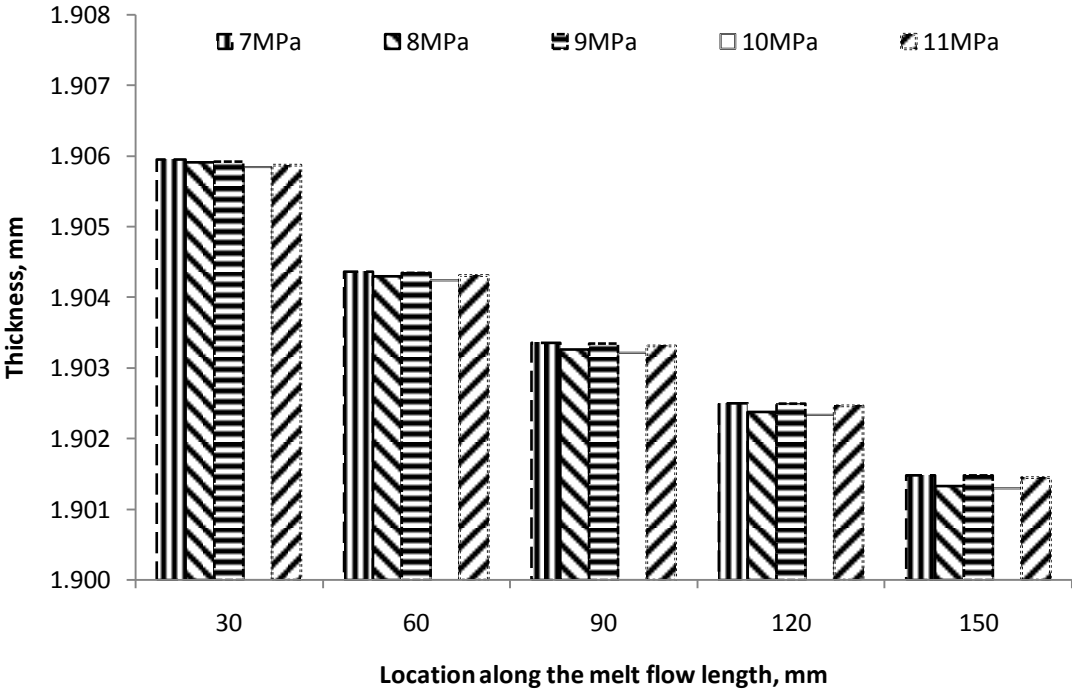

Figure 4.16: Effect of packing pressure on part thickness at melt temperature of 225 ℃

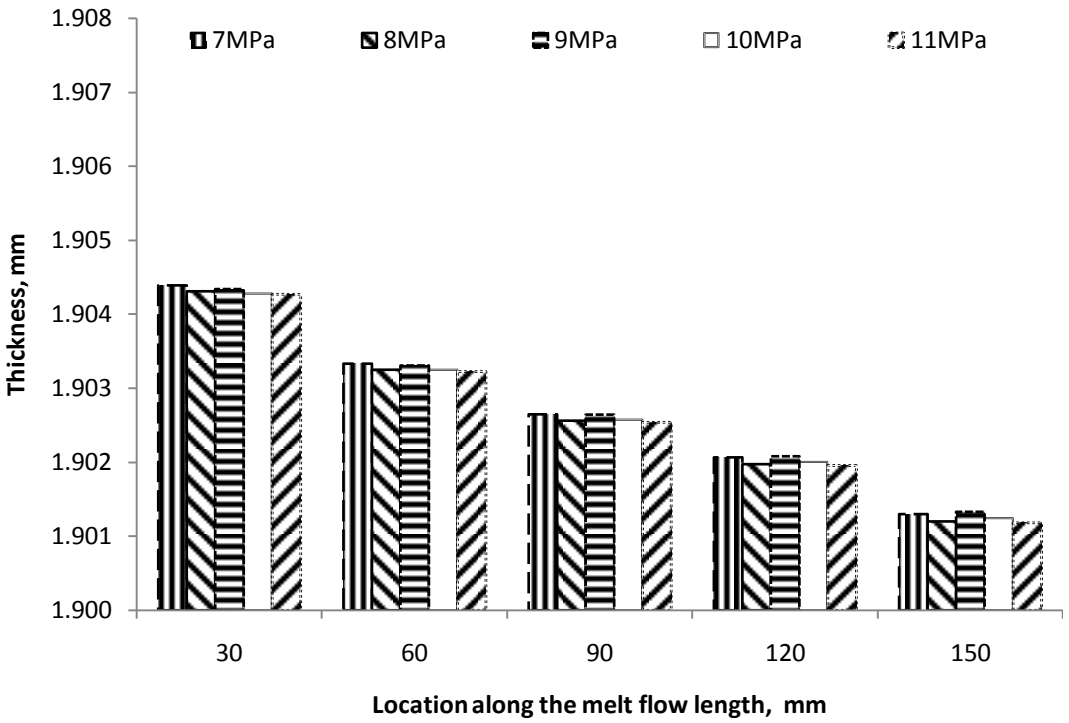

Figure 4.17: Effect of packing pressure on part thickness at melt temperature of 230 ℃

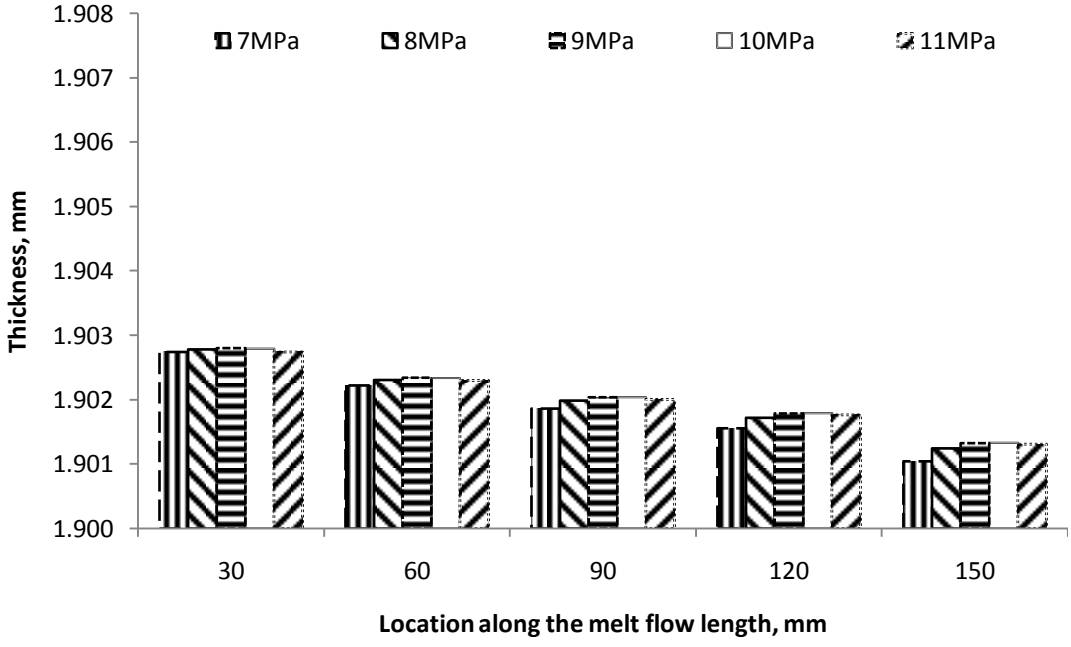

Figure 4.18: Effect of packing pressure on part thickness at melt temperature of 235 ℃

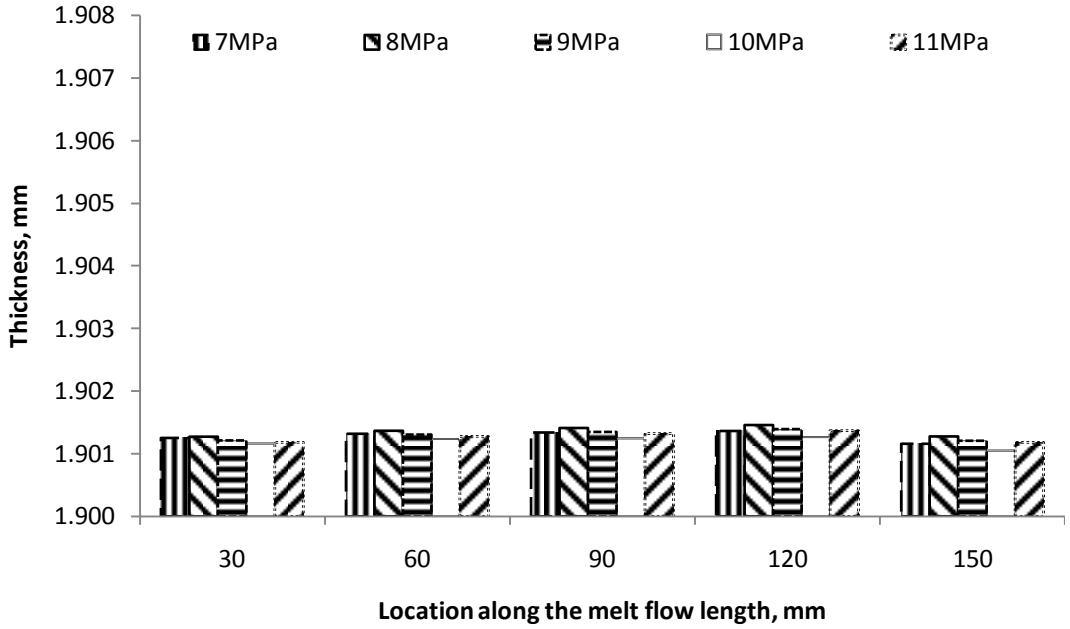

Figure 4.19: Effect of packing pressure on part thickness at melt temperature of 240 ℃

From Figures 4.15 – 4.18, the thickness of the plastic part was high at M1, which was the location nearest to the area where plastic was injected. The highest thickness recorded was 1.907, 1.906, 1.904 and 1.903 *mm* for the molding process using melt temperature of 220, 225, 230 and 235 ℃ respectively. All these readings were taken from M1. Where as for M5, the thickness reading was the smallest compared with other locations reading. The thickness value for this location was approximately 1.901 *mm* for molding using melt temperature of 220, 225, 230 and 235 ℃.

For injection molding using melt temperature of 240 ℃, the highest thickness value recorded for the plastic part was about 0.0005 *mm* greater than 1.901 *mm*, measured at M4. For other locations, the thickness readings were approximately same, 1.901 *mm.*

The results showed that the thickness of the plastic part was high at region near to the gate and low at region far from the gate for injection molding using lower melt

temperature. For molding using higher melt temperature, the reverse pattern was observed where the plastic part thickness was greater at region far from gate compared with the region near to the gate. Depending on the status and non linear behavior of polymer (HDPE), they will react differently at their respective position, temperature and pressure. Due to rapid cooling and solidification of the plastic melt when they touched the cold mold surface, most of the plastic at the end of cavity was hard to move due to the increase in viscosity and solidification resulting from heat loss. As a result, by using low melt temperature, the plastic melt at region far from gate will solidify first and become rigid. In this situation, the polymer melt added into the cavity during packing phase will be packed to the region near to the gate while the plastic melt here was still hot and with plenty of mobility.

Due to higher degree of mobility at higher melt temperature, the polymer melt can be sent into the cavity further as compared with molding using low melt temperature. The solidification rate can be extended in this situation. As the solification process was prolonged for plastic melt at region far from gate, the packing pressure applied can be used to move more plastic into the end of cavity as compared with injection molding using lower melt temperature. As a result, the thickness distribution for molding using melt temperature of 240 ℃ was more even as compared with others due to the better material distribution during the molding process.

The results as presented in Figures 4.15 – 4.19 also show that the thickness reading for point 1 to point 5 decreased with temperature. The Figure 4.14 also shows the same trend. Due to the natural behavior of polymer, they expanded when heated and shrunk during cooling. As a result, the amount of shrinkage increased with melt temperature. According to the law of polymer material, the injection molding should be conducted using

melt temperature as low as possible but not too low that the polymer melt cannot flow. But under this situation, where the plastic shape had high aspect ratio of thickness to melt flow length, this rule was not applicable. The molding using low melt temperature for plastic part as shown in **Error! Reference source not found.** will result in large thickness ariation across the part. To obtain better and more even plastic part, higher melt temperature must be used.

To eliminated the shrinkage associated with the molding using high melt temperature, it was recommended that the cavity was made larger than the actual size. To eliminate the large thickness variation associated with the injection molded plastic product using low melt temperature, it was recommended that either two or more gates were used instead of one.

4.2 Mold cavity-I product shrinkage by using two-way interaction approach

In this two-way interaction approach, both injection mass flow rate and injection melt temperature were varied at three different levels to investigate these two parameters effect on thickness distribution of the injection molded part. Five locations on the plastic part were chosen as the temperature and thickness measurement locations. These locations, as illustrated in Figure 3.2 were positioned along the flow length and transverse direction of the flow length. Along flow length direction have M10, M75 and M140 which were 10 *mm*, 75 *mm* and 140 *mm* respectively measured from gate location. The points of interest located along the transverse flow direction were L75, M75 and R 75 which were 10 *mm* and 50 *mm* measured from the left edge of the plastic part and 10 *mm* measured from the right edge of the plastic part. The numbers of experiments were reduced to nine. The injection mass flow rates used in this analysis were 0.01 *kg/s*, 0.03 *kg/s* and 0.05 *kg/s* and the melt temperatures used were 220 ℃, 230 ℃ and 240 ℃.

4.2.1 Mold filling analysis

The pressure and temperature in the mold cavity during mold filling had significant impact on part thickness since the quality of an injected part was directly reflected from the processing setting applied. As illustrated in Figure 3.14, a typical filling pattern with temperature distribution as simulated using the model described in Section 3.3.2 is presented in the figure. Under different injection mass flow rate and melt temperature, the temperature and pressure reading at M75 (50 *mm* measured from gate location and 50 *mm* measured from left edge of the plastic part) in the cavity during mold filling are presented in Figures 4.20 and 4.21. Other locations (M10, M140, L10 and L90) temperature and pressure readings are presented in Figures D-1 – D-8 in APPENDIX D.

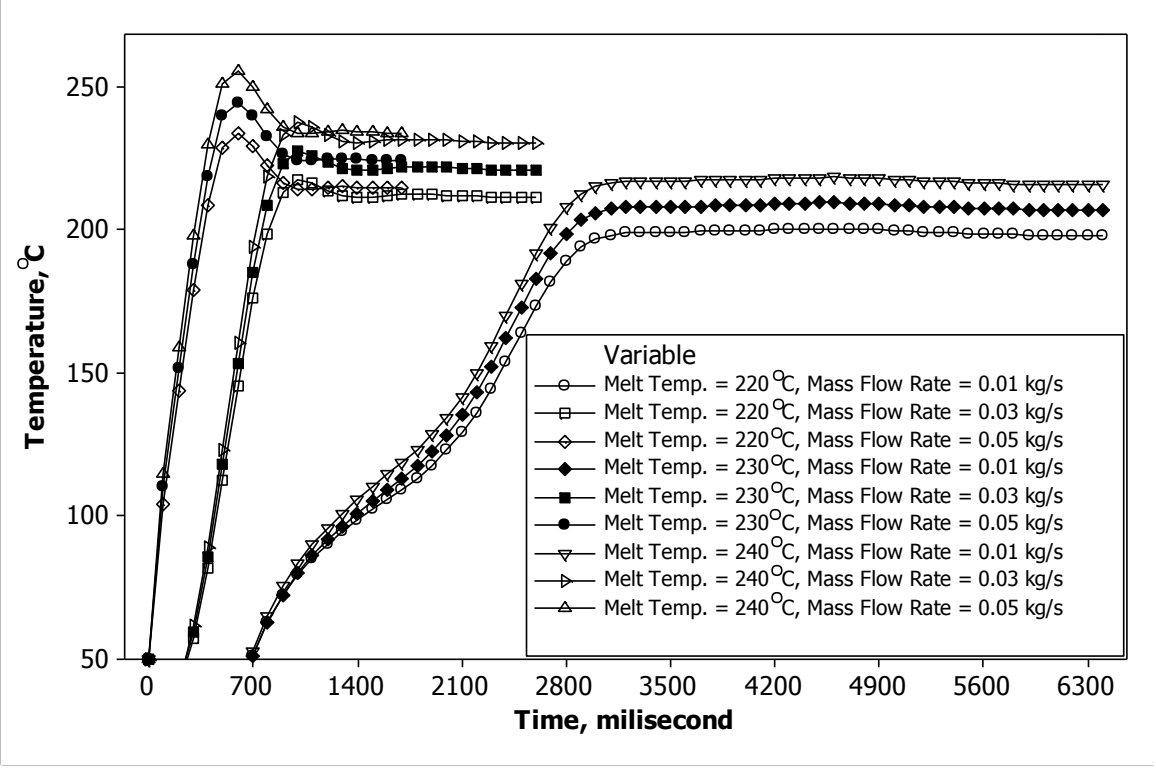

Figure 4.20: Plastic melt temperature at M75 during mold filing

Figure 4.20 shows the plastic melt temperature during injection molding for M75, which was one of the points of interest along the flow direction and situated at 75 *mm* away

from injection gate. Maximum temperature was used to indicate the arrival of plastic melt at the point of interest during mold filling. After 0.6 *s* of mold filling time, the maximum temperature was detected at this location for molding using melt temperature of 240 ℃ and injection mass flow rate of 0.05 *kg/s*. Under same injection mass flow rate but different injection melt temperature, the plastic melt speed was almost the same. For molding using injection mass flow rate of 0.05 *kg/s* but different injection melt temperature (220 and 230 ℃), the maximum melt temperature was also detected at 0.6 *s* since same mass flow rate was used. The melt speed using injection mass flow rate of 0.03 *kg/s* and 0.01 *kg/s* were 0.4 *s* and 2.4 *s* slower than that of molding procedure using injection mass flow rate of 0.05 *kg/s*. Along the flow direction, the arrival of plastic melt at distance of 10 *mm* from the gate were 0.3 *s* for molding using injection mass flow rate of 0.05 *kg/s* and 0.7 *s* for molding using injection mass flow rate of 0.01 *kg/s*. At 140 *mm* measured from injection gate and along the flow direction, the maximum temperature recorded at 1.7 *s* for molding using injection speed of 0.05 *kg/s* and different injection melt temperature ranging from 220 ℃ to 240 ℃. The melt speed for molding using injection mass flow rate of 0.03 *kg/s* was 0.9 *s* slower than the previous. The time taken for molding using injection mass flow rate of 0.01 *kg/s* to reach this position on the other hand was 6.4 *s*. The filling pattern as measured at L75 and R75 was almost identical with M75. All these locations were located along the transverse direction of the flow which respectively 10 *mm*, 90 *mm* and 50 *mm* measured from the bottom edge (as illustrated in Figure 3.2), shows almost the same maximum melt temperature, at the same flow time.

Along the flow direction, the pressure reading at 75 *mm* measured from the injection gate for molding using various processing parameter is depicted in Figure 4.21. Although under different melt temperatures but same injection mass flow rate, the recorded melt

speed was same but the pressure reading was not. The highest pressure recorded at this location were 12.22, 10.82 and 9.66*M Pa* for molding using same injection speed (0.05 *kg/s*) but different injection melt temperatures ranging from 220 to 240 ℃. The pressure reading decreased with melt temperature. The same thing applies for other locations of pressure reading. Under injection mass flow rate of 0.03 *kg/s*, the highest pressures recorded were 9.00, 8.00 and 7.12*M Pa* respectively for injection molding using melt temperature of 220, 230 and 240 ℃. The highest pressure built up in the cavity decreased with fall of injection mass flow rate. Under these temperatures but different injection mass flow rate (0.01 *kg/s*), the pressure recorded at this position was even lower, 5.40, 4.85 and 6.34*M Pa* lower than previous molding procedures using injection mass flow rate of 0.03 *kg/s* and 0.05 *kg/s*. Other locations pressure readings show the same trend. Along the transverse direction, near edge pressure reading was relatively lower than pressure reading at the middle region of the plastic part. Pressure reading at 90 *mm* away of the bottom edge of the plastic part as measured along the transverse direction was 0.7 – 2.6*M Pa* lower than pressure reading at 50 *mm* away from the bottom edge. Pressure reading at 10 *mm* away from the bottom edge of the plastic part as measured along the transverse of the plastic part was 1.1 – 5.0*M Pa* lower than pressure reading at 50 *mm* away from the bottom edge. The simulation pressure reading decreased along flow length since the pressure was converted into flow energy. The pressure reading at 10 *mm* away from injection gate as measured along the flow direction were 8- 37*M Pa* higher than pressure reading at 75 *mm* away from gate. Pressure reading at 75 *mm* as measured from injection gate was 3 – 12*M Pa* higher than pressure reading at 140 *mm* away from injection gate. Pressure loss was 97 – 99% along the flow length from injection gate area to the end of the cavity.

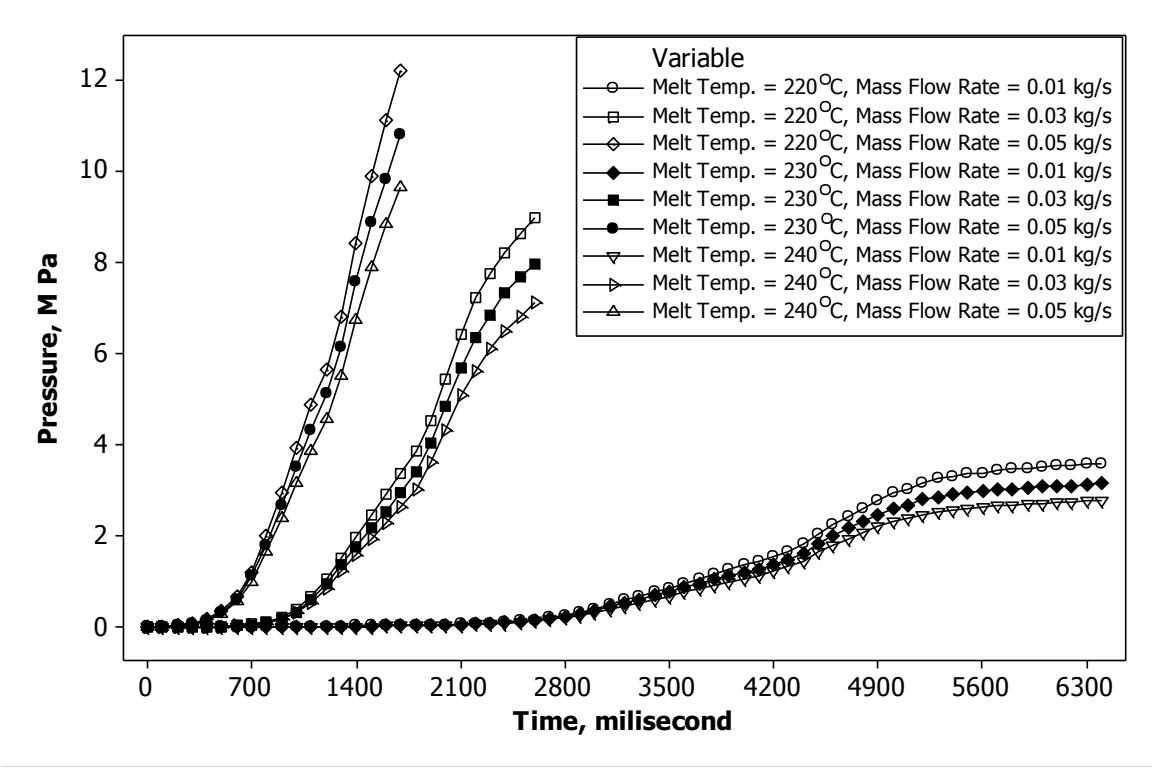

Figure 4.21: Pressure reading at M75 during mold filling

4.2.2 Shrinkage analysis

Based on the plastic melt temperature and the pressure acting on the interface in between fluid domain and solid domain, the thickness variation on M10, M75, M140, R75 and L75 as shown in Figure 4.22 was calculated using finite element method. The thickness was calculated using the mesh deformation as obtained from the finite element analysis. Under different injection mass flow rates and injection melt temperatures, the thickness variation as computed from the total mesh displacement in this finite element analysis is presented in Figure 4.22. As illustrated in this figure, the part thickness improved with injection mass flow rate since under this situation more material can be injected into the cavity with faster rate.

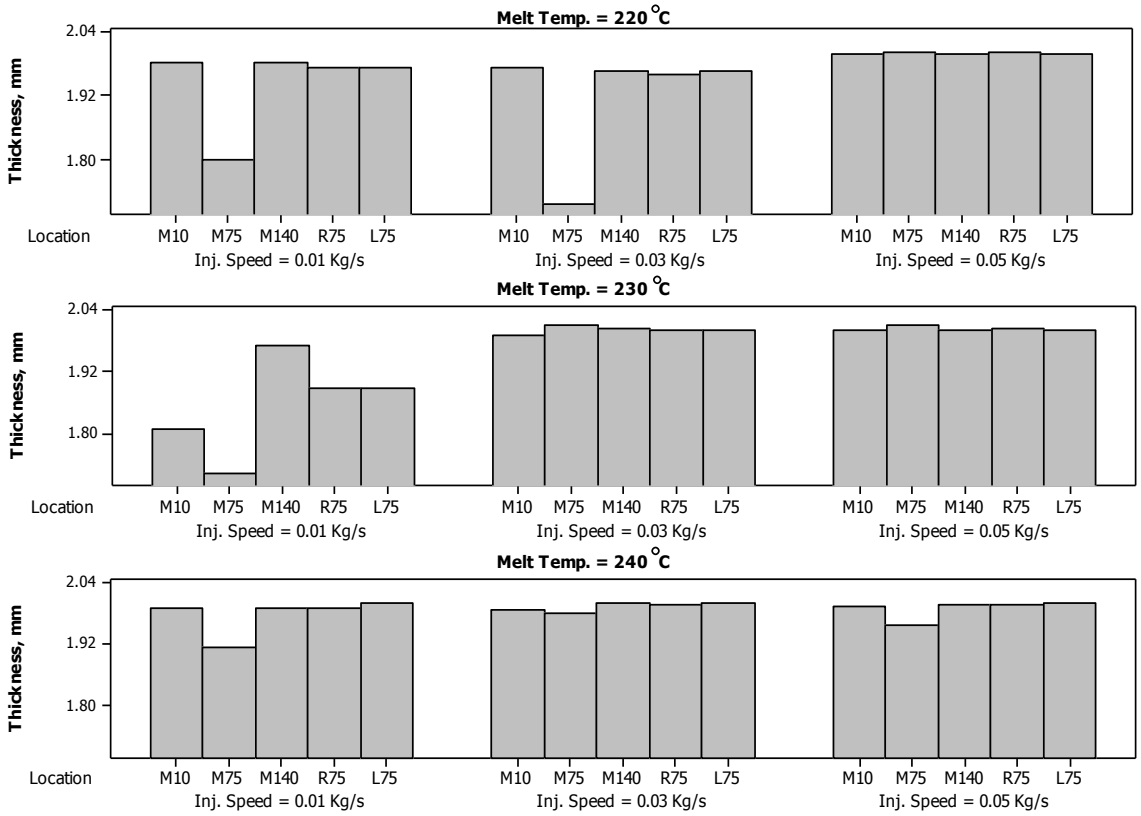

Figure 4.22: Plastic part thickness variation as obtained using different injection mass flow rates and injection melt temperatures

The part thickness was even and same with mold cavity thickness when injection mass flow rate was 0.05 *kg/s*. However, the thickness at distance of 10 *mm* and 75 *mm* away from the injection gate as measured along the flow direction were slightly lower than the actual part thickness when injection melt temperature was 240 ℃. At these locations, thicknesses were 1.99 and 1.96 *mm* respectively. Due to large shrinkage rate associated with high temperature plastic melt, slight shrinkage was found on these two locations even the injection mass flow rate applied was quite high. When injection mass flow rate was 0.01 *kg/s*: the part thickness were 1.80 – 1.98 *mm* when melt temperature was at 220 ℃; thickness were 1.72 – 1.89 *mm* for molding using melt temperature of 230 ℃; the part thickness were 1.91 – 2 *mm* when injection melt temperature was 240 ℃. Although part

thickness was low when low injection mass flow rate was used but certain improvement was made on the thickness distribution when melt temperature was adjusted from 220 ℃ to 240 ℃. The mobility of plastic melt increased with temperature. As a result, injection molding became easier although lower injection mass flow rate (0.01 *kg/s*) was used. Part thickness at 75 *mm* away from the injection gate as measured along the flow the direction was comparatively lower than other location thickness especially in the case where the melt temperature and injection mass flow rate were low. Thickness at this position was 1.80 *mm* when injection mass flow rate was 0.01 *kg/s* and melt temperature was 220 ℃. Thickness was even lower: 1.72 *mm* when injection mass flow rate was 0.03 *kg/s* and melt temperature was 220 ℃; thickness was also 1.72 *mm* too when injection mass flow rate was 0.01 *kg/s* and melt temperature was 230 ℃. Due to the plastic melt position which was located on the mid center section of the plastic part, the heat transfer rate was slower than other locations which near to the edge of mold cavity. As a result, the plastic melt in this region remained in molten state longer than other regions and resulted in higher shrinkage rate. Although the thickness on this location was low but the thickness improved with injection melt temperature and injection mass flow rate rise as a result of better temperature distribution. Thicknesses along the transverse direction were almost the same in all cases. Thicknesses at distance of 10 *mm* and 140 *mm* away from gate were almost the same in all cases but showing some difference in the case where the injection melt temperature and injection mass flow rate were 230 ℃ and 0.01 *kg/s*. In this case, part thickness at 140 *mm* away from gate was 0.16 *mm* higher than thickness measured at 10 *mm* away from injection gate. M10, M140, R75 and L75 were located at a distance of 10 *mm* from the edge of the mold cavity. The heat transfer rates for plastic melt at these positions were almost the same and thickness variation among them was not much.

The two-way interaction approach was a highly intelligent simulation model that can compute the effect of injection melt temperature and injection pressure on shrinkage with minimum data loss. However, it was not applied in the injection molding simulation of mold cavity-II since the boundary condition was not correct. In this simulation, only the deformations on the top and bottom surfaces of the plastic part were computed. In this situation, the entire plastic part was not allowed to shrink freely during the cooling process and results in significant data loss and error to the results obtained. As a result, effort was being paid on improving this current model before it was applied in injection molding simulation for mold cavity-II.

A typical example of mesh deformation as obtained from the simulation analysis is presented in Figure 4.23.

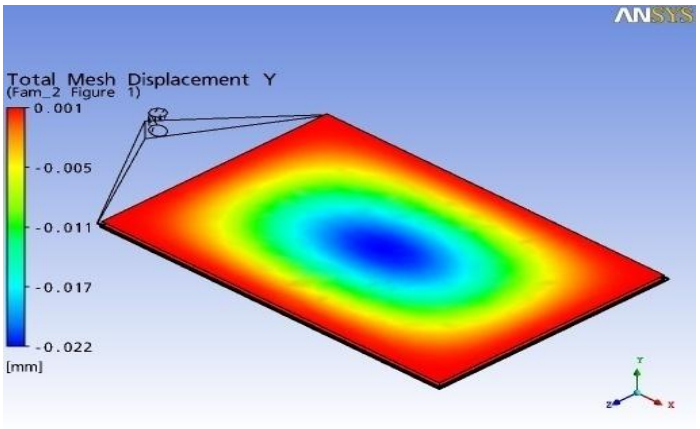

Figure 4.23: Mesh deformation of the interface in between fluid domain and solid domain

4.3 Mold cavity-II product shrinkage

The plastic product shrinkage of mold cavity-II was analyzed by using finite element analysis via one-way interaction approach. An initial guess on the molding parameter settings was made to predict the behavior of the plastic melt during mold filling and their effect on temperature distribution, pressure distribution and thickness distribution. Then

suitable parameter setting was used for the injection molding process. Before the experiment was conducted, the predicted simulation on temperature distribution and shrinkage were verified experimentally using the same injection molding processing parameter.

To optimize the parameter setting obtained from simulation, statistical tools including Taguchi method and ANOVA were used to assist the experimental study on plastic injection molding process. The obtained variables values for injection molding were varied at three levels to find out the best molding setting for plastic injection molding. Five three levels factors namely injection speed (**A**), melt temperature (**B**), packing pressure (**C**), cooling time (**D**) and packing time (**E**) were selected to investigate the effect of processing parameter on plastic part shrinkage in the experiment. The parameters used and their level value are listed in Table 3.5. The interaction effect between selected factors on shrinkage was studied in this experiment. The best molding condition for producing minimum part shrinkage was determined by using Taguchi method and the influence of each individual controlling factor on shrinkage was determined by using ANOVA analysis.

4.3.1 Mold filling of mold cavity-II

Figure 4.24 shows the initial guess simulation result on mold filling of TOYOLAC 250 ABS by using injection speed of 40 *mm/s* and melt temperature of 250 ℃. This figure shows that the molten plastic remained hot at the barrel and sprue region, about 250 ℃. The temperature of the plastic melt dropped very fast once entering the runner region. The temperature of the plastic was about 150 ℃ at gate region. The temperature difference between the plastic melt temperature at barrel and those at the gate region was around 100 ℃. At the middle section of the cavity, the plastic melt temperature was even lower, at about 120 ℃. At region near to the end of the cavity, the plastic melt temperature was 40 ℃.

Due to the heat transfer of the plastic melt once they touch the cold mold surface; the plastic melt energy was dissipated out to the room environment. As a result, the viscosity of the plastic melt became higher and the flow speed will reduce with the viscosity rise. As a result, the time required by the plastic to flow from the barrel to gate only took 1.30 *s* but the time required to fill the entire cavity took about 3.2 *s* as a result of the speed reduction of the plastic melt due to temperature falls.

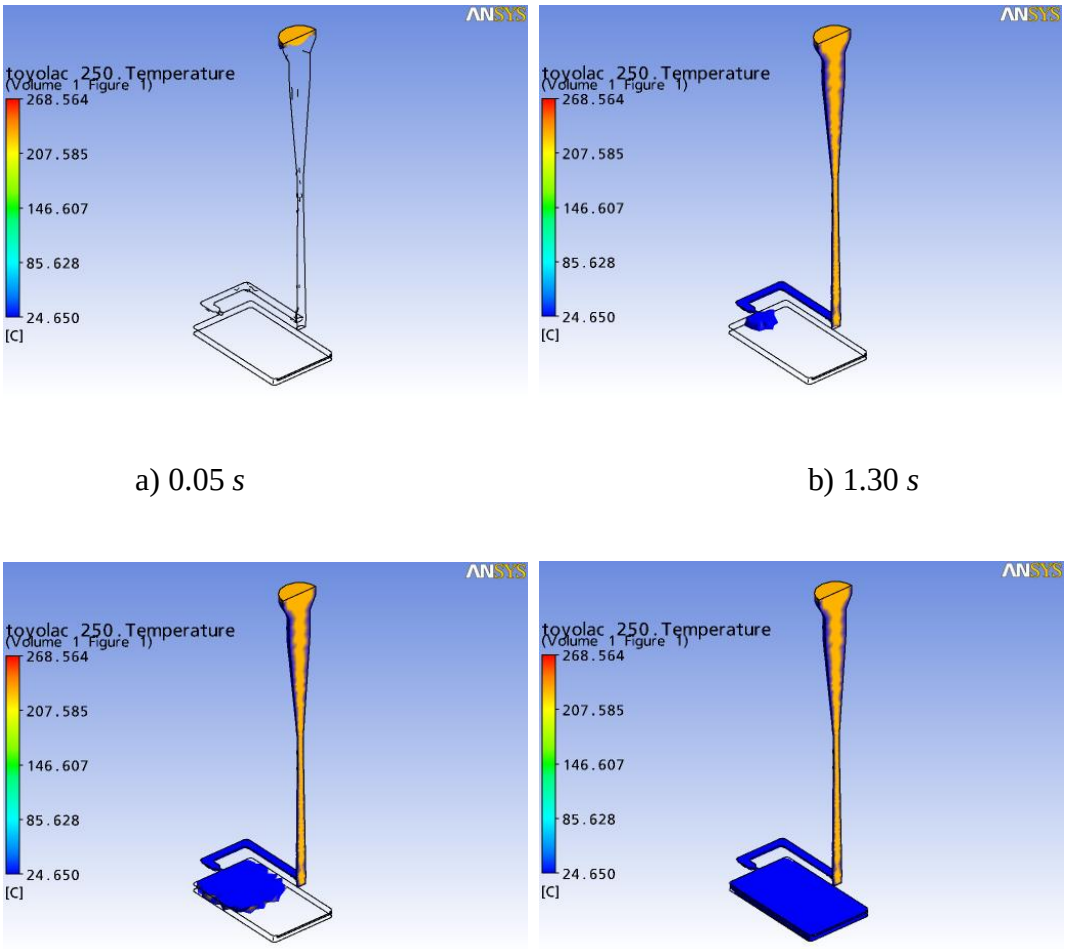

a) 0.05 *s* b) 1.30 *s*

c) 2.00 *s* d) 4.50 *s*

Figure 4.24: Flow front of plastic melt for mold cavity-II at different time intervals: a) 0.05 *s*, b) 1.30 *s*, c) 2.00 *s* and d) 4.50 *s*

Figure 4.25 shows the pressure distribution of TOYOLAC 250 ABS by using injection speed of 40 *mm/s* and 230 ℃. As presented in this figure, the mold filling was relatively smooth initially for the first two seconds. From the barrel to gate of the rectangular cavity, the time taken was just 1.3 *s*. The time taken from gate to the mid section of the cavity was 0.7 *s*. The required filling time from mid section of the cavity to end of cavity was 2.5 *s*. The plastic melt speed decreased when approaching the end of the cavity. The plastic melt became hard to move as the viscosity significantly increased at this area as the melt temperature decreased after travelling for a long distance. Moreover, the frozen layer and air trap acted as obstruction for the plastic melt to advance into the end of the cavity.

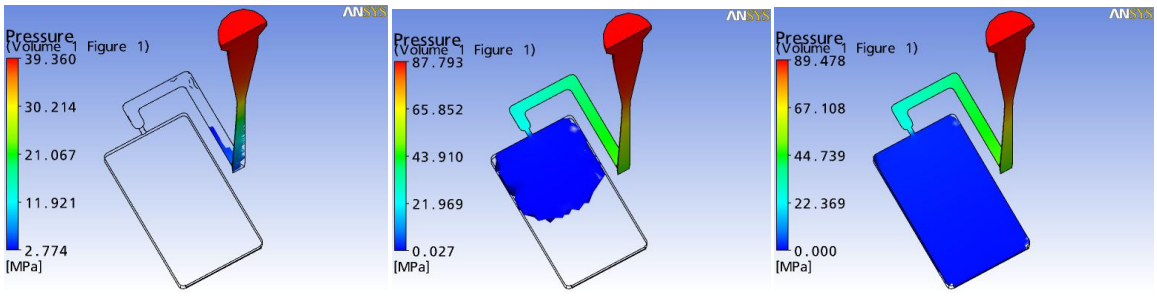

(a) 1 *s* (b) 2 *s* (c) 4.5 *s*

Figure 4.25: Pressure distributions at different time interval by using plastic injection speed of 40 *mm/s* and different plastic injection melt temperatures of 230 ℃

The simulation result on temperature distribution and pressure distribution showed that the initial guess molding parameter was suitable for mold cavity-II injection molding. The required injection pressure was 89.478*M Pa* which was within injection molding machine, BOY 22M capacity. The entire cavity can be completely filled by using injection speed of 40 *mm/s* and injection melt temperature of 230 ℃. This showed that the plastic melt had enough liquidity to be injection molded at these temperature and injection speed.

4.3.1.1 Verification of the simulation prediction on plastic melt temperature in the cavity during injection molding

A verification test was performed to compare the predicted result on injection melt temperature during injection molding with experimental result by using the same processing parameter and the result is presented in Figure 4.26. The processing parameters used were injection speed of 40 *mm/s*, melt temperature of 230 ℃, packing pressure of 10 *M Pa*, cooling time of 15 *s* and packing time of 10 *s*. For experimental result, the temperature in the cavity during injection molding was recorded by using a thermocouple at locations Y1, Y2 and Y3 as illustrated in Figure A-1 in APPENDIX A. These locations were situated along the flow direction which was respectively at 5 *mm*, 33.5 *mm* and 62 *mm* as measured from gate. The predicted temperatures were also retrieved at these positions.

As illustrated in Figure 4.26, both simulation and experimental results are almost the same. Due to the slight delay of the thermocouple sensitivity, the temperature obtained from the thermocouple showed staggered increment pattern. For simulation, the temperature in the cavity started to increase after 0.7 *s* for Y1, 1.3 *s* for Y2 and 2 *s* for Y3. On the hand, for experimental result, the temperature starts to increase after 0.65 *s* for Y1, 1.2 *s* for Y2 and 2 *s* for Y3. The travelling speed of plastic melt for experimental result was slightly faster than the result predicted by finite element analysis; however they were almost the same. The temperature reading from this figure can be used to describe the mold filling behavior of plastic injection molding. When the temperature started to increase, it acted as a good indication that the plastic melt had arrived at the recorded position. Y1 was the nearest point to gate and plastic melt will came across at this location first before Y2 and Y3. Y3 was the farthest location measured from gate and the plastic melt took about 2 *s* to reach here.

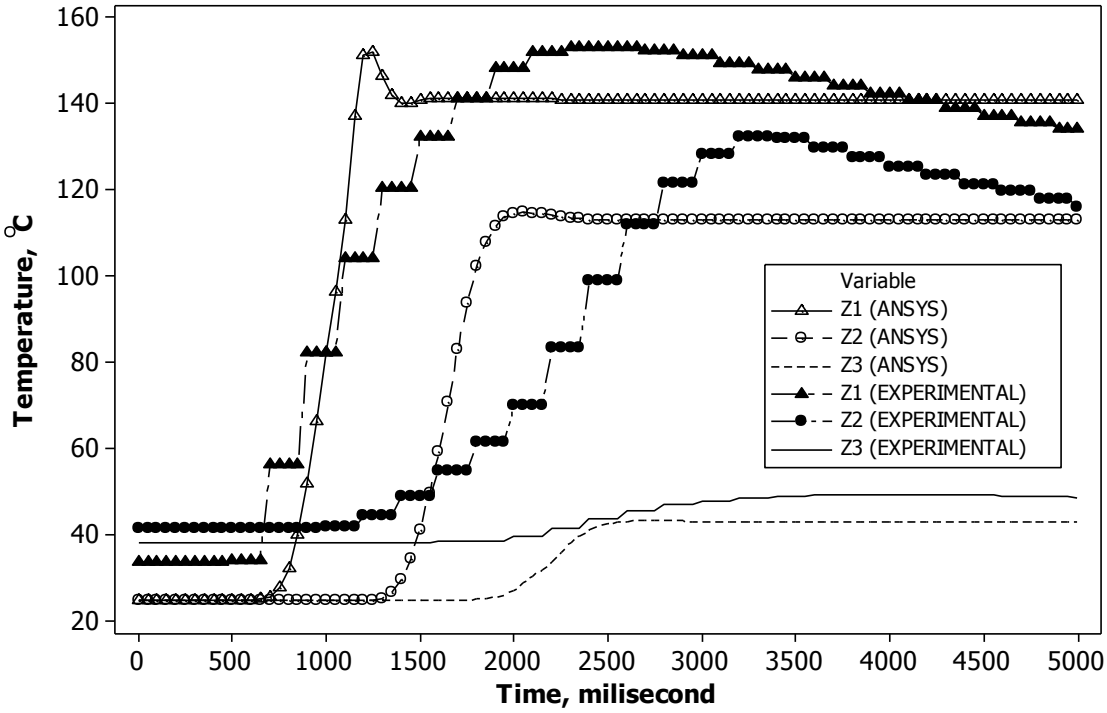

Figure 4.26: Temperature reading at different position in the mold cavity during injection molding

It is apparent that the recorded temperature reading for experimental result is relatively higher than finite element analysis prediction. At Y1, the highest temperature recorded was 153.0 ℃ for experimental result and 151.0 ℃ for finite element analysis prediction. The highest temperature recorded for Y2 was 132.3 ℃ for experimental result and 114.5 ℃ for finite element analysis. For Y3, the highest temperature readings were 49.6 ℃ and 43.4 ℃ for experimental result and finite element analysis prediction respectively. The largest temperature difference between both results was 17.8 ℃ for Y2 but for other locations, the temperature difference was below 7 ℃.

4.3.2 Finite element analysis of mold cavity-II plastic product shrinkage

A typical mold cavity-II product shrinkage predicted by using finite element analysis is presented in Figure 4.27. The undeformed mesh which is in white color was used to illustrate how the material (blue color) shrunk during the cooling process.

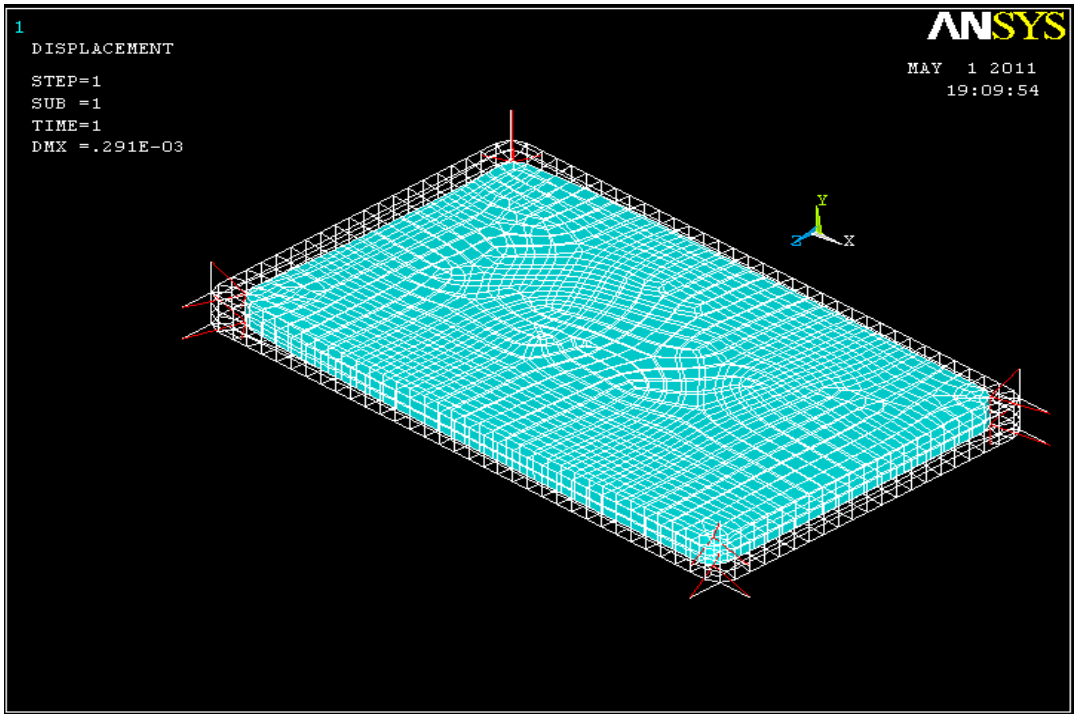

Figure 4.27: Example of a typical product shrinkage of mold cavity-II as obtained from ANSYS 12.1 finite element analysis

Figure 4.28 shows the thickness along the flow direction at three different locations, which respectively were Y1, Y2 and Y3 as illustrated in Figure A-1 for both simulation and experimental results. The plastic part was molded using injection speed of 40 *kg/s*, injection melt temperature of 250 ℃, packing pressure of 10*M Pa*, cooling time of 15 *s* and packing time of 10 *s*. As illustrated in this figure, the prediction made by the simulation on part thickness was slightly higher than experimental thickness value. At Y1, Y2 and Y3 which respectively were 5 *mm*, 33.5 *mm* and 62 *mm* as measured from the injection gate location,

the thickness values were respectively 3.96 *mm*, 3.97 *mm* and 3.97 *mm*. The experimental thickness values at these locations were respectively 3.77 *mm*, 3.93 *mm* and 3.78 *mm*. The simulation prediction over predicted the experimental result by 1 – 4.8%.

Although the simulation prediction was not exactly the same as experimental result but it served as a good initial guess on injection molding setting for a typical injection molding process. As a result, in the next section the initial guess parameter setting on injection speed, injection melt temperature, packing pressure, cooling time and packing pressure were varied at three levels according to an orthogonal array to optimize the processing condition by using Taguchi and ANOVA analysis.

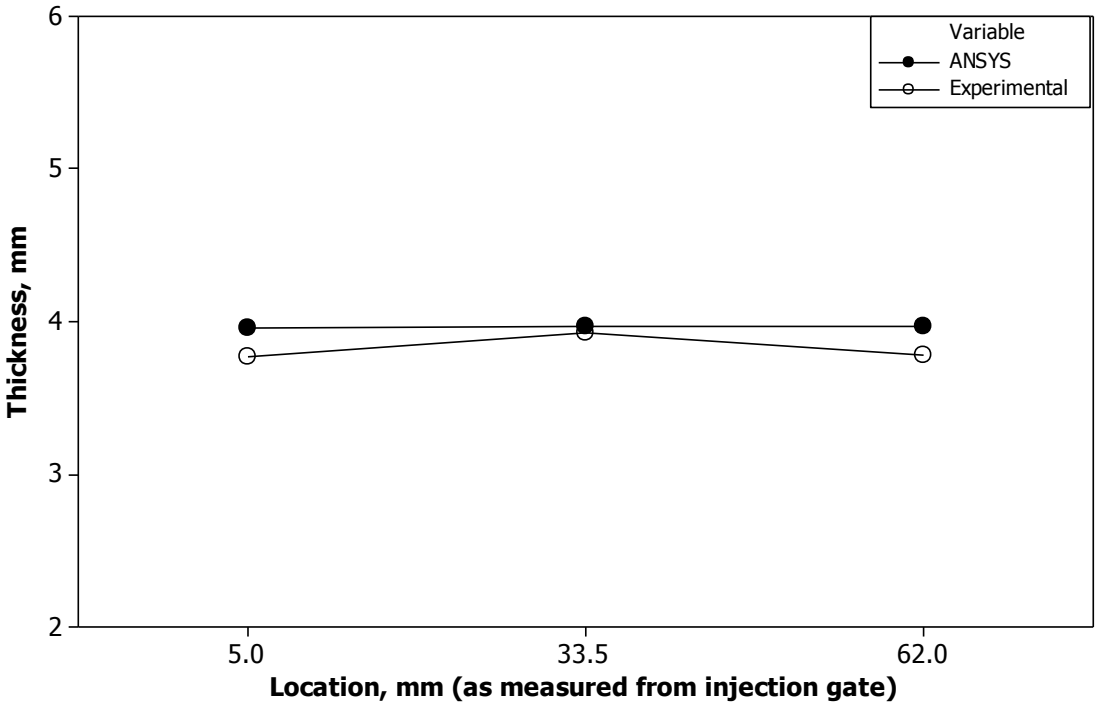

Figure 4.28: Thickness along the flow directions measured from injection gate for both simulation and experimental result

4.3.3 Optimization of mold cavity-II product shrinkage

The experimental analysis on product shrinkage was performed according to an L27 orthogonal array as discussed previously in Section 3.5. Based on the previous initial guess result on injection molding parameter setting, the injection speed was varied from 40 to 60 *mm/s*, injection melt temperature was varied from 230 to 250 ℃, packing pressure was varied from 40 to 60 *mm/s*, cooling time was varied from 10 *s* to 20 *s* and packing time was varied from 5 *s* to 15 *s*. These variables were varied at three levels as illustrated in Table 3.5. The result obtained is presented in Table C-2. Three repetitions of experimental run were conducted for each set of combination and the shrinkage values as presented in Table C-2 shows excellent repeatability of data for molding using same injection molding parameter. The variation on repetition of data for the same injection molding condition was below 6.5%. Different shrinkage values were obtained for various injection molding conditions and the minimum shrinkage was 2.5% as obtained from 13th experimental run out of the 27 experiments. On the other hand, the maximum shrinkage was 8.5% as obtained from the 25th experimental.

4.3.3.1 S/N analysis for experimental result

The S/N response diagram for experimental result is presented in Figure 4.29. The best combination of parameters for minimum part shrinkage was $\mathbf{A_2B_2C_1D_3E_2}$ namely an injection speed of 50 *mm/s*, melt temperature of 230 ℃, packing pressure of 9*M Pa*, cooling time of 20 *s* and packing time of 10 *s*. The difference in S/N ratio for a factor was used to denote which factor was significant for shrinkage in this analysis too. As illustrated in Figure 4.29, cooling time was the most significant factor on controlling shrinkage problem since the S/N ratio difference was large. Injection speed and melt temperature are also considered to be significant factors because the difference in S/N ratio for these two factors

were also quite large. Conversely, both packing time and packing pressure were not considered as significant factors as the S/N ratio difference for these two factors were low compared with other three factors.

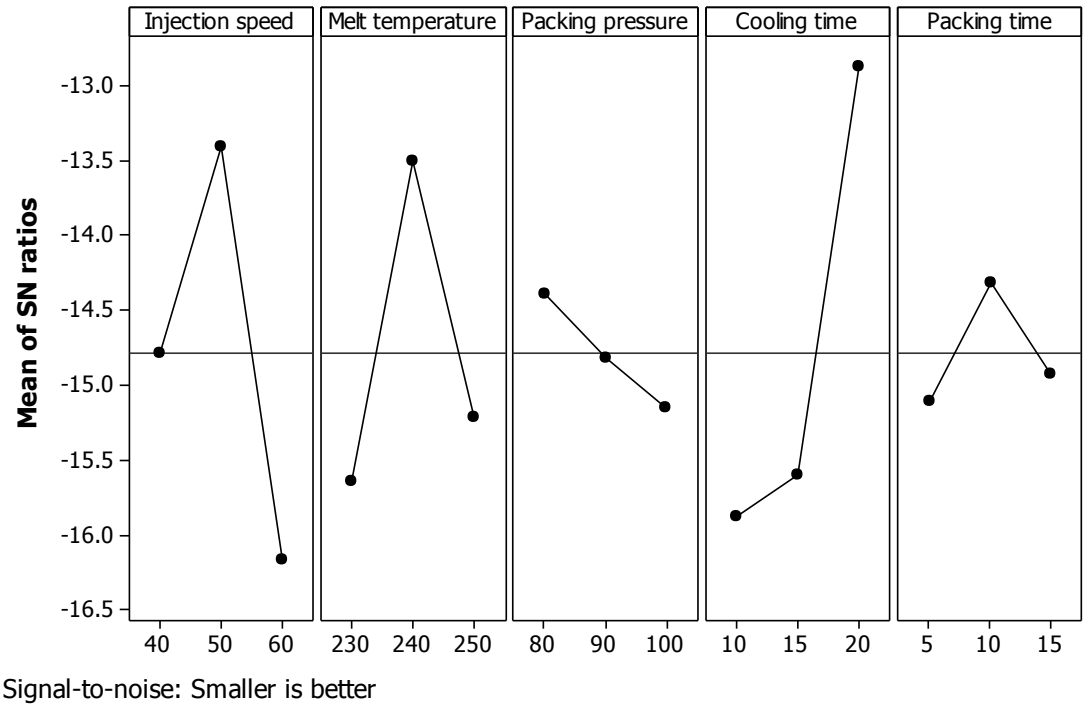

Figure 4.29: Main effects plot for experimental result

Figure 4.30 shows the interaction plot of experimental result. As shown in this figure, the interaction between melt temperature and packing pressure and the interaction between injection speed and packing pressure are significant because there were intersections among the S/N response lines of the control factors. For the third interaction plot between injection speed and melt temperature, the response line for melt temperature of 240 ℃ was completely not touching with other two response lines, hence the interaction between these two factors was not significant. To more quantitatively analyze the experimental result, ANOVA was performed in the next section.

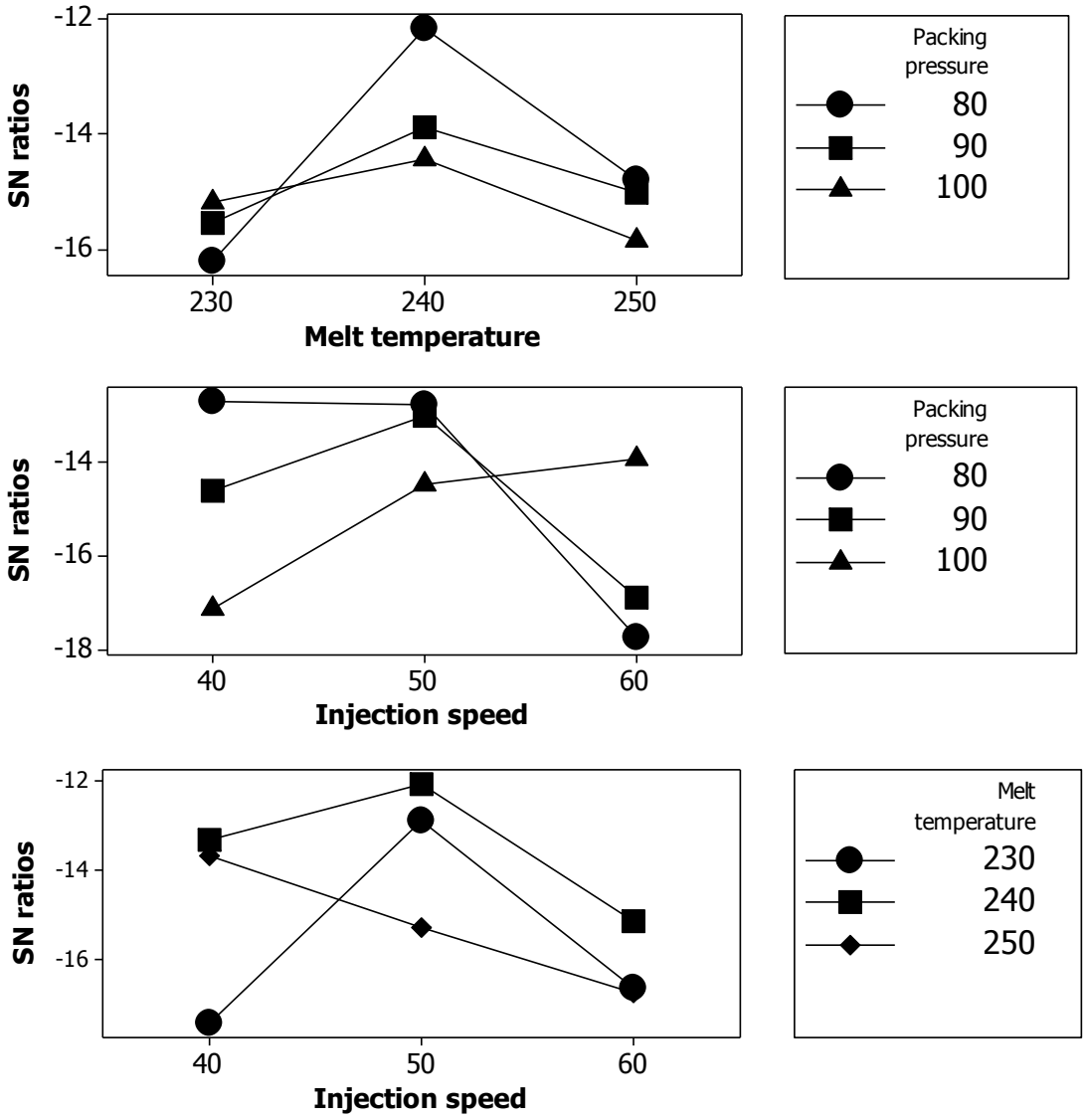

Figure 4.30: Interaction plot for experimental result

4.3.3.2 ANOVA analysis for experimental result

The ANOVA analysis for experimental result is presented in Table 4.1. The purpose of the analysis of variance (ANOVA) was to determine the ratio percentage of affecting parameters on the part shrinkage. It was apparent that *F* value calculated of factor **A**, factor **B** and factor **E** were all greater than the *F*-table value. As a result, they were considered to be significant and they were injection speed, melt temperature and cooling time. The

significant factor from this analysis was same with the significant factors obtained in S/N analysis in the previous section.

Table 4.1: ANOVA analysis for experimental result

Source	DF	SS	V	*F*-table	*F*	Contribution (%)
Injection speed (A)	**2**	**34.384**	**17.192**	**4.325**	**7.030**	**15.81**
Melt temperature (B)	**2**	**23.174**	**11.587**	**4.325**	**4.740**	**10.66**
Packing pressure (**C**)	2	2.650	1.325	4.325	0.540	1.22
Cooling time (D)	**2**	**49.817**	**24.908**	**4.325**	**10.180**	**22.91**
Packing time (**E**)	2	2.089	1.544	4.325	0.630	0.96
Injection speed × Melt temperature (**A**x**B**)	4	29.341	7.355	4.107	3.000	13.49
Injection speed × Packing pressure (AxC)	**4**	**56.056**	**14.014**	**4.107**	**5.730**	**25.78**
Melt temperature × Packing pressure (**B**x**C**)	4	9.137	2.284	4.107	0.930	4.20
Residual error	4	9.787	2.447			4.50
Total	26	217.436				100

Packing pressure and packing time were not significant factor in this analysis. Cooling time was the most significant factor and the degree of this effect on shrinkage is 22.9%. Injection speed and melt temperature effect on shrinkage on the hand, are 15.8% and 10.7% respectively.

The interaction effect of factor **A**, factor **B** and factor **C** was analyzed by using this analysis tool too. The factors selected for this study were injection speed, melt temperature and packing pressure as discussed previously. By using 90% confident level, only the interaction between injection speed and packing pressure was significant as the *F* value obtained was larger than the *F*-table value. As discussed previously in the previous Section 4.11, the interaction between melt temperature and packing pressure was considered

significant too. But after running this analysis, this interaction effect on shrinkage was not strong enough to be included as one of the significant interaction.

4.3.3.3 Confirmation test for experimental result

A confirmation experimental was executed at the optimum combination of factor levels to verify the validity of the results of the Taguchi analysis. At first, the significant factors were chosen from process parameters based on the prediction of S/N ratio at optimum combination of parameters. The optimum combination of parameters for minimum shrinkage was $\mathbf{A_2B_2C_1D_3E_2}$ as discussed previously. The most significant factor was cooling time (**D**), then followed by injection speed (**A**) and melt temperature (**B**). As the factors **A**, **B** and **D** were considered significant, the performance at the optimum condition will be estimated using only these three factors. The results of the confirmation test for optimum factor combination were then compared with the predicted value to verify the validity of the Taguchi L27 experiment. The average S/N ratio, $\bar{T}$ was -14.79 as illustrated in Table C-2 and the confirmation experimental was performed as follows:

$$n_{CT} = \bar{T} + (\bar{\boldsymbol{D}}_3 - \bar{T}) + (\bar{\boldsymbol{A}}_2 - \bar{T}) + (\bar{\boldsymbol{B}}_2 - \bar{T}) \quad (4.1)$$

where n_{CT} was used to denote the signal to noise ratio calculated from the confirmation test. The calculated n_{CT} value was -10.20 which corresponded to shrinkage value of 3.2%. The calculated n value was almost identical with the shrinkage value at optimum processing parameters which was 2.5%. The difference between them was just 0.7% and hence it can be concluded that the experimental result obtained by using Taguchi and ANOVA analysis was valid too.

4.3.4 Effect of significant parameters on shrinkage

From Taguchi and ANOVA analysis, the optimum processing parameter were injection mass flow rate of 50 *kg/s*, melt temperature of 240 ℃, packing pressure of 8*M Pa*, cooling time of 20 *s* and packing time of 10 *s*. Shrinkage at these molding conditions was 2.5%, which corresponding to 0.102 *mm*. Compared with the initial guess processing parameter which were injection speed of 40 *kg/s*, injection melt temperature of 250 ℃, packing pressure of 10*M Pa*, cooling time of 15 *s* and packing time of 10 *s*, the experimental result showed that there was significant difference between the initial guess parameter setting and optimum processing parameter setting for minimum shrinkage.

The initial guess on mass flow rate and cooling time were respectively 10 *kg/s* and 5 *s* lower than the best processing parameter. This indirectly means that the mass flow rate must be high enough for the cavity-II molding so that the plastic melt can fill the entire cavity before solidification. Slow injection mass flow rate can result low thickness value at the end of the cavity because of the cold plastic material at the end of the cavity experience difficulty to move as the viscosity increased and injection force decreased at this region. In addition, the best processing parameter for minimum shrinkage showed that the cooling time must be higher for injection molding. During mold cooling, the plastic part was constrained by the mold cavity shape. Moreover, the plastic material will have higher strength before ejection if the cooling time was long enough for solidification. As a result, shrinkage will be lowered if the cooling time was long enough.

The initial guess on packing pressure and melt temperature were respectively 2*M Pa* and 10 ℃ higher than the best processing parameter packing pressure and melt temperature. Theoretically, the higher the packing pressure the better the part shrinkage. Due to the small dimension of the gate (1 *mm* thick), high pressure did not have much effect on part

shrinkage. It was believed that the plastic material at the gate will solidified very fast as a result of the large heat transfer versus small dimension of the gate plastic material. If the molten material had solidified, the additional packing pressure will have no effect in densifying the molten material in the cavity. The applied melt temperature must be lower according to the Taguchi and ANOVA analysis. Although, the plastic melt had lower viscosity and better mobility at high melt temperature but the density at the same time will decrease with applied temperature. As a result, the plastic melt temperature must be lower so that more material can be injected into the cavity but not too low that the molten plastic cannot move.

Both initial guess and best processing parameter showed that the packing time was 10 *s*. However, this variable was not significant factor for cavity-II molding. As discussed previously, packing pressure had no effect on reducing the shrinkage problem due to the small dimension of the gate. As a result, the packing period applied had no effect on reducing the shrinkage as well. As a solution to this, the size of the gate must be enlarged so that more material can be added into the cavity during packing to reduce as much shrinkage as possible.

4.4 Summary

From analysis obtained from one-way interaction approach for mold cavity-I, it was found that the fan gate used has resulted in uniform plastic melt speed and temperature distribution. The simulation result for mold cavity-I was compared with previous researcher's experimental result. Both results showed almost identical thickness distribution. The plastic product shrinkage of mold cavity-I was found to increase with melt temperature. Evenness of the plastic product was found to increase with plastic melt temperature. The thickness distribution showed that the thickness of the plastic part was

high at region near to the gate and low at region far from the gate for injection molding using lower melt temperature. For molding using higher melt temperature, the reverse pattern was observed where the plastic part thickness was greater at region far from gate compared with the region near to the gate. The thickness distribution for molding using high melt temperature was more even. From the result obtained from two-way interaction approach for mold cavity-I, it was found that the plastic product had no shrinkage at all when high injection mass flow rate. The shrinkage improved with melt temperature when low mass flow rate was used. Thickness at the central location of the plastic part was found to be lowest compared with other locations which were near to edge of the plastic part. From the optimization of mold cavity-II plastic product, it was found that the packing pressure and packing time as insignificant. In contrast, injection speed, melt temperature and cooling time were significant. The best combination of parameters for minimum part shrinkage were injection speed of 50 *mm/s*, melt temperature of 230 ℃, packing pressure of 9*M Pa*, cooling time of 20 *s* and packing time of 10 *s*.

CHAPTER 5: CONCLUSION & RECOMMENDATIONS

5.1 Conclusions

The following conclusions can be made on the basis of finite element analysis and experimental verification of melt temperature and product shrinkage in injection molding:

- According to the result obtained by using one-way interaction approach, the plastic product shrinkage of mold cavity-I was found to increase from 4.7-4.8% to 4.9-5.0% when the melt temperature used adjusted from 220 ℃ to 240 ℃. The evenness of the plastic product was found to increase with plastic melt temperature.
- From two-way interaction approach result for mold cavity-I, it was found that the plastic product had no shrinkage at all when high injection mass flow rate, 0.05 *kg/s* was used. As low mass flow rate, 0.01 *kg/s* was used, the shrinkage improved with melt temperature. Shrinkage was 1 – 10% when melt temperature was 220 ℃, shrinkage was 5.5 – 14% when melt temperature was 230 ℃ and shrinkage was 0 – 4.5% when melt temperature used was 240 ℃. Thickness at the central location of the plastic part was found to be lowest compared with other locations which were near to edge of the plastic part.
- From the comparison between previous researcher result and simulation prediction made by one-way interaction approach, It was found that the plastic melt speed during injection molding for both results were almost the same. The plastic melt flow of experimental study was slightly faster than the simulation prediction, about 0.05 – 0.10 *s* faster than the simulation prediction. The recorded temperature was

relatively higher than the simulation, 8 – 18 ℃ higher than the simulation. One-way interaction approach model under predicted the experimental plastic part shrinkage. However the differences between them were 1 – 4.8%, less than 5%.

- It was found that both packing pressure and packing time as insignificant because the dimension of the injection gate in this study was too small. The plastic in the gate region cooled down and solidified very fast to the extent that the packing pressure had no more important function on pushing more material into the cavity during packing phase.

5.2 Recommendation for future works

- Recommendation of the use of intel fortran to modify the governing equation for density and solidification in one-way interaction approach to include the effect of compressibility effect due to holding and packing pressure in injection molding simulation.
- Since two-way interaction can calculate the structural deformation of solid material due to hydraulic force, it is recommended that this model to be used in injection forming or hydraulic forming process to study sheet metal forming process.
- It is recommended that pressure transducer to be used together with thermocouple to monitor the behavior of the plastic melt in the cavity during injection molding so that more detail output can be obtained to estimate the best processing parameter for an injection molding process.

REFERENCES

ANSYS. (2006). ANSYS CFX-Solver Theory Guide (Version 11.0). Canonsburg.

Bikas, A., Pantelelis, N., & Kanarachos, A. (2002). Computational tools for the optimal design of the injection moulding process. *Journal of Materials Processing Technology, 122*(1), 112-126.

Cengal, Y. A., & Cimbala, J. M. (2006). *Fluid Mechanics* (1st ed.). New York: McGraw-Hill.

Chen, X., & Gao, F. (2003). A study of packing profile on injection molded part quality. [doi: DOI: 10.1016/S0921-5093(03)00290-9]. *Materials Science and Engineering A, 358*(1-2), 205-213.

Chen, X., Gao, F., & Chen, G. (2004). A soft-sensor development for melt-flow-length measurement during injection mold filling. *Materials Science and Engineering A, 384*(1-2), 245-254.

Choi, D.-S., & Im, Y.-T. (1999). Prediction of shrinkage and warpage in consideration of residual stress in integrated simulation of injection molding. [doi: DOI: 10.1016/S0263-8223(00)00045-3]. *Composite Structures, 47*(1-4), 655-665.

Galantucci, L. M., & Spina, R. (2003). Evaluation of filling conditions of injection moulding by integrating numerical simulations and experimental tests. [doi: DOI: 10.1016/S0924-0136(03)00276-0]. *Journal of Materials Processing Technology, 141*(2), 266-275.

Dimla, D.E., Camilotto, M,. & Miani, F. (2005). Design and optimization of conformal cooling channels in injection moulding tools. [doi: 10.1016/j.jmatprotec.2055.02.162]. *Journal of Materials Processing Technology, 164-165*(0), 1294-1300.

Dumitrescu, O. R., Baker, D. C., Foster, G. M., & Evans, K. E. (2005). Near infrared spectroscopy for in-line monitoring during injection moulding. [doi: 10.1016/j.polymertesting.2004.10.003]. *Polymer Testing*, 24(3), 367-375

Galantucci, L. M. & Spina, R. (2003). Evaluation of filling conditions of injection moulding by integrating numerical simulations and experimental tests. [doi: 10.1016/S0924-0136(03)00276-0]. *Journal of Materials Processing Technology, 141*(2), 266-275.

Hassan, H., Regnier, N., Pujos, C., Arquis, E., & Defaye, G. (2010). Modeling the effect of cooling system on the shrinkage and temperature of the polymer by injection molding. [doi: DOI: 10.1016/j.applthermaleng.2010.02.025]. *Applied Thermal Engineering, 30*(13), 1547-1557.

Huang, H. C., & Usmani, A. S. (1994). *Finite Element Analysis for Heat transfer - Theory and Software*. London: Springer

Hwang, S.-s., Hsu, P. P., & Chiang, C.-w. (2008). Shrinkage study of textile roller molded by conventional/microcellular injection-molding process. [doi: DOI: 10.1016/j.icheatmasstransfer.2008.02.011]. *International Communications in Heat and Mass Transfer, 35*(6), 735-743.

Imihezri, S. S. S., Sapuan, S. M., Ahmad, M. M. H. M., & Sulaiman, S. (2005). A study of the comparison of 'V' and 'X' ribbing in a composite pedal using mold flow analysis software. [doi: 10.1016/j.matdes.2004.05.011]. *Materials & Design, 26*(2), 157-166.

Kansal, G., Rao, P. N., & Atreya, S. K. (2001). Study: temperature and residual stress in an injection moulded gear. [doi: 10.1016/S0924-0136(00)00659-2]. *Journal of Materials Processing Technology, 108*(3), 328-337.

Kenneth, H. H., Donald, L. D., Douglas, E. S., & Ted, G. B. (2001). *The finite element method for engineers* (4th ed.). New York: John Wiley & Sons, Inc.

Kim, C. H., & Youn, J. R. (2007). Determination of residual stresses in injection moulded flat plate: Simulation and experiments. [doi: 10.1016/j.polymertesting.2007.05.006]. *Polymer Tesing, 26*(7), 862-868.

Kurt, M., Saban Kamber, O., Kaynak, Y., Atakok, G., & Girit, O. (2009). Experimental investigation of plastic injection molding: Assessment of the effects of cavity pressure and mold temperature on the quality of the final products. [doi: DOI: 10.1016/j.matdes.2009.01.004]. *Materials & Design, 30*(8), 3217-3224.

Li, C. L. (2001). A feature-based approach to injection mould cooling system design. [doi: DOI: 10.1016/S0010-4485(00)00144-5]. *Computer-Aided Design, 33*(14), 1073-1090.

Liu, S.-J., Su, P.-C., & Lin, K.-Y. (2009). In-situ temperature measurements in the depths of injection molded parts. [doi: DOI: 10.1016/j.measurement.2009.01.002]. *Measurement, 42*(5), 771-777.

Lu, X., & Khim, L. S. (2001). A statistical experimental study of the injection molding of optical lenses. *Journal of Materials Processing Technology, 113*(1-3), 189-195.

MatWeb. (1990). Material property data, from http://www.matweb.com/search/datasheet.aspx?matguid=833fb237c7554115954120d9da5e1e96

Michaeli, W., & Starke, C. Ultrasonic investigations of the thermoplastics injection moulding process. *Polymer Testing, 24*(2), 205-209.

Min, B. H. (2003). A study on quality monitoring of injection-molded parts. [doi: DOI: 10.1016/S0924-0136(02)00445-4]. *Journal of Materials Processing Technology, 136*(1-3), 1-6.

Mirigul, A. (2010). Reducing shrinkage in injection moldings via the Taguchi, ANOVA and neural network methods. [doi: 10.1016/j.matdes.2009.06.049]. *Materials & Design*. 31(1), 599-604.

Moaveni, S. (1999). *Finite element analysis - theory and application with ANSYS*. Upper Saddle River, New Jersey: Prentice-Hall, Inc.

Moldflow. (2011). Autodesk Moldflow Adviser (Version Educational). Kuala Lumpur.

Oktem, H., Erzurumlu, T., & Uzman, I. (2007). Application of Taguchi optimization technique in determining plastic injection molding process parameters for a thin-shell part. *Materials & Design, 28*(4), 1271-1278.

Ozcelik, B., & Erzurumlu, T. (2006). Comparison of the warpage optimization in the plastic injection molding using ANOVA, neural network model and genetic algorithm. *Journal of Materials Processing Technology, 171*(3), 437-445.

Ozcelik, B., & Sonat, I. (2009). Warpage and structural analysis of thin shell plastic in the plastic injection molding. [doi: DOI: 10.1016/j.matdes.2008.04.053]. *Materials & Design, 30*(2), 367-375.

Postawa, P., & Koszkul, J. (2005). Change in injection moulded parts shrinkage and weight as a function of processing conditions. *Journal of Materials Processing Technology, 162-163*, 109-115.

Roy, R. K. (2010). *A Primer on the Taguchi method* (2 ed): Society of Manufacturing Engineers.

Shen, Y.-K., Wu, C.-W., Yu, Y.-F., & Chung, H.-W. (2008). Analysis for optimal gate design of thin-walled injection molding. [doi: DOI: 10.1016/j.icheatmasstransfer.2008.01.014]. *International Communications in Heat and Mass Transfer, 35*(6), 728-734.

Spina, R. (2004). Injection moulding of automotive components: comparison between hot runner systems for a case study. [doi: 10.1016/j.jmatprotec.2004.04.359]. *Journal of Materials Processing Technology, 155-156*(0), 1497-1504.

Sridhar, L., & Narh, K. A. (2000). The effect of temperature dependent thermal properties on process parameter prediction in injection molding. [doi: DOI: 10.1016/S0735-1933(00)00113-5]. *International Communications in Heat and Mass Transfer, 27*(3), 325-332.

Tang, S. H., Kong, Y. M., Sapuan, S. M., Samin, R., & Sulaiman, S. (2006). Design and thermal analysis of plastic injection mould. [doi: DOI: 10.1016/j.jmatprotec.2005.06.075]. *Journal of Materials Processing Technology, 171*(2), 259-267.

Tsai, K.-M., Hsieh, C.-Y., & Lo, W.-C. (2009). A study of the effects of process parameters for injection molding on surface quality of optical lenses. *Journal of Materials Processing Technology, 209*(7), 3469-3477.

Wan Abdul Rahman, W. A., Sin, L. T., & Rahmat, A. R. (2008). Injection moulding simulation analysis of natural fiber composite window frame. [doi: DOI: 10.1016/j.jmatprotec.2007.06.014]. *Journal of Materials Processing Technology, 197*(1-3), 22-30.

Wang, J., Xie, P., Ding, Y., & Yang, W. (2009). On-line testing equipment of P-V-T properties of polymers based on an injection molding machine. [doi: 10.1016/j.polymertesting.2008.09.003]. *Polymer Testing, 28*(3), 228-234.

Wang, T.-H., & Young, W.-B. (2005). Study on residual stresses of thin-walled injection molding. *European Polymer Journal, 41*(10), 2511-2517.

Wei-Bin, Y. (2004). Residual stress induced by solidification of thermoviscoelastic melts in the postfilling stage. [doi: 10.14016/jmatprotec.2003.07.015]. *Journal of Materials Processing Technology, 145*(3), 317-324.

Yokoi, H., Masuda, N., & Mitsuhata, H. (2002). Visualization analysis of flow front behavior during filling process of injection mold cavity by two-axis tracking system. *Journal of Materials Processing Technology, 130-131*(0), 328-333.

Zhil'tsova, T. V., Oliveira, M. S. A., & Ferreira, J. A. F. (2009). Relative influence of injection molding processing conditions on HDPE acetabular cups dimensional stability. [doi: DOI: 10.1016/j.jmatprotec.2008.09.018]. *Journal of Materials Processing Technology, 209*(8), 3894-3904.

APPENDIX A : Mold and Part Design

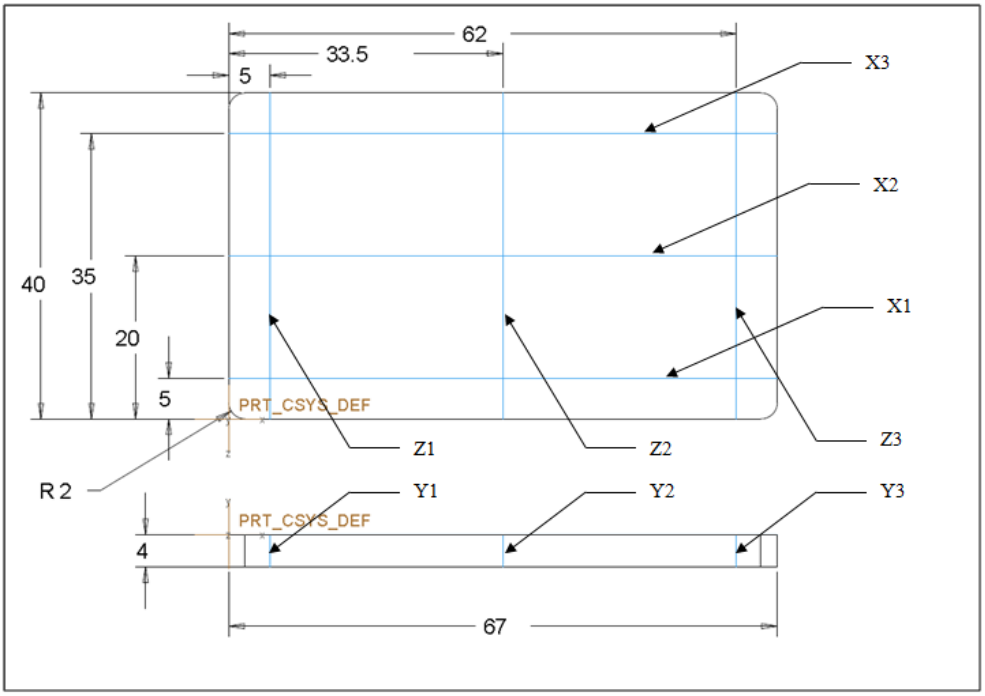

Figure A-1: Plastic part dimension and measurement locations of mold cavity-II

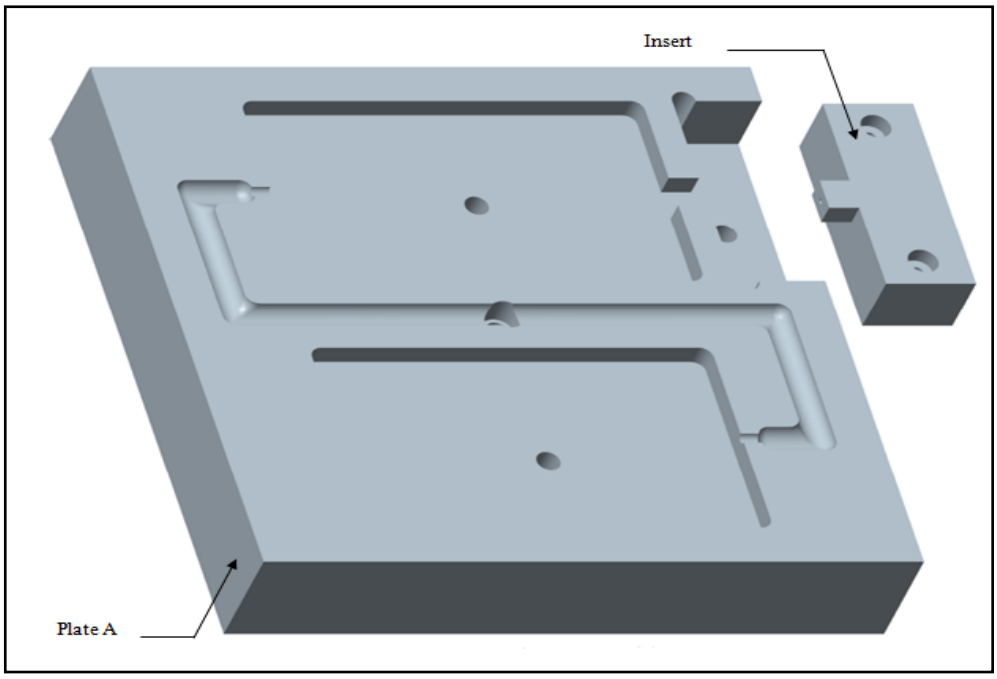

Figure A-2: Plate A and mold insert of mold cavity-II

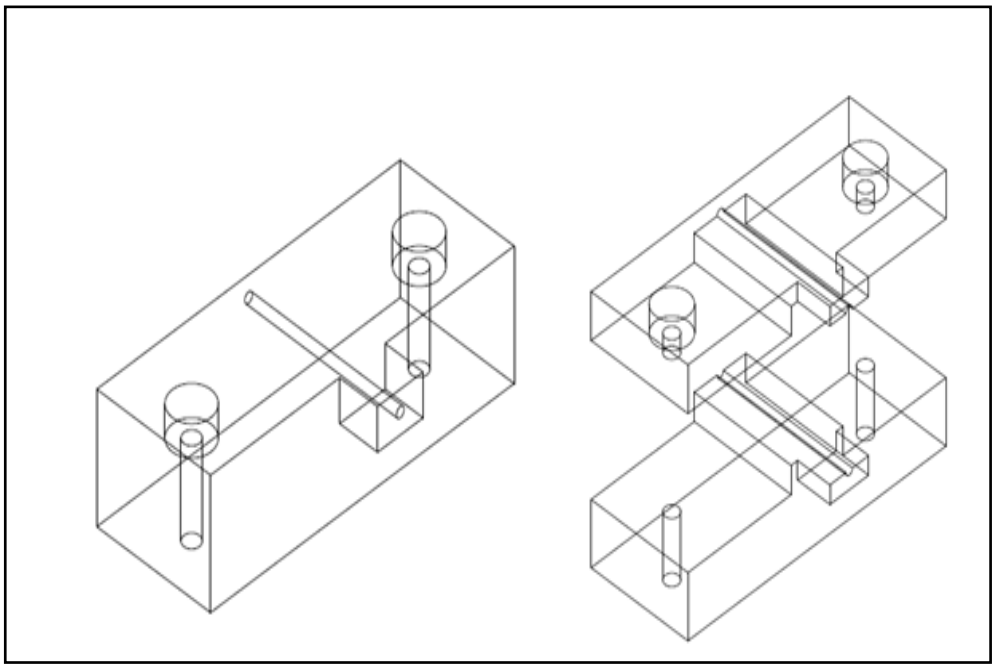

Figure A-3: Combined and non combined state of mold insert for plate A of mold cavity-II

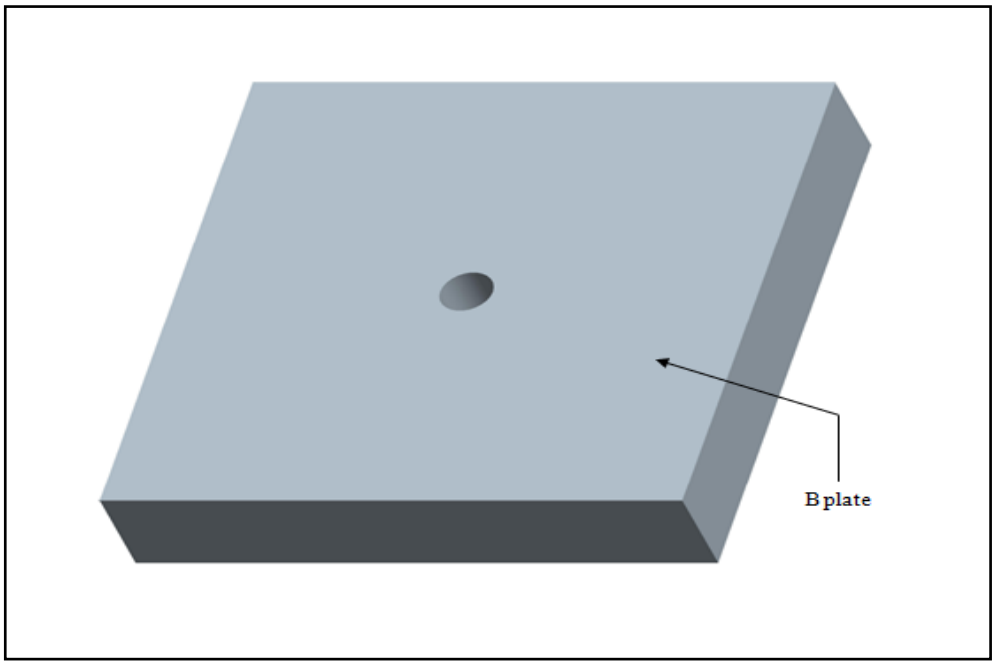

Figure A-4: Plate B of mold cavity-II

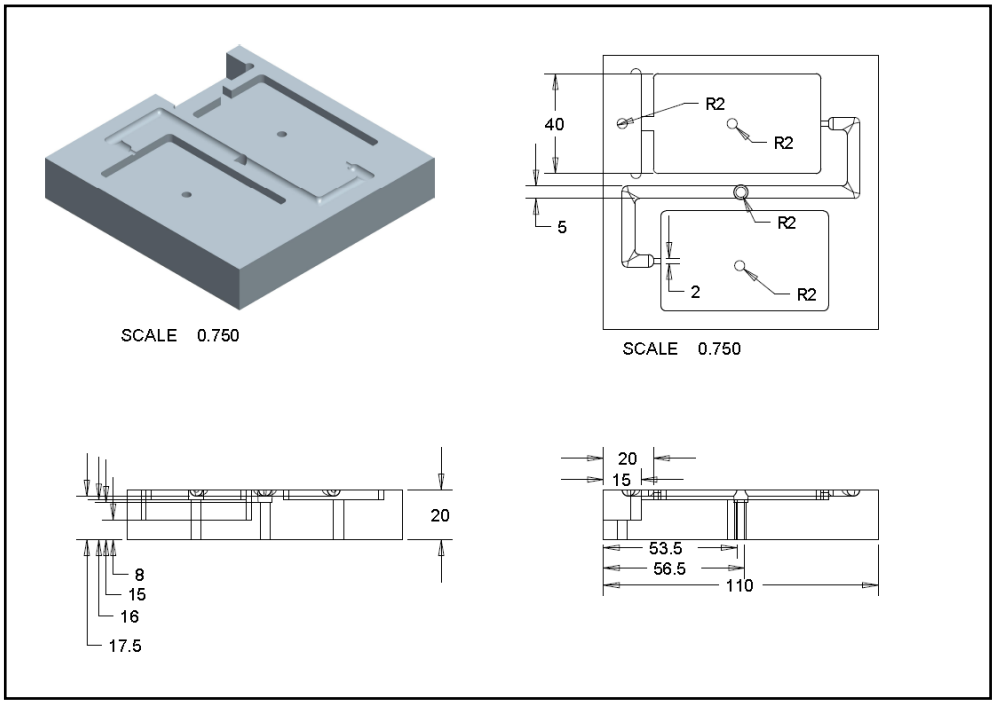

Figure A-5: Dimension for plate A of mold cavity-I

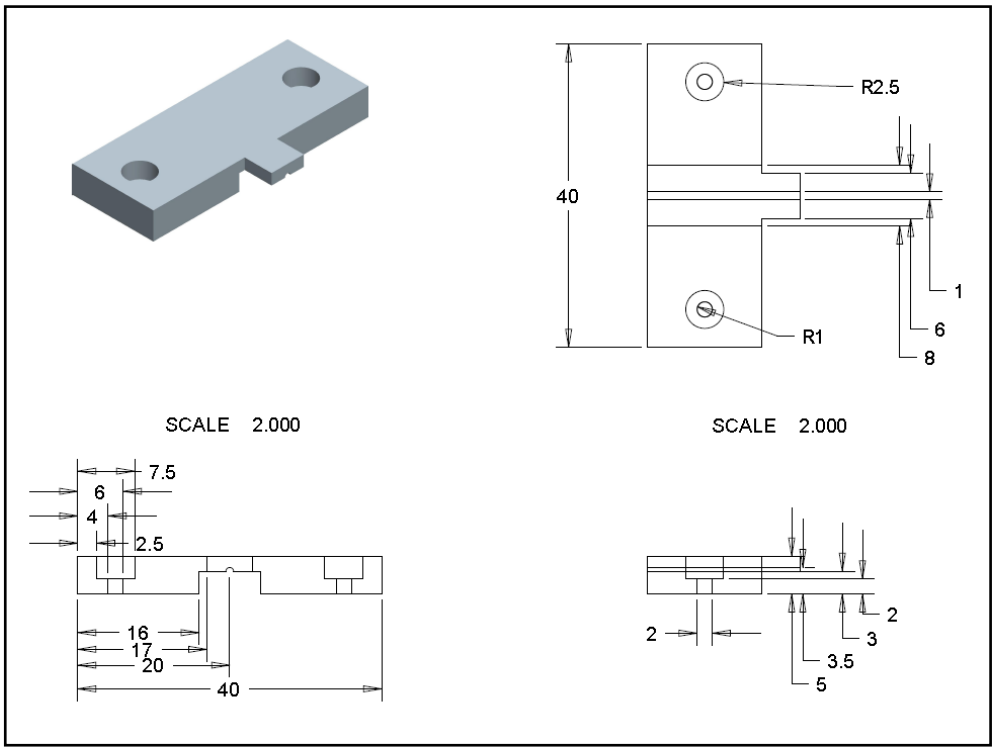

Figure A-6: Dimension of mold insert 1 for mold cavity-II

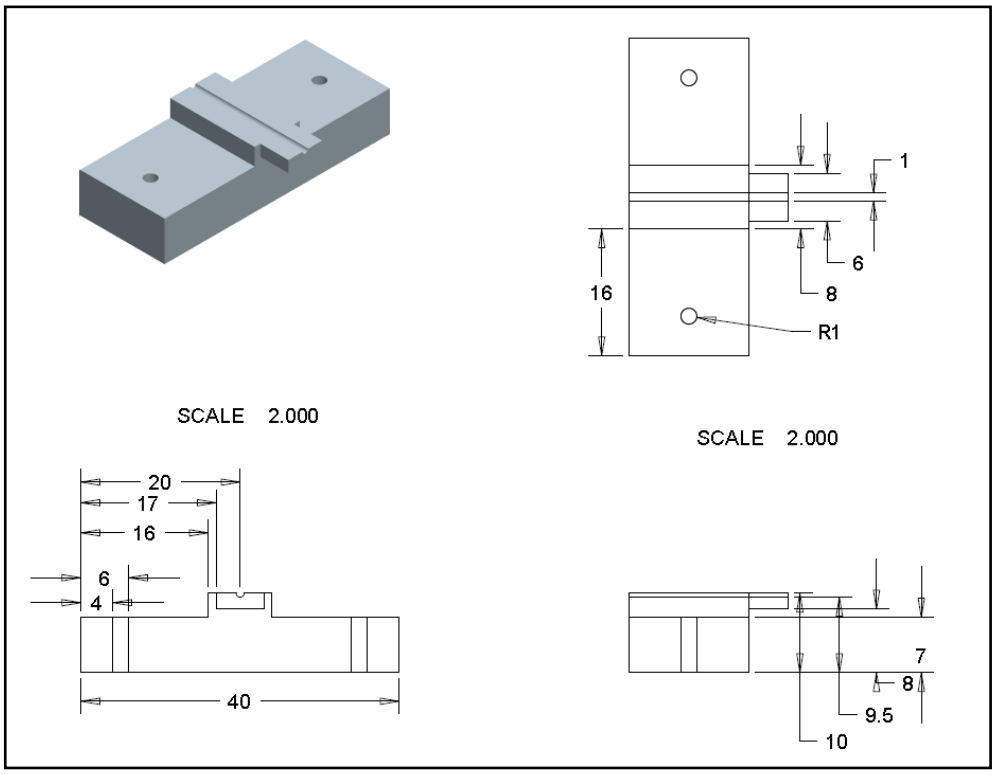

Figure A-7: Dimension for insert 2 of mold cavity-II

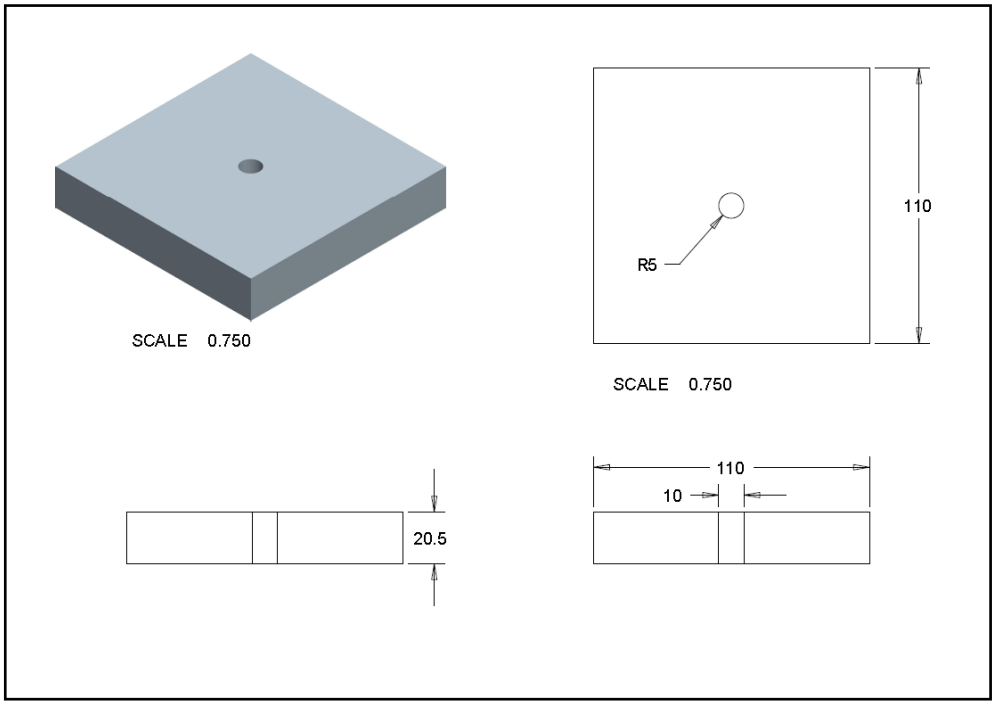

Figure A-8: Dimension for plate B of mold cavity-II

APPENDIX B : Mold Cavity used in experimental analysis

Figure B-1: Mold cavity-II (core and cavity)

Figure B-2: Mold cavity-II core part at different view positions

Figure B-3: Cavity plate of mold cavity-II

Figure B-4: Mold cavity-II components (From left to right: Retainer block, ejection system, mold cavity)

Figure B-5: Mold cavity-II ejection system (Ejector plate and pin)

Figure B-6: Mold cavity-II retainer block

APPENDIX C : Layout of Design of Experimental

Table C-1: Layout of orthogonal array, L_{27} (3^{13})

Experimental No.	Column and factor												
	1(**A**)	2(**B**)	3(**A**x**B**)	4	5(**C**)	6(**A**X**C**)	7	8(**B**X**C**)	9(**D**)	10(**E**)	11	12	13
1	1	1	1	1	1	1	1	1	1	1	1	1	1
2	1	1	1	1	2	2	2	2	2	2	2	2	2
3	1	1	1	1	3	3	3	3	3	3	3	3	3
4	1	2	2	2	1	1	1	2	2	2	3	3	3
5	1	2	2	2	2	2	2	3	3	3	1	1	1
6	1	2	2	2	3	3	3	1	1	1	2	2	2
7	1	3	3	3	1	1	1	3	3	3	2	2	2
8	1	3	3	3	2	2	2	1	1	1	3	3	3
9	1	3	3	3	3	3	3	2	2	2	1	1	1
10	2	1	2	3	1	2	3	1	2	3	1	2	3
11	2	1	2	3	2	3	1	2	3	1	2	3	1
12	2	1	2	3	3	1	2	3	1	2	3	1	2
13	2	2	3	1	1	2	3	2	3	1	3	1	2
14	2	2	3	1	2	3	1	3	1	2	1	2	3
15	2	2	3	1	3	1	2	1	2	3	2	3	1
16	2	3	1	2	1	2	3	3	1	2	2	3	1
17	2	3	1	2	2	3	1	1	2	3	3	1	2
18	2	3	1	2	3	1	2	2	3	1	1	2	3
19	3	1	3	2	1	3	2	1	3	2	1	3	2
20	3	1	3	2	2	1	3	2	1	3	2	1	3
21	3	1	3	2	3	2	1	3	2	1	3	2	1
22	3	2	1	3	1	3	2	2	1	3	3	2	1
23	3	2	1	3	2	1	3	3	2	1	1	3	2
24	3	2	1	3	3	2	1	1	3	2	2	1	3
25	3	3	2	1	1	3	2	3	2	1	2	1	3
26	3	3	2	1	2	1	3	1	3	2	3	2	1
27	3	3	2	1	3	2	1	2	1	3	1	3	2

Table C-2: Shrinkage value at three repetitions for each experimental run and S/N ratio

Experimental No.	Experimental result				
	Shrinkage value (%)				
	1	2	3	Average	S/N ratio
1	3.68	9.03	8.01	6.91	-17.25
2	7.83	8.07	8.05	7.98	-18.04
3	6.99	6.61	7.49	7.03	-16.95
4	3.50	3.38	3.10	3.32	-10.45
5	3.65	3.69	3.62	3.65	-11.25
6	7.91	8.07	8.40	8.13	-18.20
7	3.02	3.41	3.44	3.29	-10.36
8	5.12	5.56	5.20	5.29	-14.48
9	7.58	3.87	7.15	6.20	-16.15
10	8.70	2.62	2.89	4.74	-14.81
11	2.30	3.82	4.10	3.40	-10.87
12	4.99	5.06	2.91	4.32	-12.93
13	2.45	2.78	2.38	2.54	-8.11
14	5.31	4.22	4.31	4.61	-13.33
15	5.65	5.50	5.27	5.47	-14.77
16	6.72	6.01	4.60	5.78	-15.34
17	5.30	5.60	5.53	5.48	-14.78
18	5.84	6.48	5.89	6.07	-15.67
19	9.12	5.61	4.59	6.44	-16.55
20	4.88	9.18	8.29	7.45	-17.70
21	9.37	3.81	2.92	5.37	-15.67
22	8.83	6.35	8.39	7.86	-17.99
23	5.76	9.04	6.25	7.02	-17.10
24	4.51	2.53	2.33	3.12	-10.31
25	9.13	7.76	8.73	8.54	-18.65
26	6.99	5.71	5.66	6.12	-15.78
27	5.94	5.77	6.61	6.11	-15.73
				Average	-14.79

Table C-3: Available Taguchi designs (with number of factors)

Designs	Single level designs			
	2 level	3 level	4 level	5 level
L4	2-3			
L8	2-7			
L9		2-4		
L12	2-11			
L16	2-15			
L16			2-5	
L25				2-6
L27		2-13		
L32	2-31			

APPENDIX D Two-way interaction approach simulation results

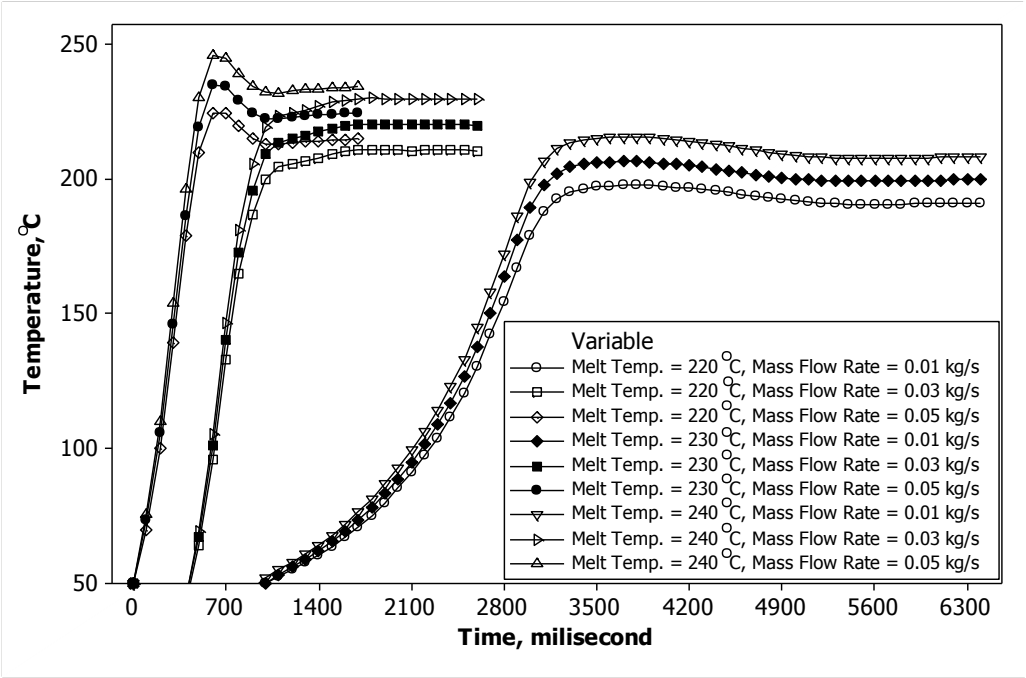

Figure D-1: R75 temperature reading during mold filling

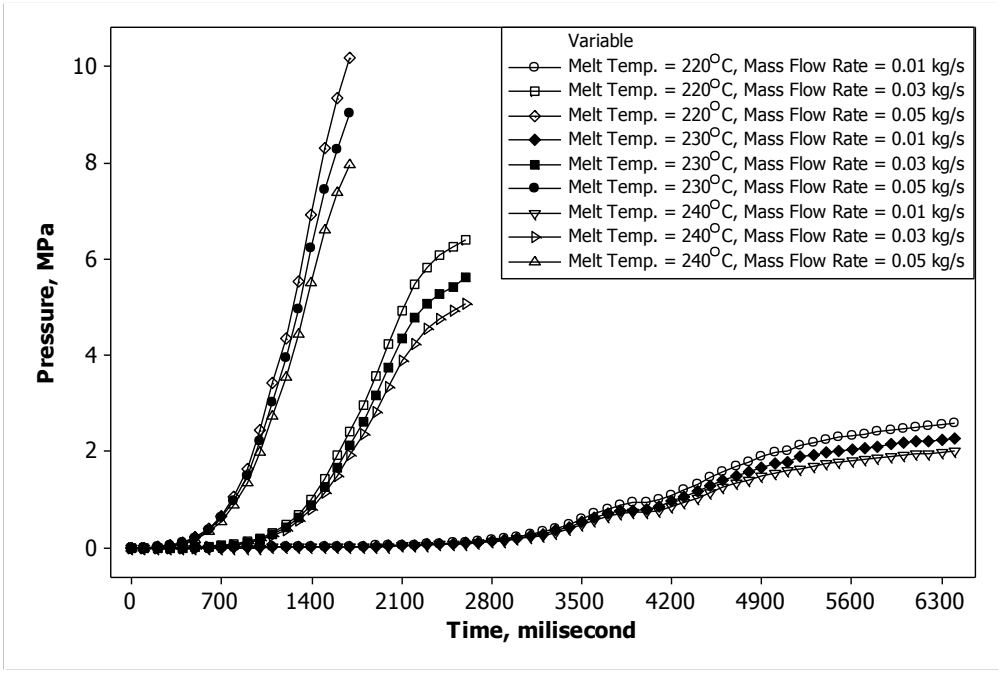

Figure D-2: R75 pressure reading during mold filling

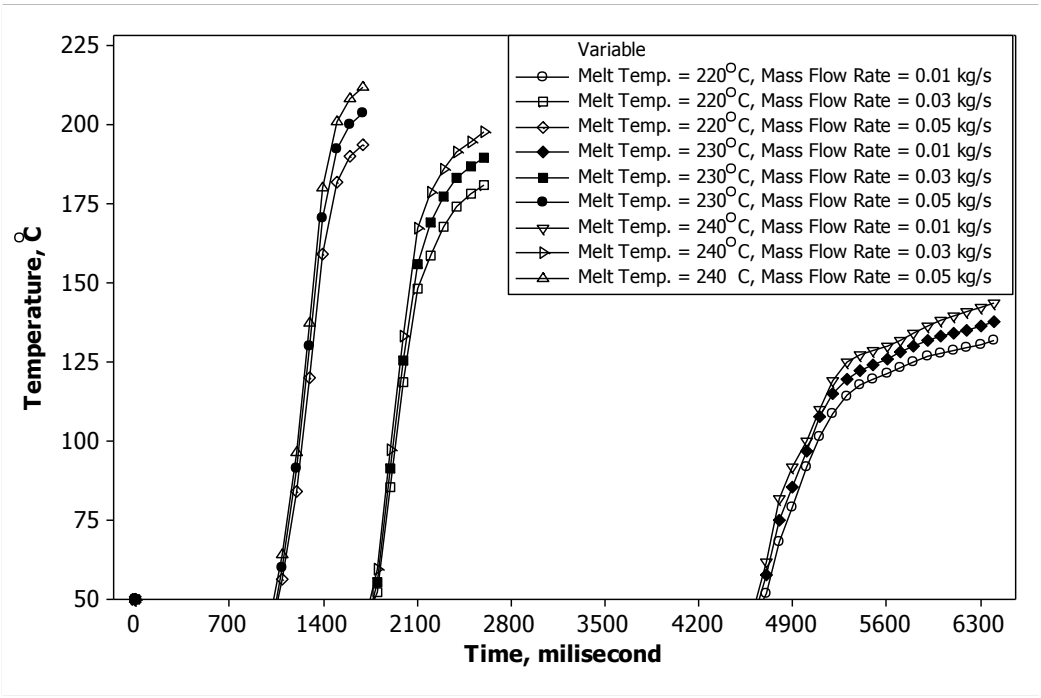

Figure D-3: M140 temperature reading during mold filling

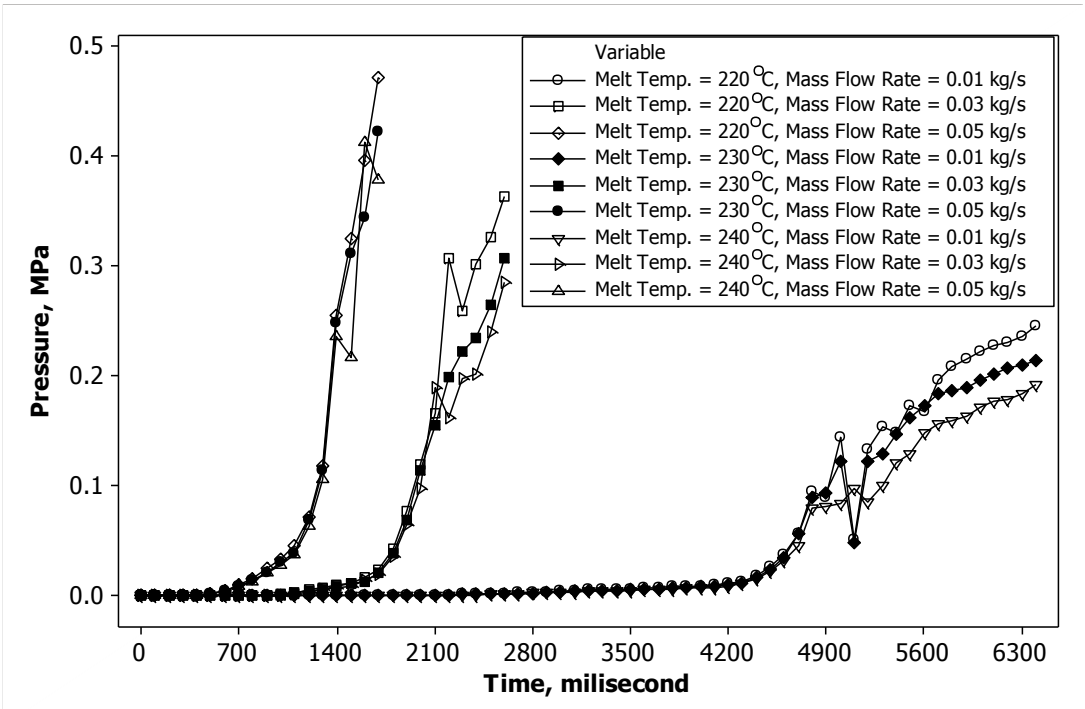

Figure D-4: M140 pressure reading during mold filling

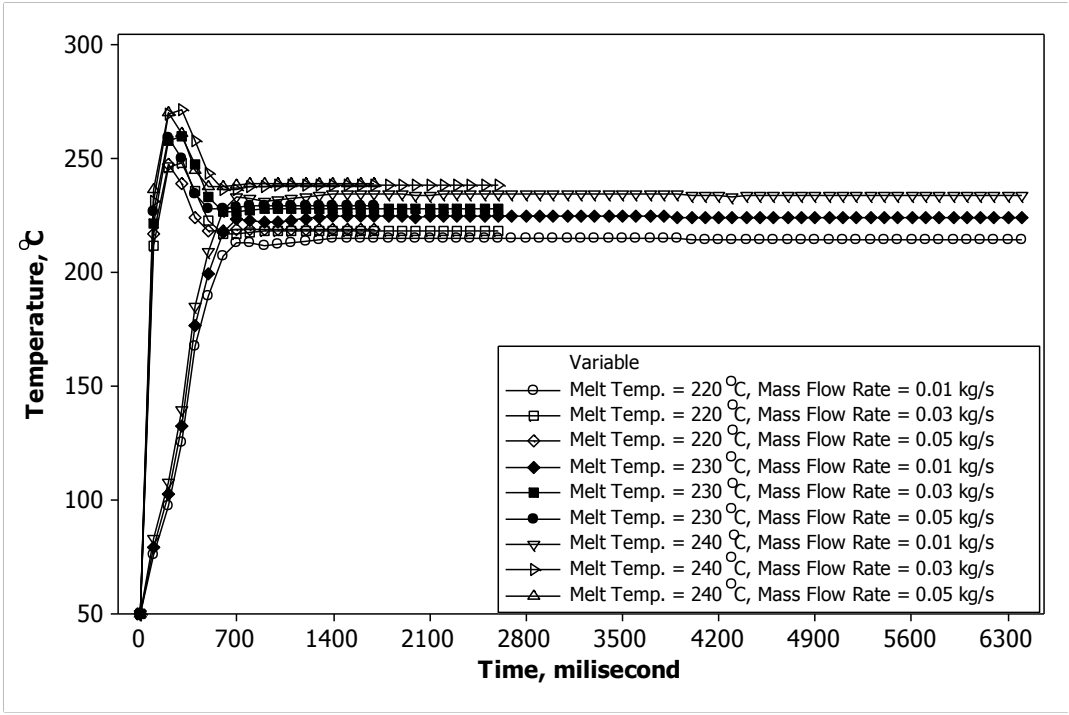

Figure D-5: M10 temperature reading during mold filling

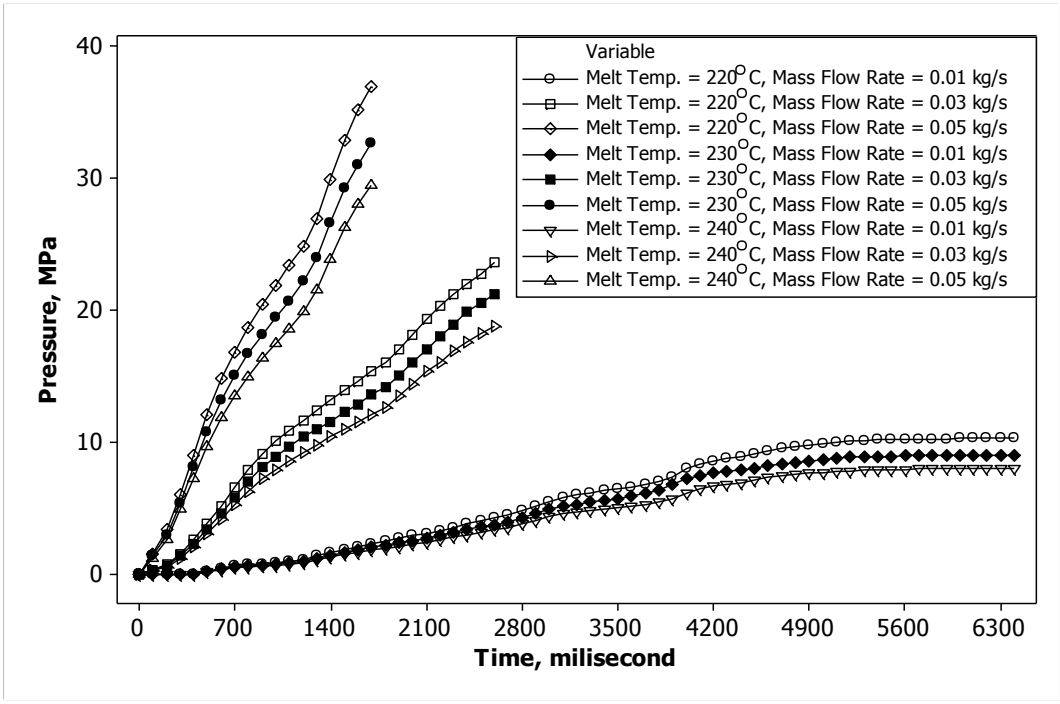

Figure D-6: M10 pressure reading during mold filling

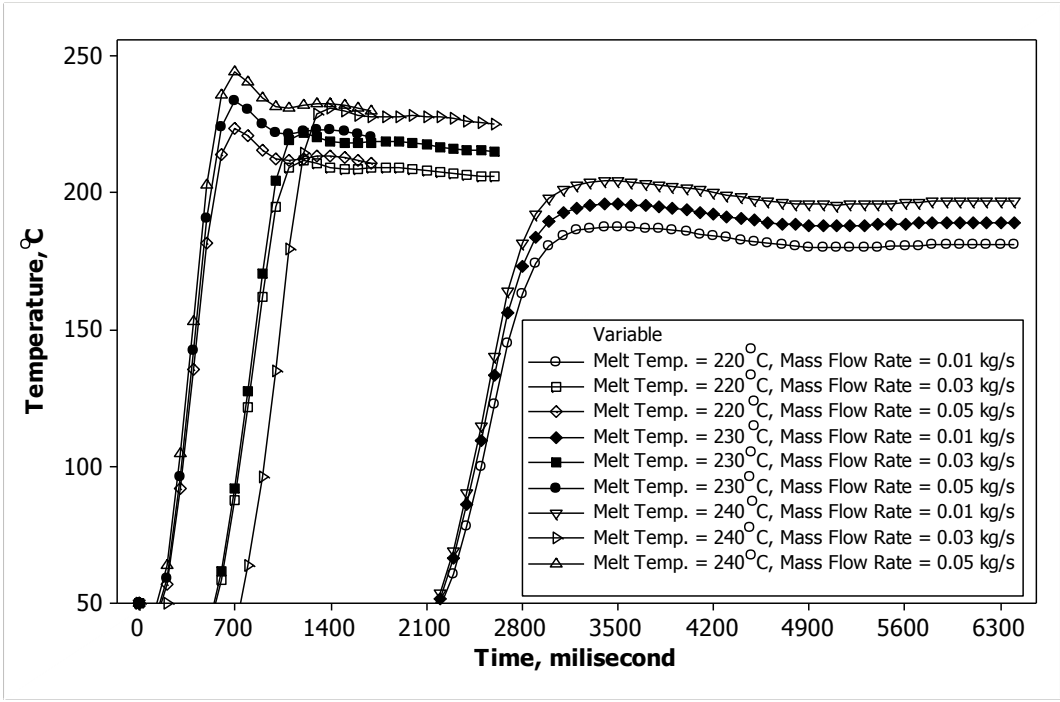

Figure D-7: L75 temperature reading during mold filling

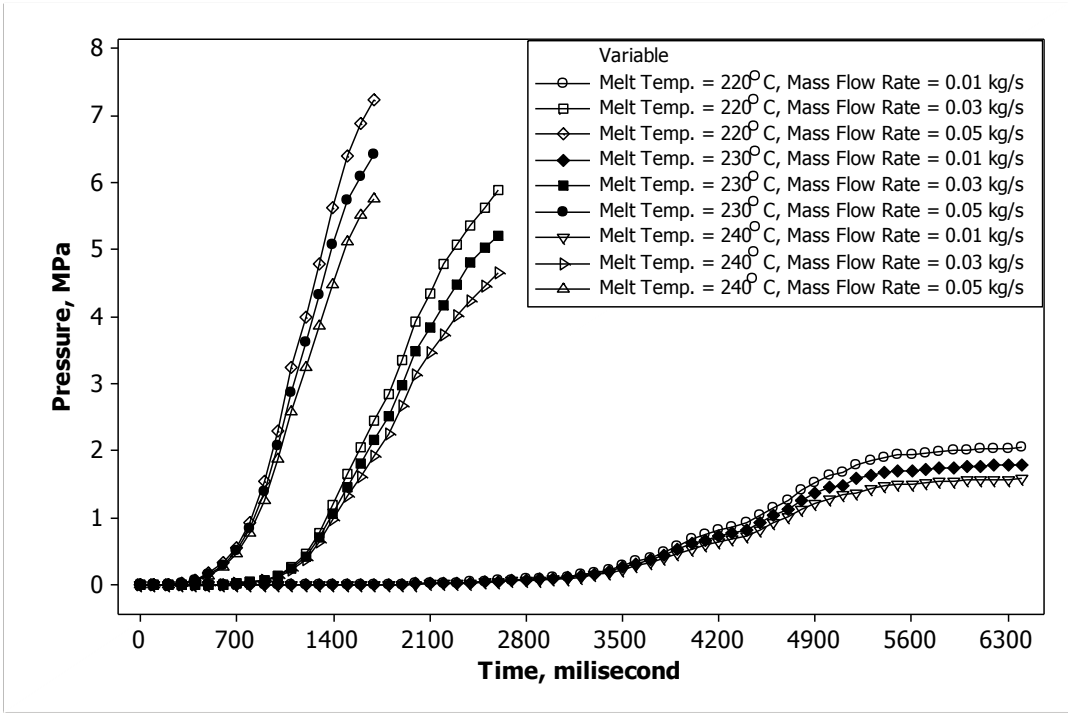

Figure D-8: L75 pressure reading during mold filling

APPENDIX E List of publications

Journal papers:

- Gan, T. W., Choudhury, I. A., & Nukman, Y. Effect of Injection Speed and Melt Temperature on The Thickness of Rectangular Shape Product Made by Injection Molding.

  [Submitted to J. Materials & Design for Publication]

- Gan, T. W., Choudhury, I. A., & Nukman, Y. Numerical Analysis on Injection Molded Plastic Part Thickness by Using Two-way Interaction Approach.
  [Submitted to International Journal of Heat and Mass Transfer for Publication]

Conference paper:

- Gan, T. W., Choudhury, I. A., & Nukman, Y. (2010). Mold Filling Analysis by Using Finite Volume Method. Paper presented at The 11th Asia Pacific Industrial Engineering and Management System Conference, Melaka, Malaysia.